VOLUME III JULY, 1938 NUMBER 3

GEOPHYSICS

A Journal of General and Applied Geophysics

DISCOVERIES*

ALEXANDER DEUSSEN†

What are the reserves of oil?

This question has been a serious matter of concern to us ever since oil has come to occupy the dominant position in our national economy which it now occupies.

With the problem of reserves the problem of discovery is inseparably related. Discovery means reserves—without discovery we know that the end of oil is in sight. We likewise know that we must continue with discovery if we can continue with oil.

The oil business started with a discovery, that of the Drake well in Pennsylvania in 1859. Its growth to its present position has been determined by a long series of additional discoveries in different portions of the country since that time. Its demise, as we now know the business, will occur when discovery fails, as fail it must, some day.

Discovery and the ability of the industry to continue it is of especial concern to the geologist and geophysicist. It is the phase of the business with which he is primarily concerned, and in which he is primarily engaged.

When discovery finally fails the work of the oil geologist and oil geophysicist will be done.

Because of the importance of discovery in relation to reserves the past history of discovery has been reviewed by a number of students,[1]

* Paper read by invitation at the Joint Annual Meeting of the Society and the A.A.P.G., New Orleans, La., Mar. 17, 1938. The writer wishes to acknowledge the assistance and collaboration of Dr. Ionel I. Gardescu, Petroleum Engineer, of Houston, Texas, in assembling the data on which this paper is based.

† Consulting geologist, Houston, Texas.

[1] Discovery Rates in Oil Finding. Pratt, W. E., Bulletin, American Association of Petroleum Geologists, Vol. 21, p. 697 et seq.

with the purpose in view of drawing some conclusions as to what its future may be, on the premise, and to an extent a sound premise, that what has happened in the past will give some inkling as to what may occur in the future.

This present paper is an additional review of some phases of the history of discovery—not heretofore covered I believe—likewise in the hope that from this particular review a conclusion may be

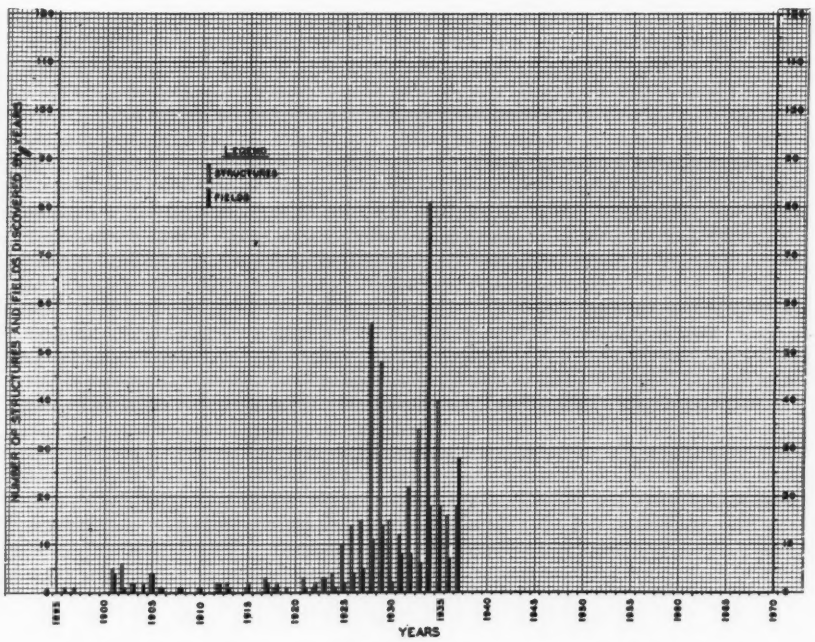

FIG. 1. Number of structures and fields discovered by years in the Texas and Louisiana Gulf Coast area.

drawn that may be of some cheer to the geologists and geophysicists here assembled.

There is one matter at least about which the geologist knows he can be certain and this is that there is a definite limit to the barrels of oil that remain in the ground. Correspondingly he knows that there must be a definite limit to discovery, that at some time and in some place, the last barrel of oil will be removed, the last oil field will be discovered, the last structure will be tested, the last well will be drilled, and the last geophysical party will be disbanded. These things are certain.

Knowing these things to be true, it is but natural, since our business (as we now know it) must one day terminate, that we (at least some of us) should try to take inventory of what we have. Also in this connection the attempt has been made to visualize something about the future of discovery.

We have been taking inventory for a number of years. The history

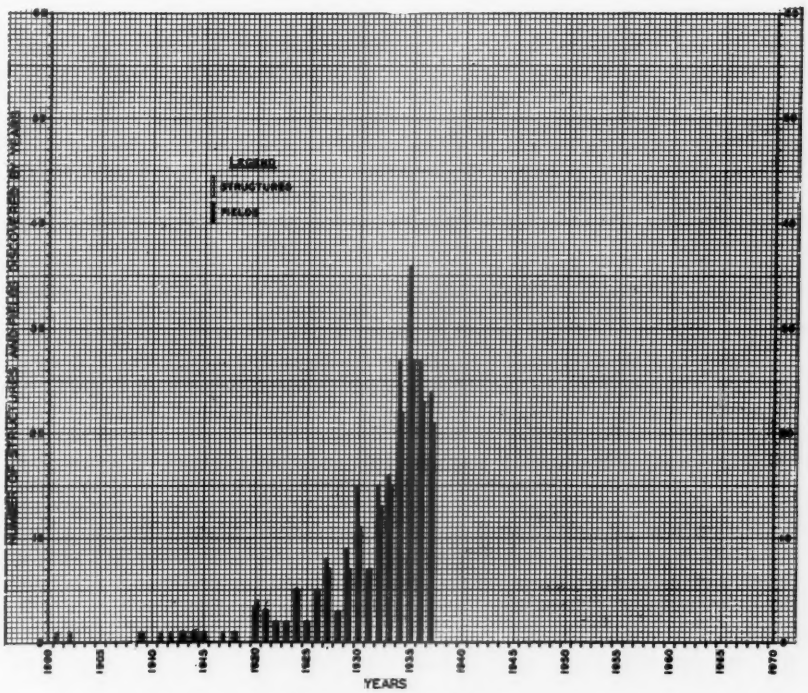

FIG. 2. Number of structures and fields discovered by years in the Southwest Texas area.

of this inventory taking has disclosed an interesting fact that may likewise have a bearing on the future of discovery.

This interesting fact is that since we have been estimating our oil reserves we have constantly underestimated them. These matters of course have been brought to your attention a number of times heretofore, but a brief repetition in this connection may not be out of order.

David T. Day in 1908 made the first serious attempt to estimate the oil reserves of the United States. His figure was a minimum of

8,000,000,000 barrels and a maximum of 22,000,000,000 barrels, a very large margin as between the minimum and maximum.

It is to be noted that these figures included both the proven and the undiscovered reserves and it is likewise worthy of note that the proven reserves at that time were relatively small, about 4,000,000,000 barrels.

As of January 1, 1908, the United States had produced

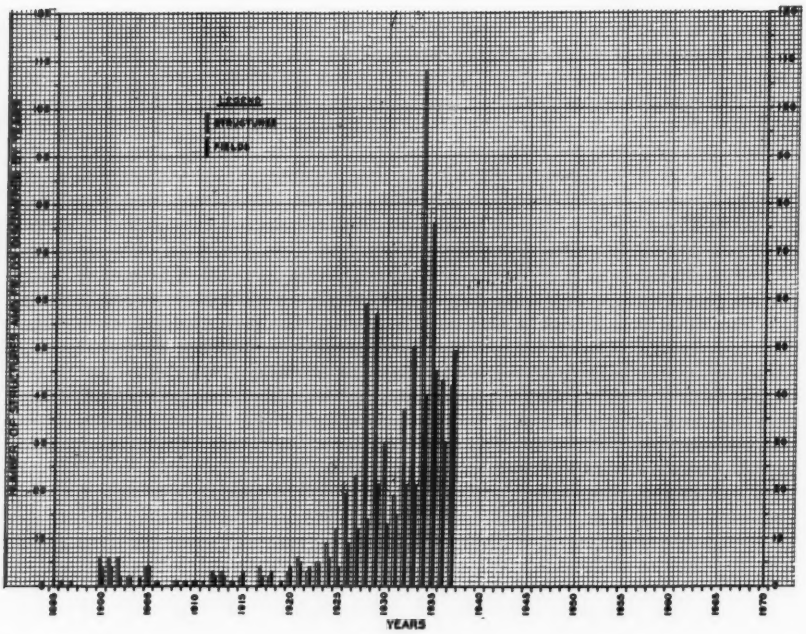

FIG. 3. Number of structures and fields discovered by years in the Texas and Louisiana Gulf Coast area, including Southwest Texas.

1,806,600,000 barrels of oil, so that taking Day's figures, the total ultimate production of the United States at that time was estimated at from 9,806,600,000 to 23,806,600,000 barrels.

Arnold in 1915 revised Day's figures upwards. In 1918 David White revised Arnold's figures upwards.

In 1921 a joint committee of the American Association of Petroleum Geologists and the United States Geological Survey made another estimate. This time the figure was 9,150,000,000 barrels, of which approximately 6,750,000,000 barrels were considered proven

and the remaining 2,400,000,000 barrels were from fields remaining to be discovered.

In 1921 the total accumulated production of the United States was 5,429,900,000 barrels (up to January 1, 1921). Adding the estimate of 9,150,000,000 barrels to this, gives a figure of 14,579,900,000

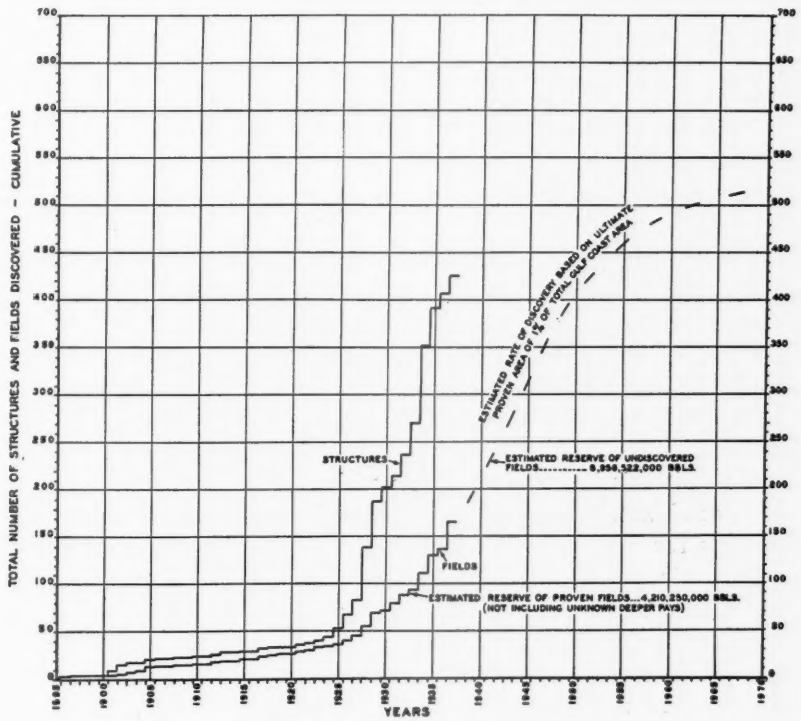
TOTAL NUMBER OF STRUCTURES AND FIELDS DISCOVERED - CUMULATIVE
YEARS
STRUCTURES
FIELDS
ESTIMATED RATE OF DISCOVERY BASED ON ULTIMATE PROVEN AREA OF 1% OF TOTAL GULF COAST AREA
ESTIMATED RESERVE OF UNDISCOVERED FIELDS..... 9,950,522,000 BBLS.
ESTIMATED RESERVE OF PROVEN FIELDS...4,210,250,000 BBLS. (NOT INCLUDING UNKNOWN DEEPER PAYS)

FIG. 4. Total cumulative number of structures and fields discovered in the Texas and Louisiana Gulf Coast area.

barrels for the total ultimate production of the United States, as it was visualized at that time.

Now, what has happened since 1921? Our total accumulated production to January 1, 1938, was 19,972,100,000 barrels; our proven reserves are now estimated at something like 15,507,300,000 barrels; we place no figure on the oil from the undiscovered fields. Counting the past production and only the oil in sight from proven fields, the total ultimate of these two items for the United States is 35,479,400,000 barrels.

In 1921 all that we could see for the ultimate total was 14,579,900,000 barrels; in 1938 (17 years later) we see 35,479,400,000 barrels, or 20,899,500,000 barrels more than we thought we had in 1921. We have produced since 1921 14,542,200,000 barrels of oil, only 37,700,000 barrels less than we figured as the total remaining oil at that time, and today after we have produced and consumed approximately the amount of oil we figured we had on hand in 1921, we have 15,507,300,000 barrels of oil still in sight, with an undetermined amount of oil to be found in as yet undiscovered fields.

These facts are summarized in Table I, page 183.

Two conclusions may be drawn from these facts:

We certainly in the past have constantly underestimated our oil reserves.

Certainly discovery has been very active in these 17 years, exceeding by far any anticipation that we could apparently justify at the time.

One further significant fact is apparent from a study of the table. It is to be noted that in the last estimate there is no figure for the undiscovered oil. We have undershot the mark so badly that we have quit (since 1925) estimating the undiscovered oil.

Yet it is this undiscovered oil in which we are most interested as a matter of fact. That which we know we have is of course important, but it is the undiscovered oil that is the more important from the nation's viewpoint, and likewise that is of primary interest to the geophysicist and exploration geologist.

Now the question may be asked that since we have done such a poor job of estimating our oil, and likewise estimating our ability to discover new oil, whether this will continue to be our experience, notwithstanding the fact that we must know that some time or other a limit must be reached.

Have we reached the peak? And how near is the end?

I will not attempt to answer these questions for the world as a whole, or even for the United States as a whole.

It may be safe to assume that so far as discovery is concerned in the world as a whole its end (of discovery) is still very far distant in the future.

There are unquestionably in countries other than the United States large areas yet to be explored, not only by geologic and seismic investigation, but also by drilling, and it seems safe to assert that very many years will be required to complete this task. In other lands and

TABLE I

ESTIMATES OF OIL RESERVES IN THE UNITED STATES

Year	Authority	Proven (Bbls.)	Undiscovered (Bbls.)	Total (Bbls.)	Production to Date of Estimate[a] (Bbls.)	Indicated Total Ultimate Production	
						Proven (Bbls.)	Proven and Undiscovered (Bbls.)
1908	David T. Day	4,000,000,000	4,000,000,000 min. 18,000,000,000 max.	8,000,000,000 min. 22,000,000,000 max.	1,806,600,000	5,806,600,000	9,806,600,000 min. 23,806,600,000 max.
1915	Ralph Arnold			5,700,000,000	3,335,500,000		9,035,500,000
1918	David White			6,700,000,000	4,252,600,000	4,252,600,000	10,952,600,000
1921	A.A.P.G. and U.S.G.S. Jointly	6,750,000,000	2,400,000,000	9,150,000,000	5,429,900,000	12,179,900,000	14,579,900,000
1938	A.P.I.	15,507,300,000			19,972,100,000	35,479,400,000	

[a] As reported by Oil Weekly.

distant countries the geologist and geophysicist unquestionably have many years of work ahead of them.

The United States of course more so than any other country, due in my judgment to the system of free enterprise under which we have heretofore operated, has been most extensively explored and our oil resources have likewise been more extensively exploited than those of any other nation.

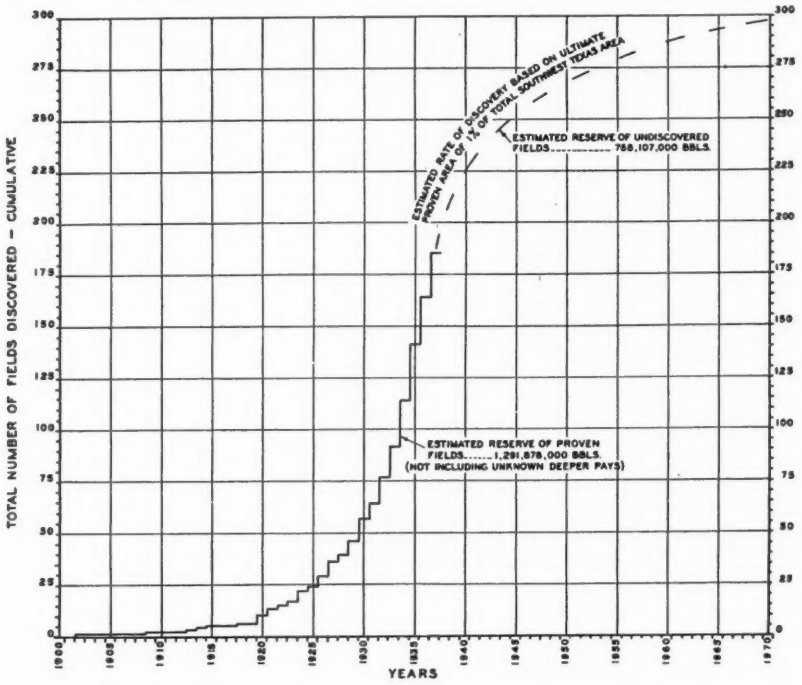
TOTAL NUMBER OF FIELDS DISCOVERED - CUMULATIVE
YEARS
ESTIMATED RATE OF DISCOVERY BASED ON ULTIMATE PROVEN AREA OF 1% OF TOTAL SOUTHWEST TEXAS AREA
ESTIMATED RESERVE OF UNDISCOVERED FIELDS..... 758,107,000 BBLS.
ESTIMATED RESERVE OF PROVEN FIELDS..... 1,291,878,000 BBLS. (NOT INCLUDING UNKNOWN DEEPER PAYS)

FIG. 5. Total cumulative number of fields discovered in Southwest Texas area.

And yet I think all of us will agree there still remains in the United States a large area to be explored and drilled, which I firmly believe will yield additional and important discoveries over the years with additional and important increments to our oil reserves.

The purpose of the present inquiry is addressed primarily to the Texas-Louisiana Gulf Coast, as a type region, one of the important oil areas (if not the most important) of the United States, one that has heretofore been extensively explored, one that has at present more

oil in reserve than any other area of the United States,[2] and one that has led the march of progress, not only in the art of exploration, but likewise in the exploitation of these resources.

It was in the Gulf Coast that the rotary drill was for the first time successfully used in the drilling of an oil well. The contribution that the rotary drill has made to the art of oil exploration would be very difficult to measure.

It was likewise in the Gulf Coast that the core barrel was first devised and used, and the contribution that the core barrel has made to the development of our oil resources would likewise be difficult to measure in terms of barrels of oil.

It was in the Gulf Coast that the value of micro-paleontology, in the attempt to improve correlation and by this means to find new structures, was successfully demonstrated.

It was likewise in the Gulf Coast that geophysics was for the first time successfully applied, and from these beginnings geophysics has come to assume its present dominating position in the exploratory end of the oil business.

In the matter of deep drilling the Gulf Coast has likewise led the march of progress and has pointed the way.

It was likewise in the Gulf Coast that electric logs were first put to practical use, and the contribution that these electric logs are making in the discovery of new oil fields and new oil reserves would likewise be very difficult to estimate.

As a result of these important and history making achievements the Gulf Coast has been explored probably more extensively than any other oil producing province of the United States. One would naturally suppose that having been so thoroughly explored the end of discovery might possibly be in sight for the Gulf Coast.

What does the future hold in the way of discovery in the Gulf Coast—in an area that has been the scene of these intense activities during the past 37 years?

There is offered for your consideration in this connection another study of the past history of discovery in the Gulf Coast, a slightly different approach to this history from that used by Pratt in his paper presented a year ago.[3]

[2] As of January 1, 1938, the proven oil reserves of the Texas-Louisiana Gulf Coast and the Southwest Texas area are estimated at 5,502,128,000 barrels of oil, representing approximately 35.5 per cent of the proven reserves of the United States.

[3] Pratt, W. E., *op. cit.*

In the following table we have tabulated by years structures reliably reported to be found in the several years (using for this purpose reports of the Oil Weekly) and consider as oil fields discovered,

TABLE II

DISCOVERIES OF STRUCTURES AND FIELDS BY YEARS IN THE TEXAS-LOUISIANA GULF COAST AREA AND INCLUDING THE TEXAS SOUTHWEST AREA

Year	Tex. G. C.		La. G. C.		Total G. C.		Tex. S. W.		Total G. C. & Tex. S. W.	
	St.	F.	St.	F.	St.	F.	St.	F.	St.	F.
1862			1		1				1	
1895			1		1				1	
1896			1		1				1	
1897			1		1				1	
1898										
1899										
1900										
1901	4	3	1	1	5	4	1		6	4
1902	4		2	1	6	1		1	6	2
1903	1	1	1	1	2	2			2	2
1904		2				2				2
1905	4	4			4	4			4	4
1906	1	1			1	1			1	1
1907										
1908	1	1			1	1			1	1
1909							1	1	1	1
1910			1	1	1	1			1	1
1911							1		1	
1912			2	2	2	2	1		3	2
1913	2	1			2	1	1	1	3	2
1914							1	1	1	1
1915	1	2			1	2	1	1	2	3
1916										
1917		1	3	1	3	2	1		4	2
1918	1	2			1	2	1	1	2	3
1919		1				1				1
1920							3	4	3	4
1921	2	2	1		3	2	3	3	6	5
1922	1	2			1	2	2	2	3	4
1923	3	3			3	3	2	2	5	5
1924	2		2	1	4	1	5	5	9	6
1925	8	2	2		10	2	2	2	12	4
1926	2	2	12	2	14	4	5	5	19	9
1927	3	2	12	3	15	5	8	7	23	12
1928	30	7	26	4	56	11	3	3	59	14
1929	30	7	18	7	48	14	9	7	57	21
1930	9	1	6	1	15	2	15	11	30	13
1931	10	3	2	5	12	8	7	7	19	15
1932	20	6	2	2	22	8	15	13	37	21
1933	30	5	4	1	34	6	16	15	50	21
1934	50	11	31	7	81	18	27	22	108	40
1935	20	11	20	7	40	18	36	27	76	45
1936	9	2	7	5	16	7	27	23	43	30
1937	10	15	8	13	18	28	24	21	42	49

TABLE III

CUMULATIVE NUMBER OF DISCOVERIES OF STRUCTURES AND FIELDS BY YEARS IN THE TEXAS-LOUISIANA GULF COAST AREA AND INCLUDING TEXAS SOUTHWEST AREA

Year	Texas S. W.		G. C. Area		G. C. & Texas S. W.	
	St.	F.	St.	F.	St.	F.
1862			1		1	
1895			2		2	
1896			3		3	
1897			4		4	
1898			4		4	
1899			4		4	
1900			4		4	
1901	1		9	4	10	4
1902	1	1	15	5	16	6
1903	1	1	17	7	18	8
1904	1	1	17	9	18	10
1905	1	1	21	13	22	14
1906	1	1	22	14	23	15
1907	1	1	22	14	23	15
1908	1	1	23	15	24	16
1909	2	2	23	15	25	17
1910	2	2	24	16	26	18
1911	3	2	24	16	27	18
1912	4	2	26	18	30	20
1913	5	3	28	19	33	22
1914	6	4	28	19	34	23
1915	7	5	29	21	36	26
1916	7	5	29	21	36	26
1917	8	5	32	23	40	28
1918	9	6	33	25	42	31
1919	9	6	33	26	42	32
1920	12	10	33	26	45	36
1921	15	13	36	28	51	41
1922	17	15	37	30	54	45
1923	19	17	40	33	59	50
1924	24	22	44	34	68	56
1925	26	24	54	36	80	60
1926	31	29	68	40	99	69
1927	39	36	83	45	122	81
1928	42	39	139	56	181	95
1929	51	46	187	70	238	116
1930	66	57	202	72	268	129
1931	73	64	214	80	287	144
1932	88	77	236	88	324	165
1933	104	92	270	94	374	186
1934	131	114	351	112	482	226
1935	167	141	391	130	558	271
1936	194	164	407	137	601	301
1937	218	185	425	165	643	350

not a field of any given magnitude, but one in which a commercial well has been discovered.[4]

[4] In the vast number of cases, with only a few exceptions, experience indicates that a commercial well in a given area is the forerunner of a commercial field, although a

The table is made of five columns—first, Texas Gulf Coast; second, Louisiana Gulf Coast; third, total,Texas-Louisiana Gulf Coast; fourth, southwest Texas; fifth, total, Texas-Louisiana Gulf Coast and Southwest Texas.

The columns list separately by years the structures found and the fields discovered.

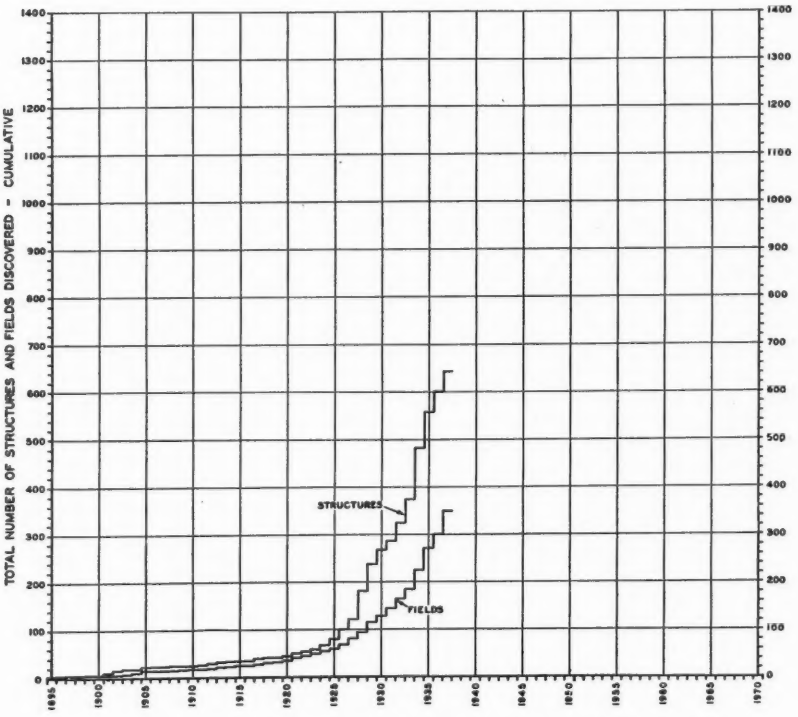

FIG. 6. Total cumulative number of structures and fields discovered in Gulf Coast area, including Southwest Texas.

In Table III the cumulative discoveries for the respective years are listed.

These results are likewise shown graphically in the series of graphs and curves, Figs. 1, 2, 3, 4, 5 and 6.

It is interesting to note from these curves that the trend of discovery, both of structures and of oil fields has been an ascending one

number of years may elapse between this first well and the later commercial importance of the particular area.

over the years. Each year has added either a new structure or a new oil field, and of course as new methods have been introduced such as torsion balance, refraction and reflection seismograph there has been a rapid increment in the number of discoveries, followed by their active exploitation.

If one would rely on the evidence of these curves as is commonly done in the statistical approach to any problem of this kind, it is

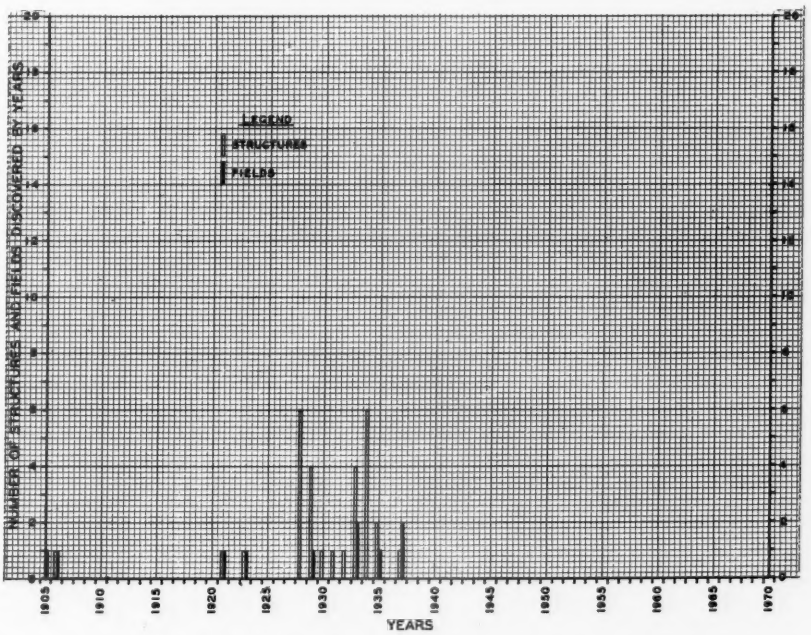

FIG. 7. Number of structures and fields discovered by years in Harris County, Texas.

noted that neither curve shows any tendency to flatten thus far, and on the basis of these curves so far as they afford any information on the subject, it may be safely concluded that the end of discovery in the Gulf Coast is yet far distant in the future.

We have attempted another approach to the solution to this problem, and for this purpose we have selected a typical area within the Gulf Coast, concerning which we have attempted some speculations.

Harris County is selected as a typical oil producing county of the Gulf Coast.

Similar tables (IV and V) and similar curves have been platted for Harris County, both as to structures and oil fields found during the years of its oil history (Figs. 7 and 8). It will be noted that so far as Harris County is concerned the curves in general are similar to those for the Gulf Coast as a whole.

And yet if one should give credence to the theory of the structural

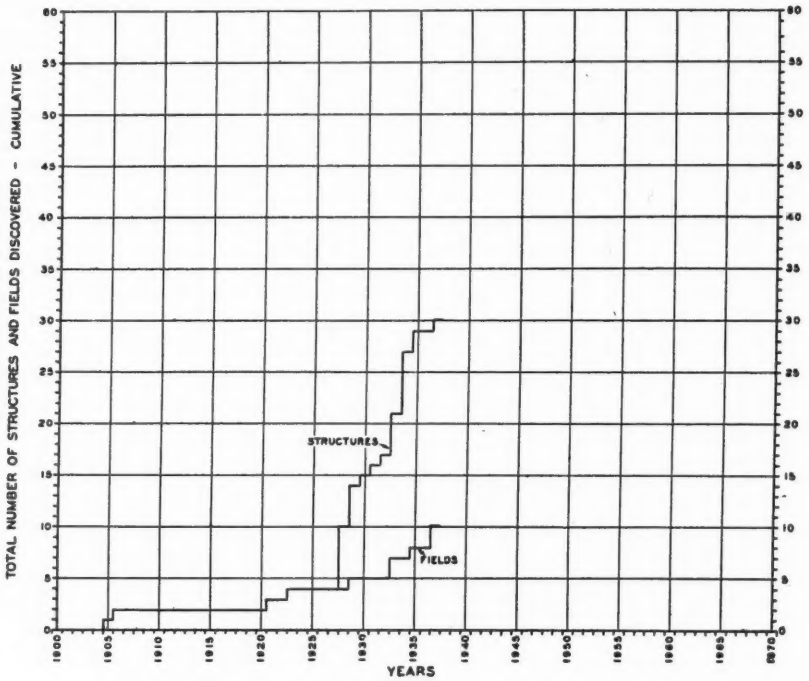

FIG. 8. Total cumulative number of structures and fields discovered in Harris County, Texas.

control of oil it is apparent there must be a limit to the number of structures and the number of oil fields that it might be possible to find in Harris County.

The accompanying map of Harris County (Fig. 9), shows the location of the present oil fields and the present structures. The map has been compiled with the idea in view that when these structures have attained a certain density then the limit of discovery will be reached.

I think it will be readily conceded by all that around each oil field

there must be a corresponding area in which no accumulation can occur, otherwise it would be impossible to have an oil field in the first instance. This is of course entirely at variance with the commonly expressed view on the part of laymen who are not acquainted with the

TABLE IV

DISCOVERIES OF STRUCTURES AND FIELDS BY YEARS IN HARRIS COUNTY, TEXAS

Year	Structures	Fields	Proven	Main Fields Discovered
1905	1	1	Oil	Humble
1906	1	1	Oil	Goose Creek
1907				
1908				
1909				
1910				
1911				
1912				
1913				
1914				
1915				
1916				
1917				
1918				
1919				
1920				
1921	1	1	Oil	Pierce Junction
1922				
1923	1	1	Oil	
1924				
1925				
1926				
1927				
1928	6			
1929	4	1	Gas	Mykawa
1930	1			
1931	1			
1932	1			
1933	4	2	Gas & Oil	Tomball
1934	6			
1935	2	1	Oil	South Houston
1936				
1937	1	2	Gas & Oil	Friendswood
	30	10		

conditions of oil occurrence, that eventually, for example all of Harris County will be found to be underlain by oil. I believe that we can safely assume that this cannot be the case.

We have tabulated the area of these structures and fields in Table VI.

As the present picture shows we have 30 structures proven or

supposed to be proven for Harris County—on the average 1 structure for each 35,285 acres of land, or if you try to evaluate it in number of oil acres against the number of dry acres, assuming that each structure may have in it as much as 1,483 acres of oil land, we have 43,150 acres

TABLE V

CUMULATIVE DISCOVERIES OF STRUCTURES AND FIELDS BY YEARS IN HARRIS COUNTY, TEXAS

Year	Structures	Fields
1905	1	1
1906	2	2
1907	2	2
1908	2	2
1909	2	2
1910	2	2
1911	2	2
1912	2	2
1913	2	2
1914	2	2
1915	2	2
1916	2	2
1917	2	2
1918	2	2
1919	2	2
1920	2	2
1921	3	3
1922	3	3
1923	4	4
1924	4	4
1925	4	4
1926	4	4
1927	4	4
1928	10	4
1929	14	5
1930	15	5
1931	16	5
1932	17	5
1933	21	7
1934	27	7
1935	29	8
1936	29	8
1937	30	10

of oil land as against 1,015,410 acres of dry land. Assuming all of the structures eventually to carry oil the percentage of oil acres to dry acres is 4.076 per cent, at best a woefully small percentage in a limited area where structural conditions are extremely favorable and an area which has been most extensively explored.

These facts are summarized in Table VII.

While the structures in Harris County appear to be extremely dense, it appears that the limit has not yet been reached, that there

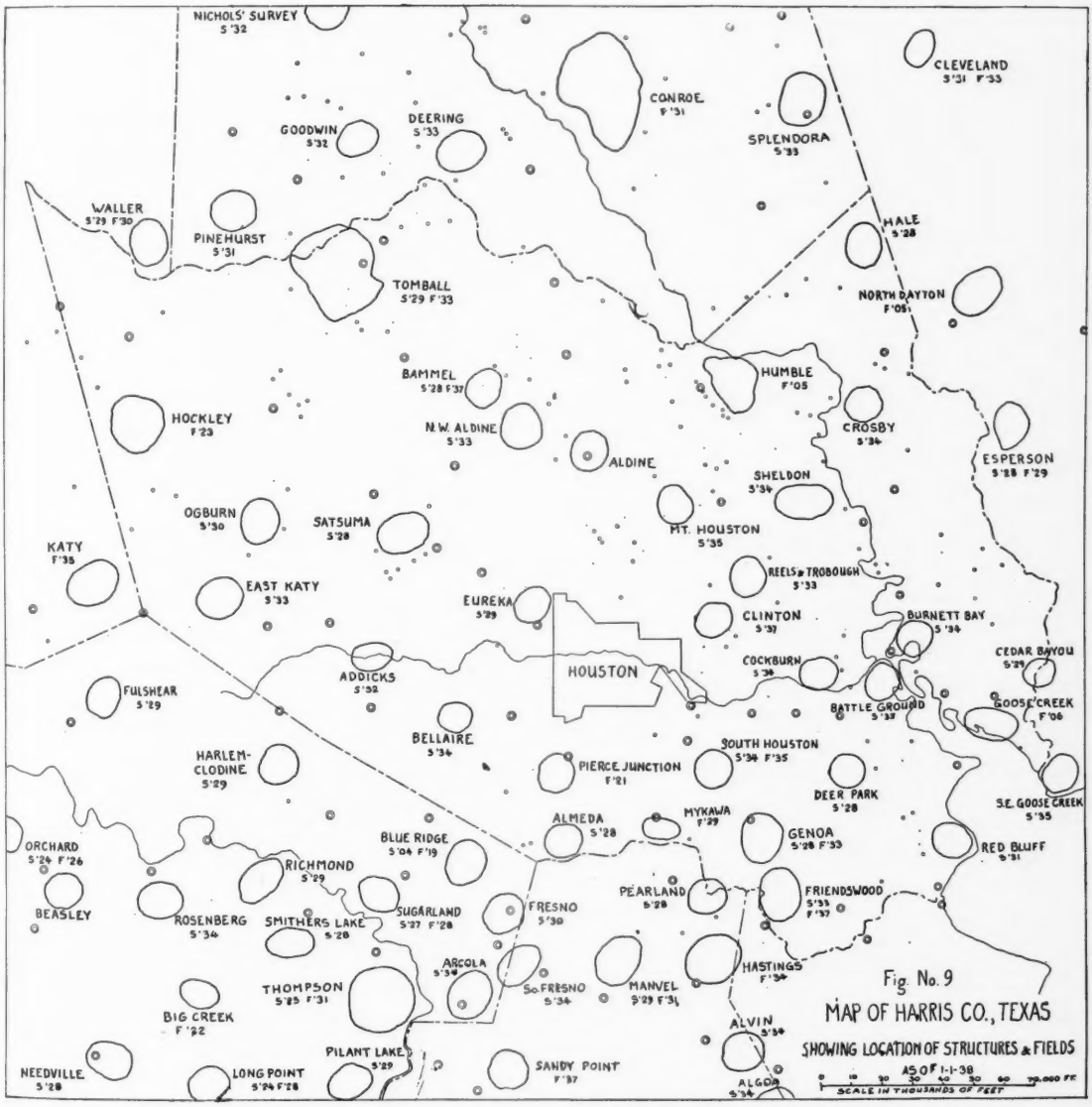

FIG. 9. Map of Harris County, Texas, showing location of structures and fields as of January 1, 1938.

TABLE VI

ESTIMATED AREAS OF PROSPECTIVE STRUCTURES AND OIL & GAS FIELDS IN HARRIS COUNTY, TEXAS

Field	Structures		Fields		Proven
	Year	Acreage	Year	Acreage	Structures
Addicks	1932	1,000		500	
Almeda	1928	1,000		500	
Bammel	1928	1,000	1937	800	Gas
Battle Ground	1935	1,000		500	
Bellaire	1934	1,000		500	
Burnett Bay	1934	1,000		500	
Cedar Bayou	1929	1,000		500	
Clinton	1937	1,000		500	
Cockburn	1934	1,000		500	
Crosby	1934	1,000		500	
Deer Park	1928	1,000		500	
East Katy	1933	1,000		500	
Eureka	1929	1,000		500	
Friendswood	1933	5,000	1937	5,000	Oil
Genoa	1928	1,000	1933	500	Gas
Goose Creek	1906	1,000	1906	1,000	Oil
Hale	1928	1,000		500	
Humble	1905	3,000	1905	3,000	Oil
Hockley	1923	1,000	1923	500	Oil
Mount Houston	1935	1,000		500	
Mykawa	1929	1,000	1929	500	Gas
North West Aldine	1933	1,000		500	
Ogburn	1930	1,000		500	
Pierce Junction	1921	1,000	1921	500	Oil
Red Bluff	1931	1,000		500	
Reels & Trobough	1933	1,000		500	
Satsuma	1928	1,000		500	
Sheldon	1934	1,000		500	
South Houston	1934	1,000	1935	650	Oil
Tomball	1929	8,150	1933	8,150	Oil
		43,150		30,600	

TABLE VII

AREAS AND AREA PERCENTAGE OF STRUCTURES AND FIELDS IN HARRIS COUNTY, TEXAS

Surface of Harris County	1,058,560 Acres
Surface of Prospective Structures	43,150 Acres
Percentage of Prospective Structures	4.076%
Surface Prospective & Proven Fields	30,600 Acres
Percentage Prospective & Proven Fields	2.891%
Surface Proven Oil Fields	18,800 Acres
Percentage Proven Oil Fields	1.776%
Surface Prospective Fields	11,800 Acres
Percentage Prospective Fields	1.115%

is still room for additional structures to be found. It might easily be that the eventual percentage of oil to dry land for this particular area may reach as high as 5 or 6 per cent.

Using Harris County as a yard stick on which to base some calculations for the entire Gulf Coast, we arrive at some interesting results,

TABLE VIII

NUMBER OF PROSPECTIVE FIELDS, ESTIMATED ON THE RATIO OF PROVEN ACREAGE TO TOTAL ACREAGE IN THE GULF COAST AREA

No. of Oil & Gas Fields Discovered as of 1/1/38	165
No. of Structures Discovered as of 1/1/38	425
Area of Counties & Parishes in Gulf Coast Area	25,787,720 Acres
Percentage of Discovered Fields to Total Area	3/10 of 1%
Percentage of Discovered Structures to Total Area	1.6%

If the prospective oil and gas fields are estimated on a basis of percentage of the total acreage of the Gulf Coast Area, the ultimate number of fields to be discovered, assuming an average of 500 acres per field, would be as follows:

No. of Fields Equivalent to 1% of Gulf Coast Area	516
No. of Fields Equivalent to 2% of Gulf Coast Area	1,032
No. of Fields Equivalent to 3% of Gulf Coast Area	1,548

On a 3% basis, there should be more than 9 times as many fields discovered ultimately.

TABLE IX

NUMBER OF PROSPECTIVE FIELDS, ESTIMATED ON THE RATIO OF PROVEN ACREAGE TO TOTAL ACREAGE IN THE SOUTHWEST TEXAS AREA

No. of Oil & Gas Fields Discovered as of 1/1/38	185
No. of Structures Discovered as of 1/1/38	218
Area of Counties in the Southwest Texas Area	14,736,640 Acres
Percentage of Discovered Fields to Total Area	6/10 of 1%
Percentage of Discovered Structures to Total Area	1.5%

If the prospective oil and gas fields are estimated on a basis of percentage of the total acreage of the Southwest Texas Area, the ultimate number of fields to be discovered, assuming an average of 500 acres per field, would be as follows:

No. of Fields Equivalent to 1% of Southwest Texas Area	295
No. of Fields Equivalent to 2% of Southwest Texas Area	590
No. of Fields Equivalent to 3% of Southwest Texas Area	885

On a 3% basis, there should be nearly 5 times as many fields discovered ultimately.

both as to the number of new discoveries we might hope to expect and as to the amount of undiscovered oil we might hope to find.

In Tables VIII and IX we show these calculations for the Gulf Coast and Southwest Texas.

Note that if the Gulf Coast should ultimately attain a density of 1 per cent for the ultimate oil fields (as compared with the present

1.776 per cent proven oil land and possible 4.076 per cent ultimately for Harris County) we have 351 additional fields to discover in the Gulf Coast and 110 in Southwest Texas, making a total of *461* fields in the entire area here considered, as against the 165 fields we now have in the Gulf Coast and 185 in Southwest Texas, or a total of *350* in both areas.

We have likewise attempted to evaluate these discoveries in terms of barrels of undiscovered oil, using only the figures based on 1 per

TABLE X

ESTIMATED OIL RESERVES AS OF 1/1/38

(a) Estimated Oil Reserves of Known Fields

Area	Production to 1/1/38	Estimated Reserve	Estimated Ultimate
Gulf Coast, Louisiana.....	330,795,000	437,255,000	768,050,000
Gulf Coast, Texas.....	1,081,155,000	2,361,045,000	3,442,200,000
Gulf Coast, Total.....	1,411,950,000	2,798,300,000	4,210,250,000
Southwest Texas.....	251,707,000	1,040,171,000	1,291,878,000
Total G. C. incl. S. W. Texas	1,663,657,000	3,838,471,000	5,502,128,000

(b) Estimated Oil Reserves of Known and Undiscovered Fields

No. of Proven Fields in Gulf Coast area.....	165
Average Ultimate Production per Field.....	25,517,000 Bbls.
Ult. Prod. of 516 Fields Equiv. to 1% of G. C.....	13,166,772,000 Bbls.
Ult. Prod. of 351 Undiscovered Fields.....	8,956,522,000 Bbls.
No. of Proven Fields in Southwest Texas area.....	185
Average Ultimate Production per Field.....	6,983,000 Bbls.
Ult. Prod. of 295 Fields Equiv. to 1% of S. W. Texas....	2,059,985,000 Bbls.
Ult. Prod. of 110 Undiscovered Fields.....	768,107,000 Bbls.
Ult. Prod. Undiscovered Fields G. C. and S. W. Texas...	9,724,629,000 Bbls.

cent of the area. On this basis we find that the undiscovered oil (not including undiscovered oil in the unproven deeper sands in the present known fields) may be 8,956,522,000 barrels for the Gulf Coast and 768,107,000 barrels for Southwest Texas, or a total of 9,724,629,000 barrels for both areas.

See also Figs. 4 and 5 in this connection.

If the undiscovered oil from deeper pays in the present known fields be estimated at 25 per cent of the present proven reserves of these fields (in both areas) or 1,375,532,000 barrels, the total of the undiscovered oil in both areas may be of the magnitude of 11,100,161,000 barrels, as against our present proven reserve of

5,502,128,000 barrels, or a little more than twice as much as we now know we have.

Interesting in this connection is that the projection of the cumulative curves in both Gulf Coast and Southwest Texas (Figs. 4 and 5), on the basis of ultimate density of 1 per cent, conforms admirably to the trend of these curves based on past history, a projection that might be reasonably drawn independent of the 1 per cent density calculations.

Unfortunately no categorical answer can be made to the question I have posed in the earlier portions of the paper.

Reasoning by analogy however, it seems safe to conclude, regardless of any credence that may be given to the figures herein suggested both as to new discoveries to be made or number of barrels of oil yet to be found, that when one considers the Gulf Coast as a whole the end of discovery is not yet in sight, and that the exploration geologist and geophysicist can take comfort in the fact that he yet has very much work to do in this leading oil producing section of the United States.

THE REFLECTION OF LONGITUDINAL WAVE PULSES FROM PLANE PARALLEL PLATES*

MORRIS MUSKAT†

ABSTRACT

A wave theory treatment is given of the reflection of elastic wave pulses from plane parallel plates. The analysis automatically resolves the reflected wave system into a series of undistorted individual pulses having the same shape as that impinging on the reflecting plate, but which are characterized by varying amplitudes and phase shifts corresponding to various internal reflection and refraction processes within the plate. The numerical values for the reflection coefficients for the three most prominent longitudinal reflected pulses resulting from an incident longitudinal wave pulse are given in both tabular and graphical form, for angles of incidence between 0 and 30°, for velocity ratios between the plate and incident medium of 1.0 to 2.0, and for density ratios of 0.9 to 1.3. The actual superposition of the individual reflected waves is shown graphically for three cases where the ratio of the reflecting plate thickness to the length of the incident pulse has the values 2, 1, or ½.

INTRODUCTION

The reflection of plane wave pulses or finite wave trains from reflecting plates is usually treated by the methods of geometrical optics. By this we mean that the histories of the individual pulses are traced, as they impinge upon the various interfaces and give rise to further reflected and refracted pulses, and adjusted with amplitude and phase changes appropriate to single surfaces of discontinuity. This procedure is rather simple to carry through when there is only a single reflecting plate and when the wave system is of a single type. The latter obtains in the case of electromagnetic wave propagation, in the case of elastic waves when the medium is a fluid and hence carries only longitudinal waves, and finally when the incident wave train is composed of transverse waves polarized normal to the plane of incidence and hence gives rise to no longitudinal waves. As is to be expected, this method gives results which are fully equivalent to those indicated by a complete wave treatment of the problem, as has indeed been recently shown in detail.[1] Moreover it follows from such a wave treatment that when the reflection coefficient for the incident wave system is strictly periodic in the frequency of the waves the pulses reflected and refracted from the plate will be of exactly the same shape

* Paper read at the Annual Meeting, Mar. 16, 1938, New Orleans, La.

† Gulf Research and Development Company, Pittsburgh, Pa.

[1] M. Muskat, Journal of Applied Physics, Vol. 9, 275 (1938).

as the incident pulse. While this fact is also generally assumed in the geometrical treatment of pulse propagation, it seems to require an explicit wave treatment in order to give it a rigorous justification.

For general elastic media when both longitudinal and transverse waves are excited at the various interfaces, the geometrical method of tracing the history of each reflected or refracted pulse, while in principle still possible, obviously becomes more complicated. Moreover it requires the explicit knowledge of the reflection and refraction coefficients for both types of waves at the various interfaces involved in the system. It therefore appears to be of interest to develop the wave theory treatment of this problem. For in this the various reflection and refraction events at the individual interfaces are taken into account automatically, so as to lead to resultant amplitudes for the pulses which leave the reflecting plates without the necessity for considering in detail their previous histories. The problem here is, of course, more complicated than in the case of electromagnetic wave propagation, or where there is only one type of elastic wave traversing the medium. This manifests itself analytically by the fact that the resultant reflection or refraction coefficient for a monochromatic system is no longer strictly periodic in the frequency, unless by accident certain relations should obtain between the multiplicity of constants appropriate to the complete system. Nevertheless a systematic procedure can be developed which is quite analogous to the simpler case of exactly periodic reflection coefficients, and which permits the calculation of the resultant amplitude of any wave pulse leaving the plate having any preassigned history of multiple reflections within it. The specific analysis to be given here for this problem will be restricted to the case where the incident waves are longitudinal, and to a discussion of only the reflected wave pulses. The treatments of systems where the incident wave train is transverse and of the transmitted wave pulses may be carried through in an exactly similar manner after making obvious changes.

GENERAL THEORY

The starting point of our analysis is, as already indicated, the reflection coefficient for a monochromatic and continuous wave system. For convenience we shall deal here directly with the amplitudes of the wave dilatation rather than the wave displacements. These latter may be expressed in terms of the dilatation and shear functions, L, T by the relations:

$$u = e^{i\omega t}\left(\frac{\partial L}{\partial x} + \frac{\partial^2 T}{\partial x \partial z}\right); \qquad v = e^{i\omega t}\left(\frac{\partial L}{\partial y} + \frac{\partial^2 T}{\partial y \partial z}\right) = 0;$$

$$w = e^{i\omega t}\left(\frac{\partial L}{\partial z} + \frac{\partial^2 T}{\partial z^2} + \frac{\omega^2 T}{\beta^2}\right);$$

where it is supposed that the plane of incidence is the xz plane, and the reflecting interfaces are parallel to the xy planes. β is the transverse wave velocity, corresponding to the longitudinal wave velocity α. The whole wave system is taken to be monochromatic with the frequency ω. The functions L and T satisfy the wave equations:

$$\left(\nabla^2 + \frac{\omega^2}{\alpha^2}\right)L = 0; \qquad \left(\nabla^2 + \frac{\omega^2}{\beta^2}\right)T = 0,$$

the actual dilatation begin given by $\nabla^2 L$.

Setting up the plane wave components for the three media—above, within, and below the plate—, as:

$$L_m = A_m e^{i(a_m z - b_m x)} + B_m e^{i(-a_m z - b_m x)},$$
$$T_m = C_m e^{i(c_m z - d_m x)} + D_m e^{i(-c_m z - d_m x)},$$

and adjusting the amplitude coefficients at the interfaces to give continuity of the displacements and stresses, one obtains eight linear inhomogeneous equations in the nine significant amplitudes. Taking the incident wave as known, the others may be expressed in terms of it. Specifying its value as unity, that of the reflected longitudinal wave is given by:

$$R(\omega) = \frac{E' - F'\cos p - iH'\sin p + G'\cos \sigma p + iJ'\sin \sigma p}{E - F\cos p - iH\sin p + G\cos \sigma p + iJ\sin \sigma p}, \qquad (1)$$

where the coefficients $E', F' \cdots J', E, F \cdots J$ are defined by the following unfortunately complex notation scheme:

$$\left.\begin{aligned}
&E' = -4a_2c_2b^2\Psi_3\bar{\Psi}_1;\ F' = -(\bar{\tau}_1 + \bar{\kappa}_1)(\tau_3 + \kappa_3) + q_3\bar{q}_1;\\
&H' = (\tau_3 + \kappa_3)\bar{q}_1 - (\bar{\tau}_1 + \bar{\kappa}_1)q_3;\\
&G' = -(\bar{\tau}_1 - \bar{\kappa}_1)(\tau_3 - \kappa_3) + q_1\bar{q}_3;\ J' = (\tau_3 - \kappa_3)q_1 - (\bar{\tau}_1 - \bar{\kappa}_1)\bar{q}_3;\\
&E = 4a_2c_2b^2\Psi_1\Psi_3;\ F = (\tau_1 + \kappa_1)(\tau_3 + \kappa_3) + q_1q_3;\\
&H = q_3(\tau_1 + \kappa_1) + q_1(\tau_3 + \kappa_3);\\
&G = (\tau_1 - \kappa_1)(\tau_3 - \kappa_3) + \bar{q}_1\bar{q}_3;\ J = \bar{q}_3(\tau_1 - \kappa_1) + \bar{q}_1(\tau_3 - \kappa_3).
\end{aligned}\right\} \qquad (1a)$$

$$\left.\begin{aligned}
&\frac{\bar{\Psi}}{\Psi} = \eta\xi \mp 2ac\nu\zeta; \quad \frac{\bar{\kappa}}{\kappa} = a_2c_2(\xi^2 \mp 4ac\zeta^2b^2);\\
&\frac{\bar{\tau}}{\tau} = b^2\eta^2 \mp ac\nu^2; \quad \frac{\bar{q}}{q} = k^2k_2^2\delta(ac_2 \mp a_2c);\\
&\eta = \delta\epsilon_2 - \epsilon;\ \xi = \epsilon + 2\delta b^2;\ \nu = \delta\epsilon_2 + 2b^2;\ \zeta = \delta - 1;\ \delta = \mu_2/\mu;\\
&\epsilon = k^2 - 2b^2;\ k^2 = \omega^2/\beta^2;\ j^2 = \omega^2/\alpha^2;\ c^2 = k^2 - b^2;\ a^2 = j^2 - b^2;\\
&b = \frac{\omega \sin\theta}{\alpha_1};\ p = (c_2 + a_2)h = r\omega;\ \sigma p = (c_2 - a_2)h = \sigma r\omega
\end{aligned}\right\} \quad (1b)$$

and:

θ = angle of incidence of incident wave;
h = thickness of reflecting plate;
μ = modulus of rigidity;
γ = density. (1c)

Except for ω and b, which have the same values in all three media, the letters without subscripts are to be given subscripts to correspond to the medium to which they refer, which are namely, 1, 2, 3 for the incident medium, the reflecting plate, and the transmitting medium respectively. All these media are supposed to be neither absorbing nor dispersive. The dependence of R on ω arises, of course, from the proportionality of p to ω according to the definitions of Eq. (1).

Supposing now that the longitudinal wave pulse impinging on the plate is defined by the function:

$$\left.\begin{aligned}
&\Phi = f(\rho);\ 0 \leqq \rho \leqq b\\
&\quad 0;\ \text{otherwise};\ \rho = t + s_i/v_1,
\end{aligned}\right\} \quad (2)$$

where Φ represents the amplitude of the pulse, s_i the distance from the origin to the phase plane ρ (cf. Fig. 1), the resultant wave system in the incident medium can be expressed as:

$$\left.\begin{aligned}
\Phi = &\frac{1}{2\pi}\int_{-\infty}^{+\infty} d\omega \int_0^b f(g)e^{-i\omega(g-\rho)}dg\\
&+ \frac{1}{2\pi}\int_{-\infty}^{+\infty} R(\omega)d\omega \int_0^b f(g)e^{-i\omega(g-\rho')}dg,
\end{aligned}\right\} \quad (3)$$

where $\rho' = t - (s_r/v_1)$, and s_r defines the phase planes of the reflected wave system. The latter is evidently represented by the second integral in Eq. (3), which we shall denote by Φ_r.

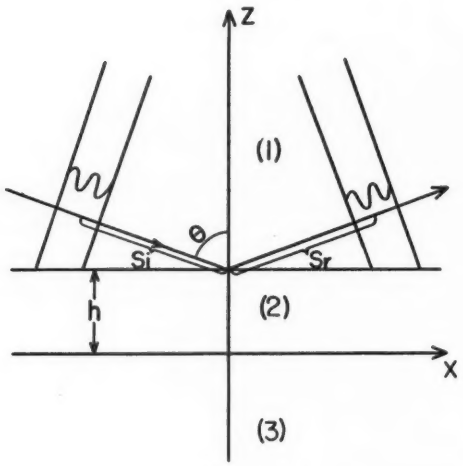

FIG. 1.

The incommensurability of p and σp in the $R(\omega)$ of Eq. (1), which arises from the presence of both longitudinal and transverse waves in the complete wave system, makes it impossible to evaluate the integrals of Φ_r directly. The nature of Φ_r can, however, be determined as follows: Denoting the numerator and denominators of $R(\omega)$ by N and Δ, respectively, they may be expressed as:

$$\left.\begin{aligned} \Delta(\omega) &= \Delta_0(\omega) + \Delta_1(\omega) \\ N(\omega) &= N_0(\omega) + N_1(\omega), \end{aligned}\right\} \tag{4}$$

where:

$$\left.\begin{aligned} &\Delta_0 = E - F\cos p - iH\sin p;\ N_0 = E' - F'\cos p - iH'\sin p; \\ &\Delta_1 = G\cos\sigma p + iJ\sin\sigma p;\ N_1 = G'\cos\sigma p + iJ'\sin\sigma p. \end{aligned}\right\} \tag{5}$$

$R(\omega)$ is then expanded as:

$$R(\omega) = \frac{N}{\Delta_0}\cdot\sum_0^\infty (-1)^n\left(\frac{\Delta_1}{\Delta_0}\right)^n. \tag{6}$$[2]

The subsequent evaluation of the integral Φ_r of Eq. (3) could then be carried through in principle in terms of a generalized Heaviside

[2] Although it is difficult to show generally that $|\Delta_1/\Delta_0| < 1$, it turns out that this inequality is actually satisfied for all numerical cases tested, except for the angles of total reflection. Of course, if for certain conditions $|\Delta_1/\Delta_0|$ exceeds 1 for all ω, the expansion of $R(\omega)$ can be made in terms of Δ_0/Δ_1, and the same analysis carried through with obvious modifications.

expansion over the poles of Δ_0, after a complex variable transformation of the infinite integral, taking note that the simple poles of Δ_0 would become nth order poles in the nth term of Eq. (6). The resulting double series—over n and the poles of Δ_0—would, however, be difficult to evaluate numerically and interpret physically. We shall, therefore, carry through the following method. Here we make the following expansions, which are obviously valid for *all* ω, due to the periodic character of N_0 and Δ_0:

$$\left.\begin{aligned} \frac{N_0(\omega)}{\Delta_0(\omega)} &= \sum b_m e^{-imr\omega}; \qquad \frac{1}{\Delta_0(\omega)} = \sum c_m e^{-imr\omega}; \\ \frac{N_0(\omega)}{\Delta_0^2(\omega)} &= \sum d_m e^{-imr\omega}; \qquad \frac{1}{\Delta_0^2(\omega)} = \sum e_m e^{-imr\omega}, \text{ etc.} \end{aligned}\right\} \tag{7}$$

Then to the order of $1/\Delta_0^2, \Phi_r$ will take the form:

$$\left.\begin{aligned} \Phi_r &= \frac{1}{2\pi} \sum_m \int_{-\infty}^{+\infty} d\omega \{ b_m + N_1 c_m - \Delta_1 d_m - N_1 \Delta_1 e_m + \cdots \} \\ &\quad \cdot \int_0^b f(g) e^{-i\omega(t-\rho'+mr)} dg \\ &\equiv \Phi_{r_0} + \Phi_{r_1} + \Phi_{r_2} + \Phi_{r_3} + \cdots, \end{aligned}\right\} \tag{8}$$

the terms Φ_{r_i} representing the resulting series with the coefficients b_m, c_m, etc. Recalling the definitions of N_1 and Δ_1 from Eq. (5), and the definition of the original pulse $f(\rho)$, the series Φ_{r_i} can be expressed as:

$$\Phi_{r_0} = \sum b_m f\left(t - \frac{s_r}{v_1} - mr \right). \tag{9}$$

$$\left.\begin{aligned} \Phi_{r_1} = \frac{1}{2} \sum c_m \Big[&(G' + J') f\left(t - \frac{s_r}{v_1} - mr + \sigma r \right) \\ &+ (G' - J') f\left(t - \frac{s_r}{v_1} - mr - \sigma r \right) \Big]. \end{aligned}\right\} \tag{10}$$

$$\left.\begin{aligned} \Phi_{r_2} = \frac{-1}{2} \sum d_m \Big[&(G + J) f\left(t - \frac{s_r}{v_1} - mr + \sigma r \right) \\ &+ (G - J) f\left(t - \frac{s_r}{v_1} - mr - \sigma r \right) \Big] \end{aligned}\right\} \tag{11}$$

$$\Phi_{r_3} = \frac{-1}{4} \sum e_m \Bigg[(G+J)(G'+J') f\left(t - \frac{s_r}{v_1} - mr + 2\sigma r \right) + 2(GG' - JJ') f\left(t - \frac{s_r}{v_1} - mr \right) + (G-J)(G'-J') f\left(t - \frac{s_r}{v_1} - mr - 2\sigma r \right) \Bigg]. \tag{12}$$

etc.

INTERPRETATION OF THE REFLECTED WAVE SYSTEM

Before entering into a detailed numerical discussion of these expressions it will be of interest to examine a little more closely their physical interpretation. Thus it is to be noted first that all the terms in these expressions represent reflected pulses of exactly the same *form* as the incident pulse, defined by Eq. (2). The composite reflected wave system therefore consists of a series of undistorted individual pulses having the same shape as that impinging on the reflecting plate. On the other hand, these individual pulses are of different amplitudes, determined by the coefficients b_m, $c_m \cdots G$, J, etc., and are mutually shifted in phase according to their arguments, except for the zero order terms—$f(t - s_r/v_1)$ in Φ_{r_0} and Φ_{r_3}—which represent the wave pulses reflected directly from the top face of the reflecting stratum. To see clearly the meaning of the phase shifts in the other terms, it is to be noted that:

$$r = h\left(\frac{\cos\theta_{t2}}{\beta_2} + \frac{\cos\theta_{12}}{\alpha_2} \right) \equiv \Delta t_3, \tag{13}$$

is the time excess of a wave traveling in the plate along the Δt_3 path (cf. Fig. 2) to reach the plane s_r over that taken by the directly reflected wave, θ_{t2}, θ_{12} being the angles with the vertical of the transverse and longitudinal waves within the plate. Hence the terms $f[t - (s_r/v_1) - mr]$ are due to wave pulses which have suffered $2m-1$ internal reflections and whose paths in the interior of the reflecting layer have been composed of an equal number of longitudinal and transverse wave segments. On the other hand:

$$r + \sigma r = \frac{2h\cos\theta_{t2}}{\beta_2} \equiv \Delta t_2, \tag{14}$$

is the time lag, per internal reflection, behind the directly reflected

wave of a pulse traveling in the interior of the plate entirely as a transverse wave. The terms $f[t-(s_r/v_1)-r-\sigma r]$ are therefore due to waves suffering one internal reflection, the whole path in the interior of the plate being traveled as a transverse wave, while the

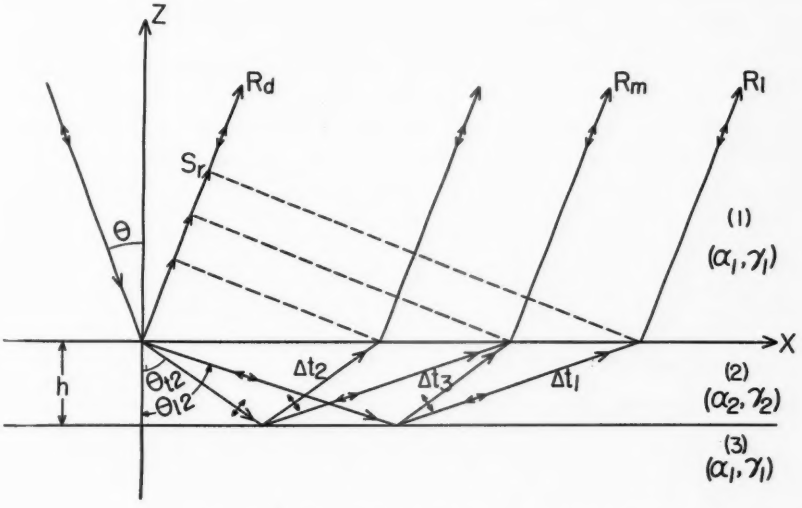

FIG. 2. Types of paths within a reflecting plate upon which is incident a longitudinal wave pulse.

$f[t-(s_r/v_1)-mr-\sigma r]$ terms represent waves like $f[t-(s_r/v_1)-r-\sigma r]$ but with $m-1$ additional internal reflections of the type Δt_3.

In a similar manner it follows that:

$$r-\sigma r=\frac{2h\cos\theta_{12}}{\alpha_2}\equiv\Delta t_1. \tag{15}$$

is the time lag per internal reflection for waves traveling in the plate entirely as longitudinal waves. Such a wave with a single internal reflection is represented by $f[t-(s_r/v_1)-r+\sigma r]$, while those with $m-1$ additional reflections of the Δt_3 type are given by $f[t-(s_r/v_1)-mr+\sigma r]$.

Finally, the more general terms as $f[t-(s_r/v_1)\pm n\sigma r-mr)]$ correspond to waves which have spent within the plate n time intervals of the type Δt_1 or Δt_2 and $m-n$ intervals of the type Δt_3.

It is thus seen that the wave theory treatment developed here automatically resolves the reflected wave system into the various

individual reflection and refraction processes. Moreover, it gives in a single step the resultant reflection coefficients—the a_m, b_m, etc.—for the different types of pulses. At the same time it confirms the generally assumed hypothesis that these reflected pulses are of exactly the same form as the incident pulse even in the present case where both longitudinal and transverse waves traverse the system.

That the expansion of Eq. (6) does give a physical separation between the various orders of multiple reflections which the emerging pulses must undergo within the plate, follows from a consideration of the effect of the general term $N\Delta_1^n/\Delta_0^{n+1}$. Making the same type of Fourier series expansions as used in Eq. (7), this term will clearly give rise to an expansion as:

$$\frac{N\Delta_1^n}{\Delta_0^{n+1}} = \Delta_1^n \sum g_m e^{-im r\omega} + N_1 \Delta_1^n \sum h_m e^{-im r\omega}. \tag{16}$$

Now it may be readily shown that:

$$g_m = 0 : m < n; \qquad h_m = 0 : m < n + 1. \tag{17}$$

The leading terms in Φ_r which Eq. (16) will contribute will, therefore, be:

$$\left.\begin{aligned} & g_n f\left(t - \frac{s_r}{v_1} - nr \pm mr\sigma\right) \\ & \quad + h_{n+1} f\left(t - \frac{s_r}{v_1} - (n+1)r \pm (m+1)r\sigma\right), \quad m \leqq n. \end{aligned}\right\} \tag{18}$$

These will remain zero until:

$$t \geqq \frac{s_r}{v_1} + nr \pm mr\sigma, \tag{19}$$

the excess over s_r/v_1 representing the time required for a wave to travel in the reflecting plate $n-m$ path elements of the type Δt_3 (cf. Fig. 2) and m of type Δt_1 or Δt_2, that is n elements of all types, involving $2n-1$ internal reflections.

The expansion of Eq. (16) therefore does separate the reflected wave system according to the number of internal reflections preceding the emergence of the various wave pulses. In particular, the first n terms of the series will give all the reflected pulses which have suffered less than $2n-1$ internal reflections within the reflecting plate. Since

each internal reflection adds to the attenuation of the wave when it finally leaves the reflecting plate, the type of expansion used here will at the same time give successively decreasing amplitudes of the resultant wave system as the higher order terms are evaluated.

NUMERICAL APPLICATIONS

In order to effect a numerical evaluation of the series of Eqs. (9)–(12), explicit expressions must be derived for the coefficients b_m, $c_m \cdots$ etc. These may be shown to be given by the following relations:

$$\left.\begin{aligned}
b_m &= -\frac{(F'-H')}{2}c_{m-1} + E'c_m - \frac{(F'+H')}{2}c_{m+1};\ m \geqq 0 \\
c_m &= \frac{1}{\sqrt{E^2-F^2+H^2}}(r_2{}^m - r_1{}^m);\ m > 0;\ c_0 = 0 \\
r_2 &= \frac{E-\sqrt{E^2-F^2+H^2}}{F+H};\quad r_1 = \frac{E+\sqrt{E^2-F^2+H^2}}{F+H} \\
d_m &= -\frac{(F'-H')}{2}e_{m-1} + E'e_m - \frac{(F'+H')}{2}e_{m+1};\ m > 0 \\
e_m &= \frac{1}{E^2-F^2+H^2}[Ec_m + m(r_2{}^m + r_1{}^m)];\ m \geqq 2;\ e_0 = e_1 = 0.
\end{aligned}\right\} \quad (20)$$

The actual values of the first few non-vanishing members of these constants are given by:

$$\left.\begin{aligned}
b_0 &= \frac{F'+H'}{F+H};\quad b_1 = \frac{2}{F+H}\left[-E' + E\frac{(F'+H')}{F+H}\right]; \\
b_2 &= \frac{F'-H'}{F+H} - \frac{4EE'}{(F+H)^2} + \frac{(F'+H')(4E^2-F^2+H^2)}{(F+H)^3}; \\
c_1 &= \frac{-2}{F+H};\quad c_2 = \frac{-4E}{(F+H)^2};\quad c_3 = \frac{-2}{(F+H)^3}[4E^2-F^2+H^2]; \\
d_1 &= \frac{-2(F'+H')}{(F+H)^2};\quad d_2 = \frac{4}{(F+H)^2}\left[E' - 2E\frac{(F'+H')}{F+H}\right]; \\
e_2 &= \frac{4}{(F+H)^2};\quad e_3 = \frac{16E}{(F+H)^3}.
\end{aligned}\right\} \quad (21)$$

For strictly numerical purposes we shall confine our discussion to the three strongest reflected pulses, which are: that directly reflected,

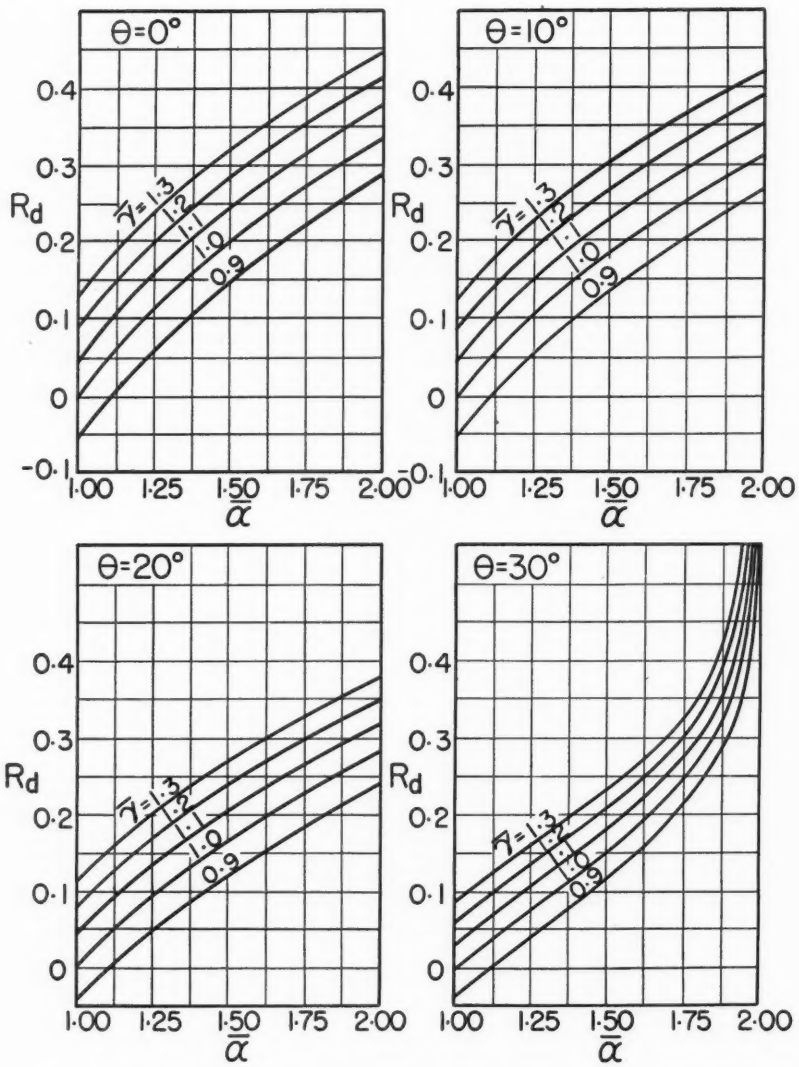

FIG. 3. Dilatation amplitudes, R_d, of the waves directly reflected from the upper face of a stratum embedded in a homogeneous elastic medium; θ=angle of incidence; $\bar{\alpha}=\alpha_2/\alpha_1$=(velocity in stratum)/(velocity above stratum) for longitudinal waves; $\bar{\gamma}=\gamma_2/\gamma_1$=(density in stratum)/(density above stratum).

that traveling in the plate as a "mixed" pulse, following the Δt_3 path (Fig. 2), and that traveling in the plate entirely as a longitudinal wave, i.e., along Δt_1, each of the latter suffering only one internal reflection. Denoting these pulses by R_d, R_m, R_1 respectively, their amplitudes are given by:

$$\left.\begin{aligned} R_d &= b_0 = \frac{(F' + H')}{(F + H)};\ R_m = b_1 = -\frac{2}{F + H}\,[E' - ER_d] \\ R_1 &= 1/2\,[c_1(G' + J') - d_1(G + J)] \\ &= \frac{1}{F + H}\,[(G + J)R_d - G' - J']. \end{aligned}\right\} \quad (22)$$

The values of these amplitudes have been calculated for the case where the medium below the reflecting stratum is identical with the incident medium, for angles of incidence between 0 and 30°, in steps of 5°, velocity ratio of velocity in plate to incident medium, $\bar{\alpha}$, of 1.0 to 2.0 in steps of 0.25, and density ratio, $\bar{\gamma}$, of 0.9 to 1.3 in steps of 0.1. The Poisson ratio was assumed to be 0.25 throughout, so that $\alpha_1/\beta_1 = \alpha_2/\beta_2 = \sqrt{3}$. Because of the accuracy of these calculations, it is felt worth recording them in tabular as well as graphical form. They are given in Tables I to III. They are plotted for several of the individual values of θ in Figs. 3–5. as functions of the velocity ratio $\bar{\alpha}$. A composite representation is given in Fig. 6. As the three pulses will arrive at the recorder at different times, they will give, in effect, a "time spectrum." In Fig. 6 the triplet groups of the three pulses are plotted horizontally against the angle of incidence and shifted vertically for the different velocity ratios, the density ratio being the same for each vertical section. Although these plots are of necessity of lesser accuracy than those of Figs. 3–5, they have the advantage of giving a composite picture of both the individual pulse amplitude variations and their interactions and relative variations as the fundamental variables θ, $\bar{\alpha}$, and $\bar{\gamma}$ are systematically changed. The first member of the "triplet" represents the value of R_d, the second of R_1, and the third of R_m. Their shifts along θ has no significance, and were made only to separate the lines and avoid overlapping.

We shall not enter here into a detailed discussion of all the various features of these curves. It will suffice for our purposes to restrict ourselves to the smaller angles of incidence which are of most practical interest, at least from the point of view of reflection shooting. For

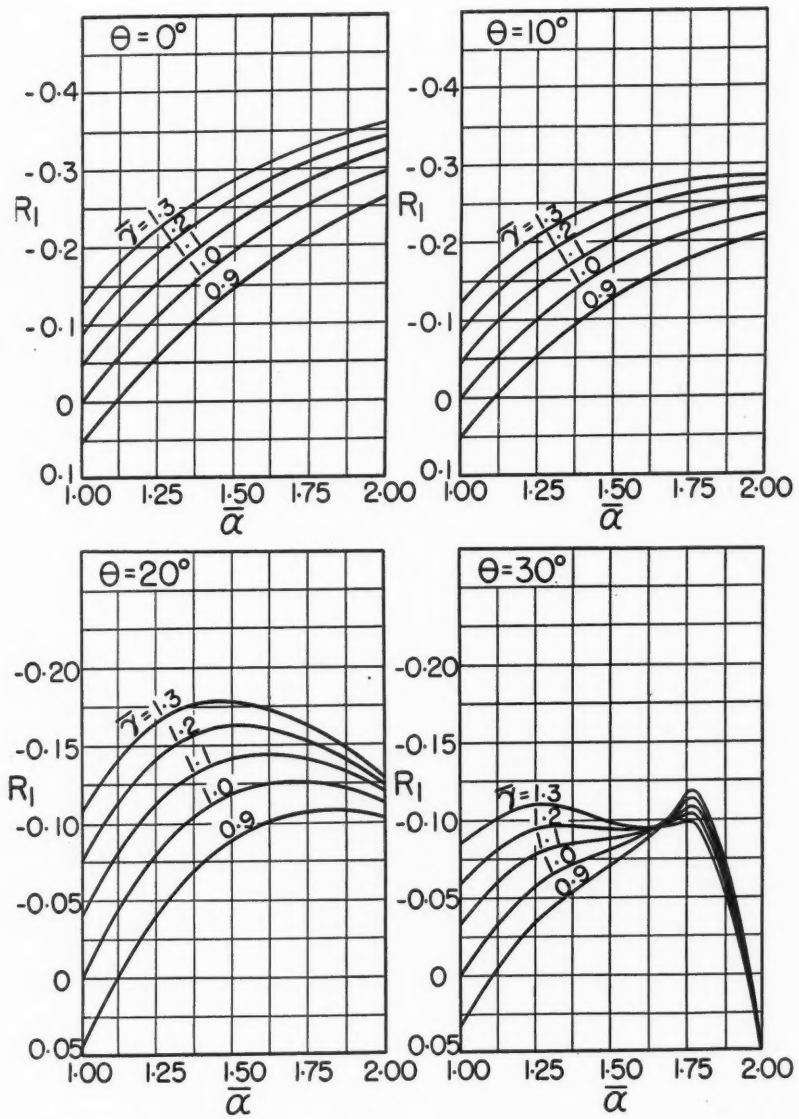

FIG. 4. Dilatation amplitudes, R_1 of the waves reflected from a stratum embedded in a homogeneous elastic medium after suffering a single internal reflection and traveling within the stratum as longitudinal waves; θ, $\bar{\alpha}$, $\bar{\gamma}$ as in Fig. 3.

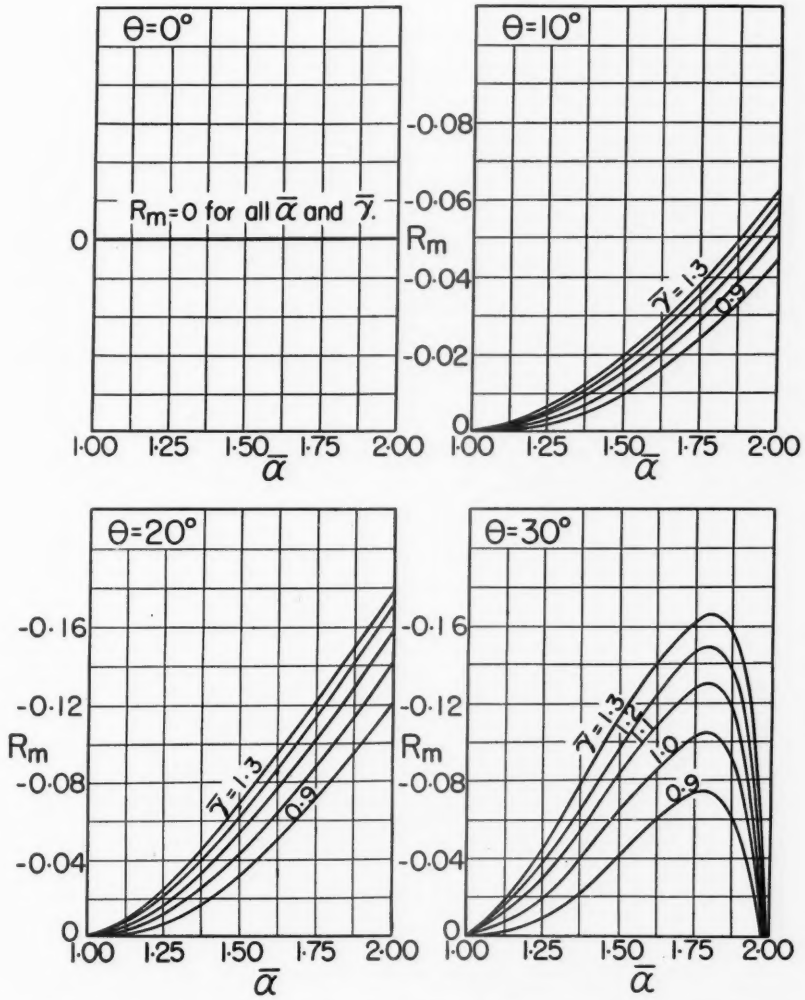

FIG. 5. Dilatation amplitudes, R_m, of the waves reflected from a stratum embedded in a homogeneous elastic medium after suffering a single internal reflection and traveling within the stratum partly as longitudinal and partly as transverse waves; θ, $\bar{\alpha}$, $\bar{\gamma}$ as in Fig. 3.

these angles the curves of Figs. 3–6 reveal the following properties of the various reflected pulses:

1. For $\bar{\alpha}\bar{\gamma} > 1$, R_d is of the same phase[3] as the incident wave, while R_1 is of opposite phase; for $\bar{\alpha}\bar{\gamma} < 1$, the phases of R_d and R_1 are reversed. R_m is always of opposite phase to the incident wave except for the case of total reflection ($\bar{\alpha} = 2.0$, $\theta = 30°$).

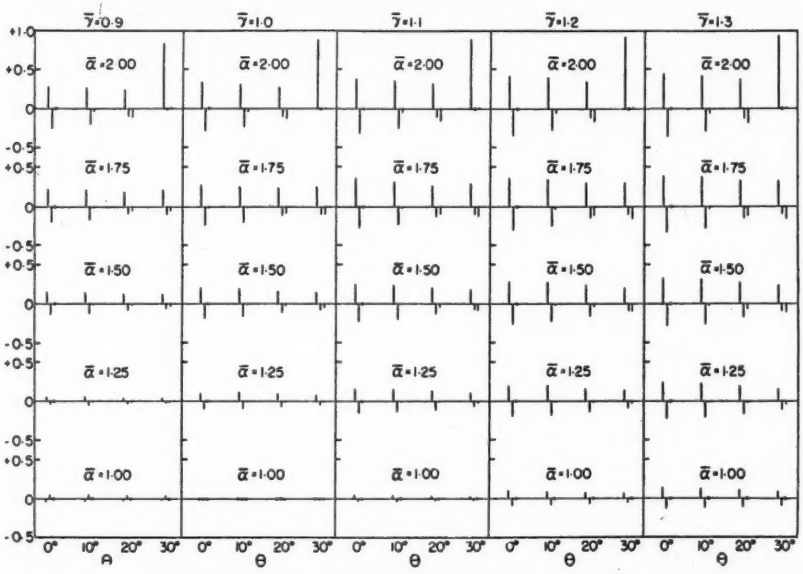

FIG. 6. Composite dilatation amplitude "spectrum" of waves reflected from a stratum embedded in a homogeneous elastic medium; left member of "triplet" is R_d, central member is R_1, right member is R_m (cf. Figs. 3, 4, 5); θ, $\bar{\alpha}$, $\bar{\gamma}$ as in Fig. 3.

2. All three wave amplitudes R_d, R_1, R_m increase algebraically as $\bar{\alpha}$ or $\bar{\gamma}$ is increased.

3. R_d and R_1 decrease slowly in numerical value with increasing θ, while R_m decreases from a vanishing value as θ increases from 0.

4. For the special case of normal incidence, R_d, R_1, R_m are given by the expressions:

$$R_d = \frac{\bar{\alpha}\bar{\gamma} - 1}{\bar{\alpha}\bar{\gamma} + 1}; \qquad R_1 = \frac{-4\bar{\alpha}\bar{\gamma}(\bar{\alpha}\bar{\gamma} - 1)}{(\bar{\alpha}\bar{\gamma} + 1)^3}; \qquad R_m = 0. \tag{23}$$

Finally, it is of interest to make an application of the above results to a specific case of a pulse reflection problem. For this purpose an

[3] By "phase," as used here, we mean essentially the sign of the value of dilatation Φ, a postive Φ implying a rarefaction wave and a negative Φ a condensation.

TABLE I[4]

DILATATION AMPLITUDES, R_d, OF THE WAVES DIRECTLY REFLECTED FROM THE UPPER FACE OF A STRATUM EMBEDDED IN A HOMOGENEOUS ELASTIC MEDIUM

$R_d=(F'+H')/(F+H)$

θ	γ_2/γ_1	$\alpha_2/\alpha_1=1.00$	1.25	1.50	1.75	2.00
0°	0.9	−0.0526	0.0588	0.1489	0.2233	0.2857
	1.0	0	0.1111	0.2000	0.2728	0.3333
	1.1	0.0476	0.1579	0.2453	0.3163	0.3750
	1.2	0.0909	0.2000	0.2857	0.3549	0.4118
	1.3	0.1304	0.2381	0.3220	0.3893	0.4444
5°	0.9	−0.0521	0.0579	0.1468	0.2202	0.2815
	1.0	0	0.1097	0.1974	0.2692	0.3294
	1.1	0.0471	0.1560	0.2422	0.3123	0.3701
	1.2	0.0900	0.1977	0.2823	0.3506	0.4067
	1.3	0.1291	0.2355	0.3183	0.3847	0.4390
10°	0.9	−0.0505	0.0553	0.1407	0.2111	0.2700
	1.0	0	0.1056	0.1898	0.2587	0.3160
	1.1	0.0457	0.1506	0.2335	0.3007	0.3564
	1.2	0.0873	0.1911	0.2724	0.3380	0.3919
	1.3	0.1253	0.2278	0.3075	0.3714	0.4236
15°	0.9	−0.0479	0.0514	0.1316	0.1978	0.2537
	1.0	0	0.0991	0.1784	0.2433	0.2976
	1.1	0.0434	0.1419	0.2200	0.2834	0.3362
	1.2	0.0829	0.1805	0.2572	0.3190	0.3702
	1.3	0.1190	0.2154	0.2906	0.3509	0.4005
20°	0.9	−0.0444	0.0470	0.1194	0.1843	0.2398
	1.0	0	0.0913	0.1652	0.2266	0.2807
	1.1	0.0402	0.1311	0.2038	0.2639	0.3165
	1.2	0.0769	0.1670	0.2384	0.2972	0.3481
	1.3	0.1104	0.1995	0.2696	0.3269	0.3763
25°	0.9	−0.0400	0.0433	0.1139	0.1799	0.2542
	1.0	0	0.0833	0.1533	0.2179	0.2903
	1.1	0.0364	0.1193	0.1883	0.2515	0.3218
	1.2	0.0695	0.1519	0.2197	0.2814	0.3496
	1.3	0.0999	0.1814	0.2480	0.3081	0.3742
30°	0.9	−0.0350	0.0423	0.1170	0.2157	0.8479
	1.0	0	0.0774	0.1513	0.2481	0.8791
	1.1	0.0318	0.1090	0.1818	0.2765	0.9042
	1.2	0.0609	0.1375	0.2091	0.3015	0.9245
	1.3	0.0876	0.1635	0.2337	0.3239	0.9409

[4] The individual values of the constants E', F', $\cdots$ H, J, in the general reflection coefficient of Eq. (1) require too much space for complete reproduction here. Even more complete tables of R_d, giving the "single interface reflection coefficient," will be published in a forthcoming paper, together with the reflection coefficients for the transverse waves and the refraction coefficients for both types of waves.

TABLE II

DILATATION AMPLITUDES, R_1, OF THE WAVES REFLECTED FROM A STRATUM EMBEDDED IN A HOMOGENEOUS ELASTIC MEDIUM AFTER SUFFERING A SINGLE INTERNAL REFLECTION AND TRAVELING WITHIN THE STRATUM AS LONGITUDINAL WAVES

$$R_1=\{(G+J)R_d-G'-J'\}/\{F+H\}$$

θ	γ_2/γ_1	$\alpha_2/\alpha_1=1.00$	1.25	1.50	1.75	2.00
0°	0.9	0.0525	−0.0586	−0.1456	−0.2122	−0.2624
	1.0	0	−0.1097	−0.1920	−0.2524	−0.2963
	1.1	−0.0475	−0.1540	−0.2305	−0.2846	−0.3223
	1.2	−0.0902	−0.1920	−0.2624	−0.3102	−0.3420
	1.3	−0.1282	−0.2246	−0.2886	−0.3303	−0.3567
5°	0.9	0.0520	−0.0573	−0.1412	−0.2035	−0.2481
	1.0	0	−0.1076	−0.1864	−0.2424	−0.2810
	1.1	−0.0470	−0.1511	−0.2240	−0.2734	−0.3052
	1.2	−0.0892	−0.1885	−0.2551	−0.2981	−0.3240
	1.3	−0.1269	−0.2205	−0.2807	−0.3175	−0.3378
10°	0.9	0.0504	−0.0535	−0.1287	−0.1789	−0.2087
	1.0	0	−0.1014	−0.1705	−0.2136	−0.2363
	1.1	−0.0456	−0.1427	−0.2053	−0.2413	−0.2575
	1.2	−0.0865	−0.1781	−0.2339	−0.2633	−0.2735
	1.3	−0.1229	−0.2086	−0.2576	−0.2806	−0.2854
15°	0.9	0.0478	−0.0480	−0.1102	−0.1435	−0.1539
	1.0	0	−0.0916	−0.1466	−0.1715	−0.1739
	1.1	−0.0433	−0.1294	−0.1767	−0.1937	−0.1892
	1.2	−0.0820	−0.1618	−0.2015	−0.2114	−0.2006
	1.3	−0.1166	−0.1896	−0.2219	−0.2252	−0.2091
20°	0.9	0.0444	−0.0416	−0.0876	−0.1065	−0.1028
	1.0	0	−0.0804	−0.1186	−0.1255	−0.1127
	1.1	−0.0401	−0.1128	−0.1424	−0.1404	−0.1198
	1.2	−0.0759	−0.1411	−0.1620	−0.1522	−0.1249
	1.3	−0.1079	−0.1652	−0.1781	−0.1612	−0.1284
25°	0.9	0.0401	−0.0362	−0.0729	−0.0849	−0.0981
	1.0	0	−0.0677	−0.0928	−0.0928	−0.0947
	1.1	−0.0361	−0.0948	−0.1090	−0.0986	−0.0911
	1.2	−0.0684	−0.1179	−0.1222	−0.1028	−0.0874
	1.3	−0.0972	−0.1376	−0.1329	−0.1112	−0.0836
30°	0.9	0.0351	−0.0344	−0.0717	−0.1186	0
	1.0	0	−0.0582	−0.0811	−0.1137	0
	1.1	−0.0317	−0.0785	−0.0885	−0.1085	0
	1.2	−0.0598	−0.0957	−0.0941	−0.1032	0
	1.3	−0.0848	−0.1103	−0.0983	−0.0979	0

incident longitudinal unit amplitude wave pulse was chosen, defined by the function:

$$\left.\begin{aligned} f(\delta) &= 14(\delta - 1/2)e^{-36(\delta-1/2)^2};\ 0 \leqq \delta \leqq 1 \\ &= 0 \text{ otherwise.} \end{aligned}\right\} \qquad (24)$$

The medium below the reflecting plate was taken to be the same as the incident medium, the velocity contrast for the plate, $\bar{\alpha}$, was chosen as 2.0, the density contrast, $\bar{\gamma}$, as 1.2, and the angle of incidence as 10°. The reflected wave system, determined by Eqs. (9) to (12) and

TABLE III

DILATATION AMPLITUDES, R_m, OF THE WAVES REFLECTED FROM A STRATUM EMBEDDED IN A HOMOGENEOUS ELASTIC MEDIUM AFTER SUFFERING A SINGLE INTERNAL REFLECTION AND TRAVELING WITHIN THE STRATUM PARTLY AS LONGITUDINAL AND PARTLY AS TRANSVERSE WAVES

$$R_1 = -2E' - ER_d/F + H$$

θ	γ_2/γ_1	$\alpha_2/\alpha_1 = 1.00$	1.25	1.50	1.75	2.00
0°	0.9	0	0	0	0	0
	1.0	0	0	0	0	0
	1.1	0	0	0	0	0
	1.2	0	0	0	0	0
	1.3	0	0	0	0	0
5°	0.9	−0.0000	−0.0004	−0.0025	−0.0064	−0.0120
	1.0	0	−0.0008	−0.0033	−0.0076	−0.0136
	1.1	−0.0000	−0.0011	−0.0040	−0.0087	−0.0148
	1.2	−0.0000	−0.0014	−0.0046	−0.0095	−0.0158
	1.3	−0.0000	−0.0017	−0.0051	−0.0102	−0.0166
10°	0.9	−0.0000	−0.0016	−0.0096	−0.0240	−0.0442
	1.0	0	−0.0031	−0.0128	−0.0288	−0.0504
	1.1	−0.0000	−0.0044	−0.0155	−0.0328	−0.0553
	1.2	−0.0001	−0.0056	−0.0178	−0.0361	−0.0591
	1.3	−0.0002	−0.0067	−0.0198	−0.0387	−0.0622
15°	0.9	−0.0001	−0.0034	−0.0198	−0.0483	−0.0862
	1.0	0	−0.0066	−0.0266	−0.0586	−0.0992
	1.1	−0.0001	−0.0095	−0.0325	−0.0671	−0.1095
	1.2	−0.0002	−0.0121	−0.0376	−0.0740	−0.1176
	1.3	−0.0004	−0.0144	−0.0419	−0.0797	−0.1239
20°	0.9	−0.0001	−0.0054	−0.0306	−0.0719	−0.1206
	1.0	0	−0.0108	−0.0422	−0.0888	−0.1414
	1.1	−0.0001	−0.0157	−0.0521	−0.1028	−0.1580
	1.2	−0.0003	−0.0201	−0.0605	−0.1142	−0.1710
	1.3	−0.0007	−0.0241	−0.0677	−0.1235	−0.1775
25°	0.9	−0.0002	−0.0070	−0.0392	−0.0848	−0.1235
	1.0	0	−0.0150	−0.0559	−0.1085	−0.1514
	1.1	−0.0001	−0.0223	−0.0701	−0.1265	−0.1736
	1.2	−0.0005	−0.0288	−0.0823	−0.1440	−0.1910
	1.3	−0.0010	−0.0346	−0.0926	−0.1569	−0.2048
30°	0.9	−0.0002	−0.0077	−0.0412	−0.0739	0.0239
	1.0	0	−0.0185	−0.0631	−0.1032	0.0203
	1.1	−0.0002	−0.0282	−0.0816	−0.1271	0.0173
	1.2	−0.0006	−0.0370	−0.0948	−0.1466	0.0148
	1.3	−0.0013	−0.0447	−0.1106	−0.1624	0.0127

(20), (21), was then calculated for plate thickness equal to 2, 1 and $\frac{1}{2}$ times the length of the pulse.

The resultant wave amplitudes for these three cases are plotted in Figs. 7, 8, and 9 as a function of $\alpha_1\delta$, which is proportional to the distance from the front of the pulse measured in the direction of emergence of the reflected wave system, the incident pulse length

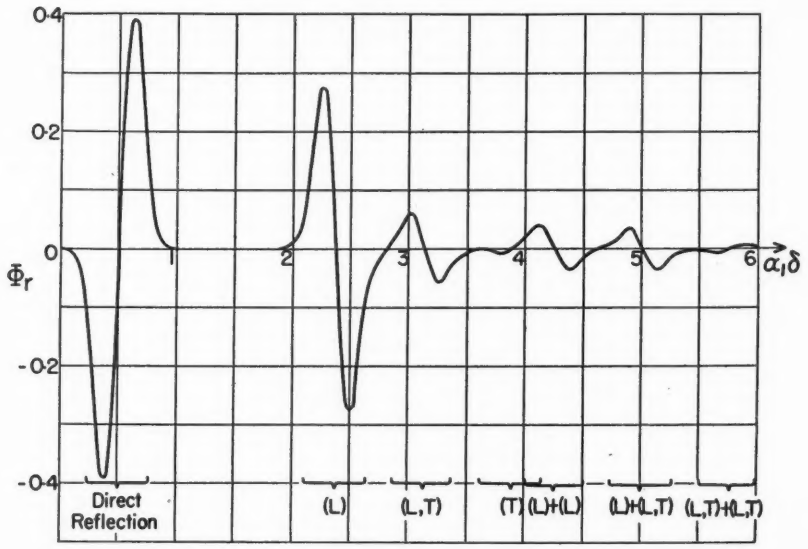

FIG. 7. Dilatation amplitudes of the reflected waves excited by incidence at 10° of a unit amplitude pulse of length equal to $\frac{1}{2}$ of reflecting stratum thickness; (velocity in stratum)/(velocity above stratum) = 2.0; (density in stratum)/(density above stratum) = 1.2. (L) represents the R_1 pulse, (L,T) the R_m pulse, (T) the pulse with one internal reflection and traveling within the plate as a transverse wave so as to have a time lag Δt_2, $(L)+(L)$ the pulse with three internal reflections and time lag $2\Delta t_1$, $(L)+(L,T)$ that with time lag $\Delta t_1+\Delta t_3$, $(L,T)+(L,T)$ that with time lag $2\Delta t_3$, and $(T)+(L,T)$ that with time lag $\Delta t_2+\Delta t_3$ (cf. Fig. 2).

being unity on this scale.[5] The shape of the incident pulse is indicated by the wave marked "direct reflection" in Fig. 7, although its actual

[5] A great number of reflected wave system diagrams such as shown in Figs. 7, 8, and 9 have been previously published in an extended series of lengthy papers by K. Sezawa and K. Kanai and their collaborators, in the Bulletins of the Earthquake Research Institute beginning with Vol. 8, 1930. In these papers are also given the wave theory treatments for both continuous and finite wave trains for a number of reflecting systems, including various types of boundary conditions at the interfaces. In the study of the pulse reflection problems, however, these authors have restricted themselves to

amplitude before impinging upon the plate was unity rather than 0.39. The contributions to the reflected wave system due to the various types of individual wave pulses discussed above are indicated by the notations at the bottoms of Figs. 7, 8, and 9. In particular, (L) represents the R_1 wave with a time lag Δt_1, (L,T) the R_m wave of time lag Δt_3, (T) the pulse with one internal plate reflection and

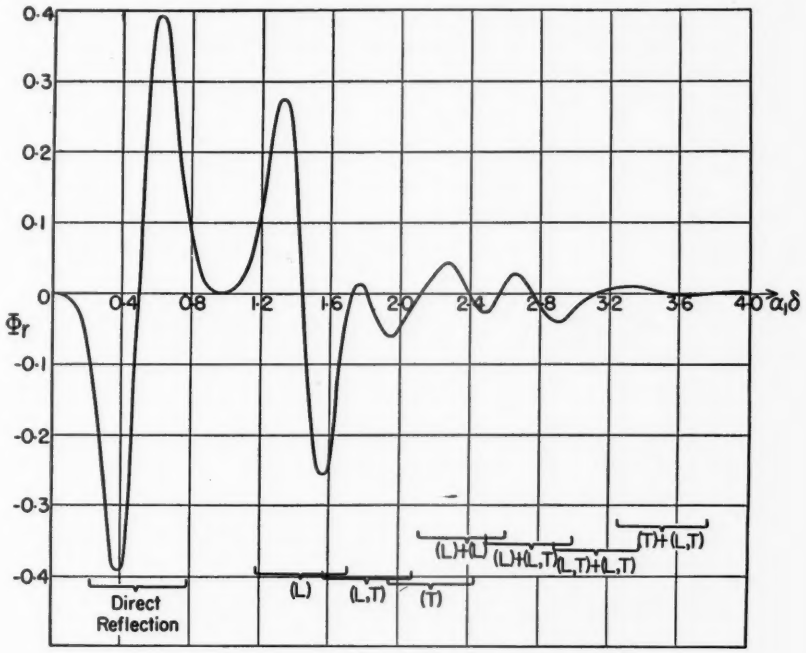

FIG. 8. Dilatation amplitudes under conditions as in Fig. 7 but with a pulse length equal to the reflecting stratum thickness.

traveling in its interior as a transverse wave so as to have a time lag Δt_2, $(L)+(L)$ the pulse with three internal reflections and time

pulse forms of sinusoidal or error function character and carried the analysis through for these cases without recognizing or pointing out the generality of the solutions such as represented by the Eqs. (9) to (12) above. Moreover, the general resolution of the reflected wave system following from the expansion of the reflection coefficient as in Eq. (6) and the subsequent developments through Eq. (19) above were not brought out in these papers. Finally no systematic tabulation of the reflection coefficients, such as given here in Tables I to III and Figs. 3 to 6 for the various types of pulses, was included in these discussions.

lag $2\Delta t_1$, $(L)+(L,T)$ the pulse with time lag $\Delta t_1+\Delta t_3$, $(L,T)+(L,T)$ that with time lag $2\Delta t_3$, and finally $(T)+(L,T)$ that with time lag $\Delta t_2+\Delta t_3$. A more detailed interpretation of these waves will be clear by reference to Fig. 2.

The tendency for the development of mutual overlapping in a reflected wave system as the plate thickness decreases in comparison to the incident pulse thickness and consequent distortion of the

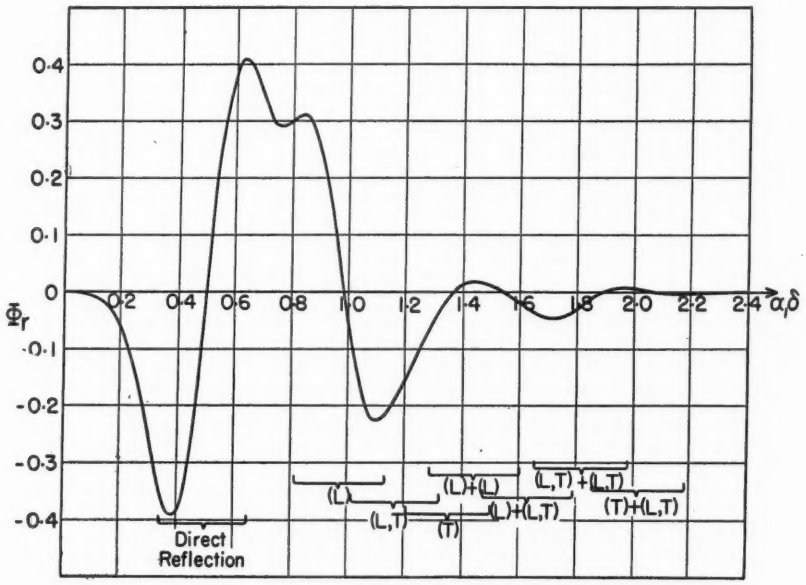

FIG. 9. Dilatation amplitudes under conditions as in Fig. 7 but with a pulse length equal to twice the reflecting stratum thickness.

resultant reflected wave system is to be noted. In fact, the most interesting conclusion to be drawn from these curves seems to lie in the observation of the pronounced amplitudes possible for the first internally reflected wave, and hence its ability to appreciably distort and mask the direct reflections to almost any arbitrary shape if the reflecting beds are thin enough.

Further applications of these considerations and methods will be obvious to the reader.

The author is indebted to Mr. M. W. Meres for carrying through the numerical calculations presented in this paper, and to Drs. P.D Foote and E. A. Eckhardt for permission to publish it.

SEISMIC EXPLORATION IN EASTERN VENEZUELA*

W. R. RANSONE†

ABSTRACT

A map and cross-section are presented to give a brief and generalized idea of the area. A limited discussion of the geology and physiography is given. Working conditions are discussed with their particular relations with physiography, climate and state of development of the country. Emphasis is placed on Anzoategui because of the amount of work done in that area.

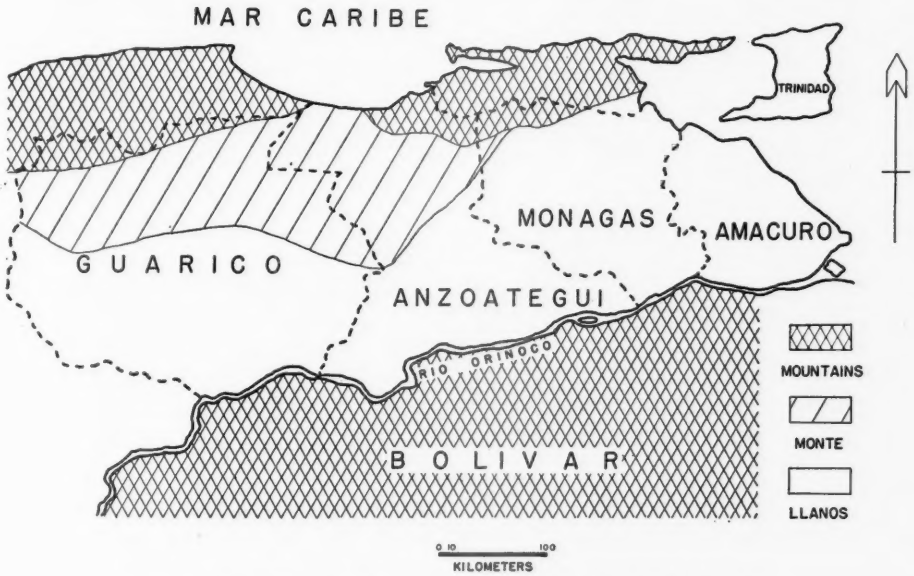

FIG. 1. Simplified map of eastern Venezuela, showing physiographic and geologic provinces. After Liddle.

INTRODUCTION

The rising tide of geophysical activity in eastern Venezuela is making this an area of increasing interest to the exploration geophysicist. This area, lying wholly within the Tropic Zone, has features which make it possible to carry on seismic prospecting at a high production rate. For these reasons it is thought that a brief discussion of this little known region is merited at this time.

* Read at the Fall meeting, Houston, Texas, Nov. 19, 1937.

† Geophysical Service, Inc., Dallas, Texas.

GEOLOGY AND PHYSIOGRAPHY

Referring to the map, Fig. 1, it may be seen at once that the geology and physiography are very directly related and that both may be illustrated in a very simple fashion. The cross-hatched portions in the north and south represent mountainous areas. In the south, beginning at the Orinoco river, are the Guayana highlands formed of a complex igneous mass, part of the old Brazilian shield. To the n orth lie the Maritime Andes, a highly folded and faulted system, with an

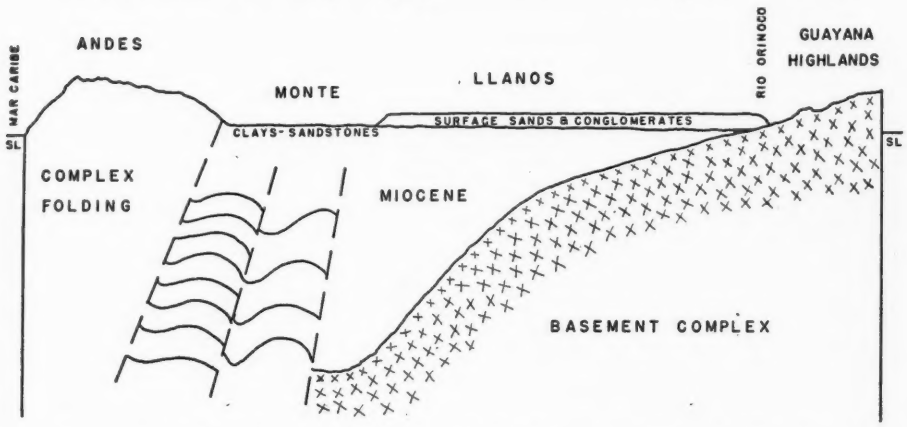

FIG. 2. A north-south cross-section through the State of Anzoategui. After Kaye.

igneous core in part, and flanked to the south by successively less metamorphosed and folded sedimentaries.

Between these two great highlands lies a broad structural and physiographic basin. The structure of this basin is illustrated in the cross-section of the State of Anzoategui. The gently north dipping basement complex changing very suddenly into steep folds presents again the asymmetry so often found in Tertiary basins. The depth and contours of the basement and its overlying sediments, and the folds in the north have engendered problems for the seismographer.

The surface of this great basis is a broad rolling plain, called by the Venezuelan "llanos." This basin may also be divided into two portions both topographically and geologically. The southern part, shown on the map in white, is the true "llanos" and is a series of mesas of nearly equal elevation which are separated by the streams which flow southward into the Orinoco river or eastwards into the Atlantic ocean. These mesas and plains are formed of Pleistocene gravels and sands which have been held together as conglomerates

by ferruginous cements. This cementing effect appears to have been caused by the upward percolation of ground waters as the cementing is always more complete at the surface. As a result of this sandy, well drained soil, few trees grow on the "llanos," except in the river courses; and transportation by car or truck is both rapid and easy. The streams themselves are usually without water in the dry season, and may be crossed without bridges as may be seen in the picture.

FIG. 3. Trucks carrying seismic equipment crossing stream in northwestern Anzoategui.

In the northern portion of the basin in the area indicated by cross-lines on the map, Miocene clays and sandstones outcrop, and as a result, topography is rougher, and the terrain is covered with brush and trees. This type of country is called "monte" by the Venezuelan as is called the same type of country in southwest Texas and Mexico. Transportation is somewhat difficult in the "monte" and a "pica" or pathway must usually be cleared before trucks can pass.

The transition from the "llanos" to the "monte" country is often abrupt and results in sharp escarpments facing north. A typical example of this is in the State of Anzoategui, near the town of Cantaura. A glance at the cross-section will show the transition point

FIG. 4. A partly constructed camp in the "monte."

FIG. 5. A view of the "llanos" with irregular mesas in the distance. The trees are Palm and Chaparro.

with the conglomerates and sands of the mesa sloping gently to the south away from the escarpment.

In the extreme east the plains gradually merge into the swamps and distributaries of the great Orinoco delta. Here transportation must be accomplished by boat.

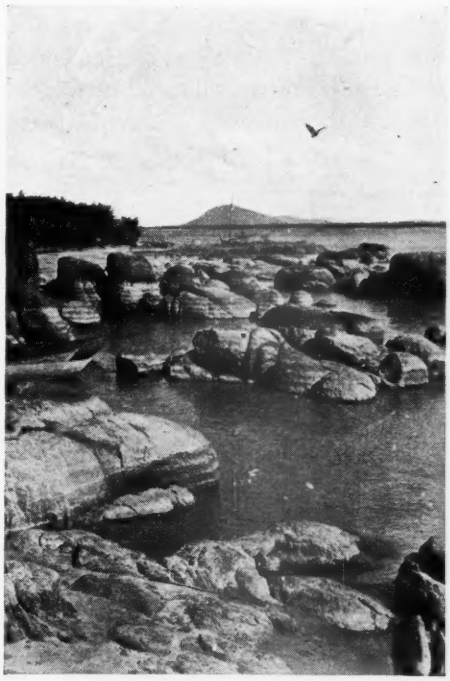

FIG. 6. Looking southeast across the Rio Orinoco with Guayana Highlands in the distance. The rocks in the foreground are igneous, the bands being silt deposited by the river at different stages.

WORKING CONDITIONS

As previously pointed out the absence of true tropical jungle and the ability to drive over considerable distances without roads or bridges are important advantages in seismic exploration in eastern Venezuela. On the other hand the sparseness of civilization and the poorness of the country itself necessitate maintaining each field crew in temporary camps. Beyond the bringing into the camp of supplies from a usually distant town, each camp must be a self-sufficient unit with transportation and mechanical facilities in addition to living

equipment and a good backlog of canned foodstuffs. All the various equipment is, of course, in portable form.

Health conditions can be good if proper care is taken. The local populace being malarial and generally diseased makes health rule number one to avoid all towns in selecting campsites. The next most important rule is to boil and filter all drinking water. Beyond these a few simple remedies appear to take care of most ills.

Climatic conditions are especially good considering the latitude which is 9°N. in the center of the "llanos" belt. Temperatures rarely deviate from a range of 72 degrees Fahrenheit at night to 92 degrees in the daytime, accompanied, of course, by high humidity. East trade winds which blow very continuously during the dry season call for a blanket at night. The rainy season lasts from May to November ordinarily, and is a series of showers, torrential in quality, but not widespread. This intermittent behavior of the rains combined with the sandy soil have permitted the carrying on of seismograph work in the rainy season. This is especially true in the "llanos" of Monagas and Anzoategui where a medium amount of rain makes the terrain more rather than less negotiable.

CONCLUSION

Available scout information indicates a 100% increase in all forms of geophysical prospecting since January 1935. The increase in seismic exploration has been the same and the discovery of new fields in the States of Monagas and Anzoategui presages a still greater increase for 1938 and the future.

PRESENT STATUS AND FUTURE ASPECTS OF GEOPHYSICAL EXPLORATION IN POLAND*

Z. A. MITERA†

Geophysical methods of prospecting were introduced in Poland in 1923, or at about the same time as in the Gulf Coast. In the first stage local seismic refraction and electrical surveys were employed for private mining and oil companies. The Mintrop's refraction method has shown success in locating extension of salt deposits near Wieliczka and in Wapno. The Sundberg electromagnetic method was not entirely successful in mapping some lead and copper ore deposits. The same refers to the use of electromagnetic methods for mapping of oil structures. Steep anticlines and complicated structures in which oil mostly occurs within the area of the Carpathian Range were not favorable to be worked out with these methods which were not entirely developed and proved at that time.

Actual results obtained in the early days of the application of geophysical methods of prospecting in Poland are not known. These results in many cases are guarded by private companies as secrets and were never published.

In 1926 the Polish Geological Survey took an interest in the application of geophysical methods to solve many problems connected with regional structural and mining geology in Poland. In the same year the Geophysical Department of the Geological Survey was formed and it introduced the original torsion balances of R. Eötvös to solve some structural problems in Carpathian Foreland.

Considerable activity in geophysical prospecting was carried on in the years 1928 to 1930 when the "Pionier Exploration Co." was created by the government and all leading oil companies in Poland. Geological and geophysical prospecting for new oil and gas reserves were the principal aims of that company. At the same time the Institute of Geophysics and Meteorology at the University of Lwów, in cooperation with the Pionier Co., undertook extensive magnetic measurements in the Carpathian Foreland in the southeastern part

* Paper read at the Annual Meeting, New Orleans, Mar. 19, 1938.

† Consulting Geophysicist, Instructor of Geophysics at the Mining Academy of Krakow, Poland.

of Poland. A temporary magnetic base station at Daszawa and later a permanent magnetic observatory at Janów were established.

Geophysical prospecting during the years 1928 and 1930 extended the area previously covered by seismic refraction and torsion balance measurements. It was possible by use of the refraction method to outline accurately the boundary of the Podolian Plateau to the north-east. The Podolian Plateau forms a rigid framework which determined the strike of folds in the Carpathian Foreland. The Foreland itself is a depression zone in which younger sediments, mostly of Miocene age, were deposited and on which the marginal folds of the Carpathian Range were overthrust.

In the north-east, the Podolian Plateau is formed of cretaceous sediments near the surface and plunges under the Carpathian Foreland Depression.

Due to the great contrast in elastic properties between the Podolian and Miocene formations it was rather easy to outline the contact of these formations and map the shallower parts of Podolian Plateau. The deeper part of that Plateau and its structural forms could not be revealed by this method due to its limited depth penetration.

Magnetometer vertical intensity surveys have been checked quite closely with the results of seismic refraction investigations. The former showed distinctive magnetic anomalies near the contact of the Podolian Plateau with younger Miocene beds.

During the same period it was found possible to outline many Miocene salt deposits located in the frontal part of the Carpathian Mountains and also some salt domes of Permian age in the plains of the western part of Poland.

In 1932, the Geophysical Department of the Geological Survey acquired its own seismic refraction instruments and conducted further refraction surveys in the same areas. During the same time the Bureau of Weights and Measures of the Department of Commerce executed intensive pendulum measurements for the government.

In 1934, the Pionier Exploration Co. introduced the reflection seismograph and formed its own geophysical department under the name: "Pionier Institute of Applied Geophysics."

With this year large scale geophysical activity began in Poland. The greater part of this activity was concentrated in the Carpathian Foreland and the Carpathian Mountains where major oil and gas deposits are located. Sundberg electromagnetic methods were also

tried in outlining some structural features in this area. Due to limited depth penetration, this method failed to map the deeper structures which present the greatest interest from the commercial point of view in this area.

The total surface of the Carpathian Foreland amounts to about 20,000 square kilometers (7800 square miles).

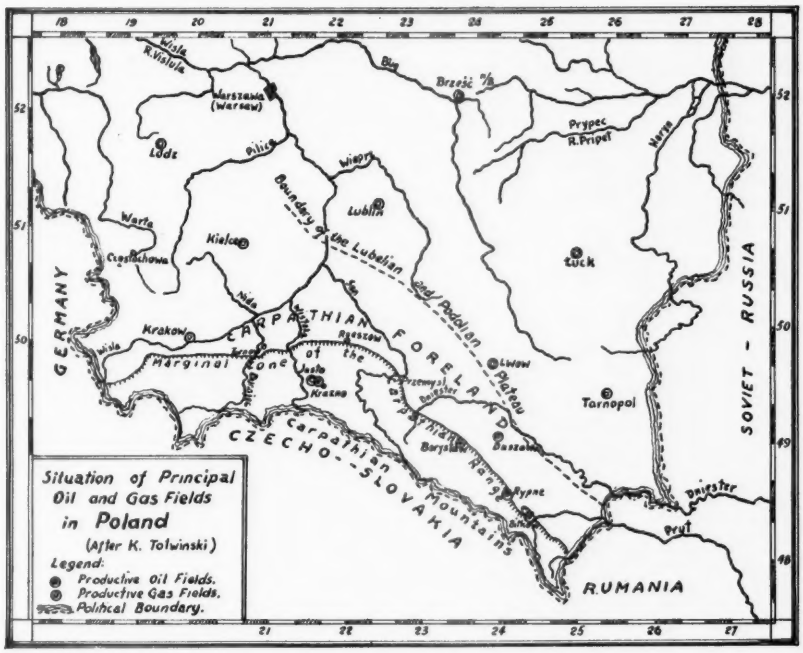

FIG. 1. Location of major oil and gas fields in reference to the Carpathian Mountain Range and its Foreland.

According to the leading oil geologists this represents one of the largest potential oil and gas areas in Poland. The southern part of this Foreland, adjoining the Carpathian Range is intensively folded, while in the northern part more gentle structures are found.

The Carpathian Mountains are characterized by sediments ranging in age from Lower Cretaceous to Lower Miocene, forming so-called Flysh facies, i.e., mostly shallow sea deposits. These are composed mostly of alternating series of shales and sandstones. These Flysh sediments were folded into systems of overthrust anticlines lying upon each other.

Due to the complicated structure of these beds, it was very difficult to obtain any reliable data from reflection surveys.

Only dip-shooting methods and continuous profiling could be applied as there was a decided lack of any beds that could be correlated or persistent reflecting horizons. In addition steep dips, amounting often to over 65°, many unconformities and faults made it impossible to obtain clear and nice-looking reflection records in that area.

Fig. 2 represents an example of experiments carried out in the geologically known area of Nahujowice, west of the Borysław Oil

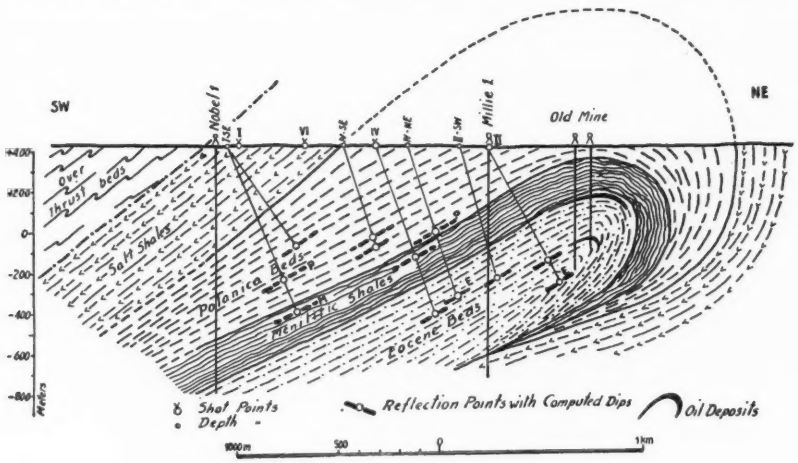

FIG. 2. Seismic Reflection Profile with geologic section through the Frontal Part of the Deep Element of Nahujowice, Eastern Poland. Geologic Section after K. Tolwinski.

field. A majority of the recorded reflections occur in the Polanica beds, Oligocene in age. The Menilitic shales, together with the hornstones at the base do not produce any outstanding reflections. Probably they are crushed and cracked by tectonic movements and therefore, they do not represent, despite their hardness, favorable conditions for the reflection of elastic waves. A few reflections originate in the Hieroglyphic shales of Lower Eocene series.

Further investigations were carried out in the region of the Deep Element of Borysław, similar to that of Nahujowice and also in the Bitków oil field in the Eastern Carpathian Range. In this last region, Polanica beds and Menilitic shales are interfolded and the whole series is covered with an overthrust sheet of Cretaceous and Eocene formations.

Experiments carried out in this area have shown very limited possibilities of the application of reflection methods to outline such complex and contorted structures.

A number of reflections have been observed in Miocene salt bearing formations, a few in Polanica and Menilitic beds and some in older Cretaceous and Eocene formations. In addition, some reflections

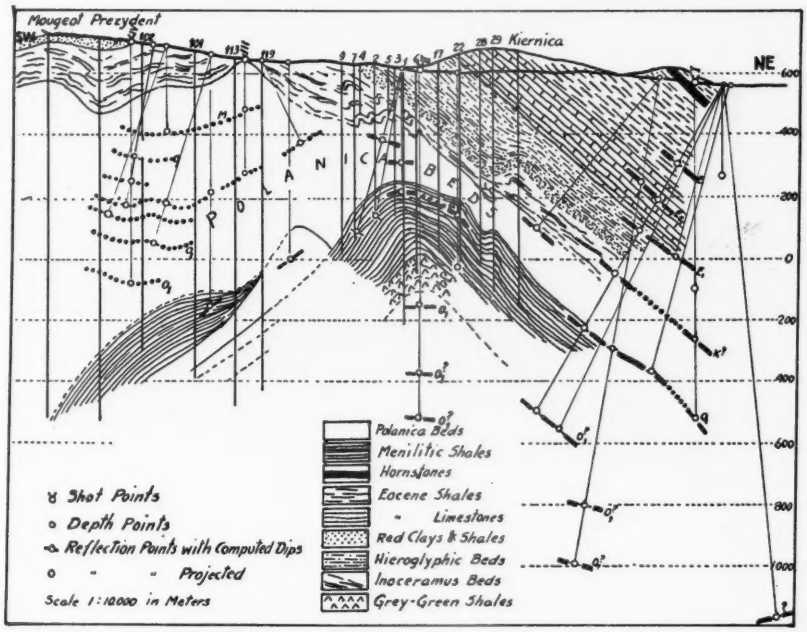

FIG. 3. Seismic Reflection Profile and Geologic Section through, the Bitków oil field. Geologic section after B. Bujalski.

are believed to have been received from the bottom of the Menilitic shales.

Generally speaking, the results obtained within the limits of the Carpathian Mountain system were not very encouraging and they failed to outline the more complicated structures. This was due not only to the definite lack of uniform beds, but also to the very small dimensions of the structures encountered. These structures do not exceed, often times, several hundred meters in length and width.

In addition to the geologic difficulties, there exist serious hindrances to transportation, due to rough and inaccessible terrain as is shown in Fig. 4.

Quite different and much better conditions for the application of seismic reflection methods exist in the Sub-Carpathian depression, called the Carpathian Foreland. In most cases there are present here a series of alternating beds of clays and sands in contact with deeper

FIG. 4. Difficult transportation conditions in application of reflection surveys in the Carpathian Foreland.

and harder layers of anhydrite and sandstones. It is believed, that these latter series belong to the known formation of the Podolian Plateau. At the surface, there are consolidated clay and gravel beds and often soft sands.

Fig. 5 reproduces typical reflection records obtained in the vicinity of the known gas field of Daszawa and in Stryj, in the eastern part of the Carpathian Foreland.

Besides a few indications of shallow reflecting horizons, one may notice a characteristic sharp reflection occurring at about 0.831 sec. By means of the average velocity, computed from actual well measurements, it has been established, that this prominent reflection may

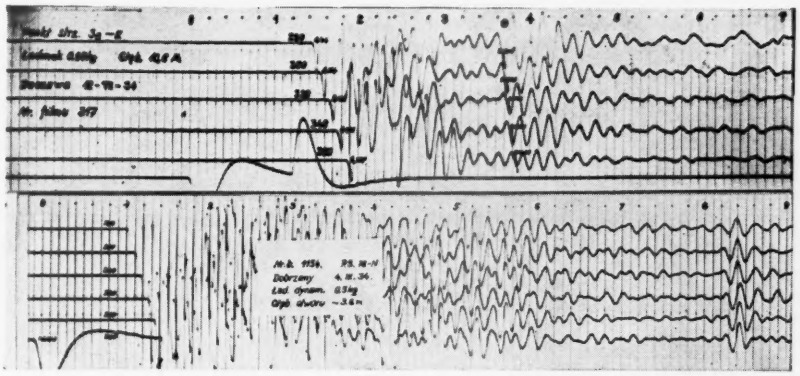

FIG. 5. Reflections obtained in Daszawa and Stryj in the Carpathian Foreland.

be identified with the anhydrite layers, occurring here at the depth of about 3,500 feet. The average thickness of this series amounts to 80–100 feet.

These outstanding and persistent reflections have been followed successfully throughout large areas of the Carpathian Foreland amounting to several thousand square miles.

Contour maps of this reflecting horizon furnished interesting information as to the geologic subsurface conditions. One may hope, that in the near future prospecting wells, recently commenced, will furnish more detailed information as to the oil and gas possibilities in that area.

In 1937 the Polish Geological Survey became again an important factor in promoting and expanding geophysical activity in Poland. There has been worked out a four-year exploration program in

which geophysical surveys, both reconnaissance and detailed, play an important role. The geophysical department of the above-mentioned institution acquired a number of new magnetometers for vertical intensity measurements, new torsion balances, and two Thyssen gravimeters. It is interesting to notice how much the gravimeter

FIG. 6. Map of Poland showing the areas covered by different geophysical methods in the period of 1923 to 1938. Total area amounts to about 150,000 sq. miles.

surveys exceed the old pendulum measurements, in that country. In the period from 1926 to 1937, about 300 pendulum stations were measured in Poland, the work being done only two or three months yearly. In 1937 alone, in only three months, over 800 new stations were made with Thyssen gravimeters, with an accuracy of ± 0.5 to

1 milligal, in regional measurements. In the same year many mining prospects have been worked out by earth resistivity measurements. The Schlumberger bore hole surveying methods have been accepted here as a standard method for bore hole correlation for three years.

Poland as a whole consists of about 80% lowlands and flat areas where there are not many possibilities for usual geologic exploration methods. Therefore there is open a large field for application of different geophysical methods of prospecting. In the eastern part of the so-called Volhynian Province the vertical magnetometer revealed large basaltic lava flows covered with diluvial and alluvial sediments. In the province of Wilno it is believed there have been found enough geological foundations to find new oil reserves in paleozoic and also younger formations in connection with the structural uplifts, which exist there according to latest geological investigations. One expects that the structural features may be better outlined by the use of known geophysical methods.

In the western part of Poland the Geologic Survey plans to extend their surveys for further salt domes which are found in this area and are very similar to those existing in the planes of north west Germany.

In the central part of Poland there have been carried out lately some self-potential and resistivity surveys in the mineralized zone of the Holy Cross Mountains. New iron, lead, and copper deposits have been recently found in small quantities in the area.

In carrying out the large prospecting program the geophysical department of the Polish Geologic Survey covered in 1937 alone 18,000 sq. miles with regional magnetic vertical intensity measurements, 4,800 sq. miles with gravimeter regional surveys and about 600 sq. miles with the detailed seismic refraction and reflection surveys.

Due to the fact that Poland shows during the last few years about 2% of steady decline in production of oil, great attention is paid to the geophysical methods as a help in the exploration and search for new oil and gas reserves. In order to keep the oil production at the same level as in 1936 (i.e., 3,775,000 barrels) in 1939 alone there will be needed about 380 new wells. This represents 740,000 feet of drilling according to Ch. Bohdanowicz, professor of Economic Geology of the Mining Academy of Krakow. Therefore one may expect again an increase in geophysical activity in Poland during the next few years.

AN INTRODUCTION TO THE SECOND DERIVATIVE CONTOUR METHOD OF INTERPRETING TORSION BALANCE DATA*

H. KLAUS†

ABSTRACT

After auspicious beginnings in the interpretation of torsion balance data, i.e., gradients and curvatures, the balance has been misused as a gravity instrument, the gradients being integrated into gravity, and the curvatures either neglected or not even observed in the field. Gravity was then made the sole basis of interpretation work, the regional effects being determined with more or less luck, subtracted from the total either before or after integration (regional gravity or regional gradient), and the residue held to be "local effect." This method appears to be now in vogue for most torsion balance and gravity meter work. In contrast to this procedure, the method here described is based on the quantities measured directly by the torsion balance, the gradients and curvatures, or second derivatives, and constitutes a considerable amplification of the original methods of investigating these quantities. Gravity is simply a by-product of this method, and is not needed at all for its functioning. The essential parts of this method are: 1) the re-determination of all second derivative components with respect to a new system of rectangular coordinates, one axis of which has been made parallel to the direction of elongation of anomalous features; 2) the contouring of these second derivative components on four separate maps; and 3), the interpretation of the resulting contour patterns. The outstanding advantages of this method over the total gravity methods are the following: 1) full utilization of the two independent aspects of the gravitational field furnished by the gradients and curvatures; 2) virtual independence from regional effects; 3) much greater resolving power when compared to gravity; and 4), complete absence of assumptions, such as are involved in estimating the regional, and in computing gravity from the gradients.

ACKNOWLEDGMENTS

The writer is greatly indebted to members of the executive and geological departments of Gulf Oil Corporation, Gypsy Division, particularly to Mr. W. B. Wilson, chief geologist, and to Dr. R. S. Knappen, assistant to the vice president, without whose encouragement and patience with experimentation the work could not have progressed initially; and to Drs. E. A. Eckhardt and L. L. Nettleton of Gulf Research and Development Company, whose criticisms and suggestions greatly aided in the further development of the method.

INTRODUCTION

When the torsion balance in its present form was used for geodetic purposes by its designer, Baron Roland von Eoetvoes, gradients and

* Published by permission of Gulf Oil Corporation, Gypsy Division; Gulf Research and Development Company; and Klaus Exploration Company. Paper read at Annual Meeting, New Orleans, La. Mar. 16, 1938.

† Consulting geologist and geophysicist, Klaus Exploration Co., Enid, Oklahoma.

curvatures were considered to be of equal importance for this work, because they furnished two separate and independent sources of information for the study of the same problem. With the application of the instrument to geological exploration, the necessity of utilizing both the gradients and the curvatures became obviously much greater, due to the much smaller size, and more complicated shape, of local subsurface objects, when compared to the large regional anomalies in the shape of the earth which Eoetvoes was investigating. Consequently, the pioneer interpreters devised methods giving full weight to the information to be derived from both the gradient and the curvature contributions to a complete torsion balance observation. These methods consisted mostly of profile or vertical section work, the components of the quantities along an observed profile being plotted in vertical sections, and compared with theoretical sections in trial and error procedure. Total gravity was then treated entirely as a by-product of a torsion balance survey, and was used merely as a convenient means of approximately representing the regional effects which had been the object of Eoetvoes' investigations.

Although good results were achieved with second derivative profiles, and although some remarkable quantitative work was done with their aid, this type of analysis seems to have fallen into disuse within the last ten years. Instead, it appears that torsion balance interpreters have preferred to investigate total gravity, thus making the original by-product the main objective of a torsion balance survey. Their procedure consisted of calculating total gravity by line-integration of the gradients, of estimating the regional effect, and of subtracting it from total gravity, or of estimating the regional gradients and subtracting them from the observed gradients before integration. In either case, the end-product, called "residual gravity" or "local gravity," was immediately identified with the gravity effects due to local geological structure, regardless of the assumptions involved both in the integration procedures and in the estimates of the regional effects. This group of methods, which shall be examined in more detail below, brought about decisive changes in the field procedure and in the design of the torsion balance. Since gravity became the main objective of a survey, the curvatures were regarded as superfluous and were neglected. The average radius of the terrain survey was shortened considerably, in order to achieve gradient corrections only, with resulting loss in the accuracy of curvature determinations, and gain in the speed of operations. Curvatures, thus made useless

through inaccuracy, as well as being considered unimportant, ceased to be observed by some operators, which was entirely logical under the circumstances. Instruments emphasizing speed soon appeared, one of which was so designed as to measure gradients only (the Shaw Gradiometer), while others decreased gradient sensitivity somewhat, and curvature sensitivity to a considerable extent, in order to shorten observation periods. The logical consequence of this misuse of the torsion balance as a gravity instrument was the greater development of apparatus for the direct measurement of gravity differences, such as pendulum and gravity meter, because such work was still more speedy, and was free of the assumptions involved in the procedures of integrating gradients.

In the total gravity methods, the principal defect is that the practical accuracy of determining gravity is of the same order of magnitude as significant gravity differences due to local structural situations. While this defect may not be serious in the qualitative determination of isolated mass anomalies, such as a salt dome miles away from others, it becomes very serious when the problem is the isolation of structural details, such as faulting and truncation, or the isolation of the individual structural and paleotopographic elements making up a complex subsurface situation. For these problems, the gradients and curvatures offer a much better line of attack, because their maxima and minima vary decisively from their regional levels, do not coincide in location, and often show increases in relief where the corresponding gravity picture loses relief due to the merging of the individual gravity effects of neighboring anomalies.

This paper, then, is based on the premise that the torsion balance is *not* a gravity instrument, but an instrument capable of measuring certain second derivatives of the gravity potential. Therefore, if we wish to investigate gravity, we should *not* use the torsion balance, but rather a gravity measuring device, such as the pendulum or the gravity meter. On the other hand, if we do use the torsion balance, we should analyze the quantities which are measured by that instrument directly, namely the gradients and curvatures. Consequently, this paper advocates two things: 1) the return to second derivative profile investigations; 2) the use of the second derivative contour method, the rudiments of which are described below. As far as the writer has been able to learn, this method has never before been described in the literature. A simple outline of the basis and the elements of the method is therefore presented here, with the hope that it

will stimulate research along the lines indicated, and that it will help to define the proper place of the torsion balance among the geophysical tools for the exploration of subsurface geology.

DESCRIPTION OF THE METHOD

1) CHOICE OF NEW REFERENCE AXES

In the field, the second derivatives are generally computed with respect to astronomic North. Naturally, this is a matter of convention, insuring uniformity of procedure. In this system, the x-axis is directed N-S with $+x$ to the N; the y-axis E-W, with $+y$ to the E, both x and y axes being contained in the horizontal plane, while the z-axis is vertical to this plane, with the positive branch directed downward. In this conventional system, it would be purely accidental, of course, if the direction of the geologic strike should coincide with one of the axes. For the new method, one of the axes, preferably the y-axis, is deliberately made parallel to the geological strike, in order to obtain second derivatives which have the most direct and most easily recognized relationships to the geologically significant mass anomaly under investigation. The new system leaves the z-axis undisturbed, but rotates the x and y-axes in the horizontal plane until the y-axis is parallel to the direction of elongation of local anomalies. This direction is determined from the data itself, without any outside information, in one of several possible ways, the easiest of which are the following: 1) prepare a contour map on the total magnitude of the horizontal gradient, and determine the direction of elongation of the contour-patterns; 2) proceed in the same manner with the curvatures. The directions so determined may be valid for the area of a single anomaly only, or they may be substantially the same for a whole survey or project. The choice of new reference axes must be undertaken accordingly.

II) REDETERMINATION OF SECOND DERIVATIVES

The second derivatives of the gravity potential which are measured by the torsion balance are U_{xz}, U_{yz}, U_Δ and $2U_{xy}$; and their relations to G, the horizontal gradient of gravity; α, its direction angle; R, the magnitude of the curvature value; and λ, its direction angle, are the following:

$$G = (U_{xz}^2 + U_{yz}^2)^{1/2},$$

$$\tan \alpha = U_{yz}/U_{xz},$$

$$R = (U_\Delta^2 + 4U_{xy}^2)^{1/2},$$

$$\tan 2\lambda = 2U_{xy}/U_\Delta,$$

where both direction angles are counted clockwise from astronomic north.

The adoption of the new system of axes does not affect G and R in the least, of course, but their direction angles are diminished by the amount of clockwise rotation of the new system as compared to the old. If we will call this angle of rotation ϵ, then the second derivatives in the new system may be obtained by using the following relationships:

$$U_{x'z} = G \cos (\alpha - \epsilon), \tag{1}$$

$$U_{y'z} = G \sin (\alpha - \epsilon), \tag{2}$$

$$U_{\Delta'} = - R \cos 2(\lambda - \epsilon), \tag{3}$$

$$2U_{x'y'} = R \sin 2(\lambda - \epsilon). \tag{4}$$

By the use of these formulae, the new second derivatives may be determined to any desired accuracy. For practical purposes, the nearest Eoetvoes unit is fully sufficient, since the contour interval will seldom be less than two or three Eoetvoes units. The new derivatives may also be found from plotted gradients and curvatures by simple graphical means.

III) CONTOURING OF SECOND DERIVATIVES

The method of contouring second derivatives is the same as that used in contouring any other quantity. It is necessary, therefore, that control points are well spread out over an area, instead of being concentrated along profile lines. Much of the torsion balance work, the primary objective of which was total gravity, has been done in profiles. Where these profiles are widely spaced, one from the other, the method under consideration cannot be applied. However, where the profiles are close to each other, and are crossed at frequent intervals by profiles at right angles to the former, contouring of the second derivatives may often be feasible. This depends on the size and intensity of the second derivative patterns in relation to the spacing of the profiles and to the probable error of the survey.

Areal control, with the stations scattered out about equidistantly throughout the survey, is best suited to the method. The distances between stations are governed by the magnitude, depth, and nature of the subsurface objectives. As a general rule, the spacing should be such that any closure in the second derivative contours should be based on more than two or three stations. The number required

may vary with surface conditions and expected probable error, and with the purpose of the survey.

One disadvantage of the areal or scatter spacing is the fact that distances between individual stations, being of the order of from half a mile to a mile and a quarter, are generally too large to permit of good line integrations into total gravity. However, since total gravity is not made the basis of the interpretation procedure, this disadvantage is fully offset by the fact that the spacing and direction control of the gradients for contouring total gravity is available in much area which is without any control whatever in the profile method, besides the fact that the primary condition for contouring second derivatives is given by this spacing.

An advantage of this type of spacing is that an experienced operator will be able to find good station sites even in fairly rough country, if a spacing of about one mile is required, whereas a more closely spaced profile through the same type of country must include many doubtful stations, which will seriously impair the usefulness of such profile.

The contour interval to be used depends on the practical accuracy of the survey, the sufficiency of the control, and the size and relief of the closures or contour patterns. Where large type balances with high sensitivity are used, and the field work has been conducted for maximum accuracy instead of speed, the contour interval for the gradient components may be as low as two or three Eoetvoes units, and that for the curvature components as low as four or five Eoetvoes. Where the second derivative relief is high, or the probable error larger than usual, an interval of five units for the gradient components, and ten for the curvature components, may be in order.

The contouring of each of the four maps should be carried out independently, so that the expression of an anomaly in any one of the maps is free from preconceived ideas, since the degree of agreement of the four individual second derivative patterns of an anomaly is the main criterion for consistency. The term "pattern" is here used to denote the configuration of the contours, such as a closure, or combination of closures, which constitutes the complete expression of a single subsurface feature in the second derivative map under consideration.

The contouring is based not only on the observed values at each point, but also on the changes, and implied rates of change, of the second derivatives from point to point; in other words, on such im-

plied third derivatives as U_{xxz}, U_{xyz}, U_{yyz}, U_{xxy}, U_{yyz}, and so on. Here is where the experience and judgment of the interpreter enters, when the control is not quite sufficient. Where the control is adequate, this personal element is held to a minimum.

Stations with a large error in one or more of the second derivatives may be eliminated in the contouring, because they will not fit in with the rate of change indicated by their neighbors, and will show up as isolated points with a number of contours around them, that is, by closures which are supported by this point alone. Fortunately, in this work, such stations disturb the continuity of the evidence only for the very small area which they represent, and they may be either disregarded or checked, according to the importance of their positions in the survey as a whole, having been brought to one's attention forcefully in the contouring. In contrast hereto, such stations are a serious handicap in the total gravity method, since their adjustment affects the whole of the survey, and since in total gravity work it is not often possible to spot stations with large errors as certainly as in the second derivative contouring.

IV) INTERPRETATION OF CONTOUR PATTERNS

Within the limits of this paper, it is impossible to do more than give a bare outline of the interpretation procedure. The points to be considered are the following: 1) the normal shape of the contour pattern of each derivative for a certain subsurface feature, and the relationship of these patterns to each other; 2) the effect of the regional on the patterns; 3) the effect of neighboring anomalies; and 4) the effect of strike deviations.

To illustrate the first point, Fig. 1 shows the normal second derivative contour patterns due to an elongated anticlinal dome with a positive density contrast. A representative structural contour is shown by the dotted line. The apex of the dome coincides with the origin of the new system of axes, and the y-axis is parallel to the direction of elongation of the dome, in other words, to the geological strike. For U_{zz}, the zero contour coincides with the y-axis; there are negative closures straddling the positive branch of the x-axis and positive closures straddling the negative branch of the x-axis. The U_{yz} pattern is very similar, but is rotated clockwise through 90 degrees with respect to the U_{xz} pattern, and it has some distinguishing characteristics, such as a greater distance between maximum and minimum, a wider spacing of the contours, and less elongation of the

closures. The U_Δ pattern is characterized by a central positive area, which straddles the long axis of the structure and is pinched in the apex region while it flares out at both ends, and two negative closures, one on each flank. The $2U_{xy}$ pattern exhibits four closures, two maxima and two minima; the zero lines coincide with the axes; the

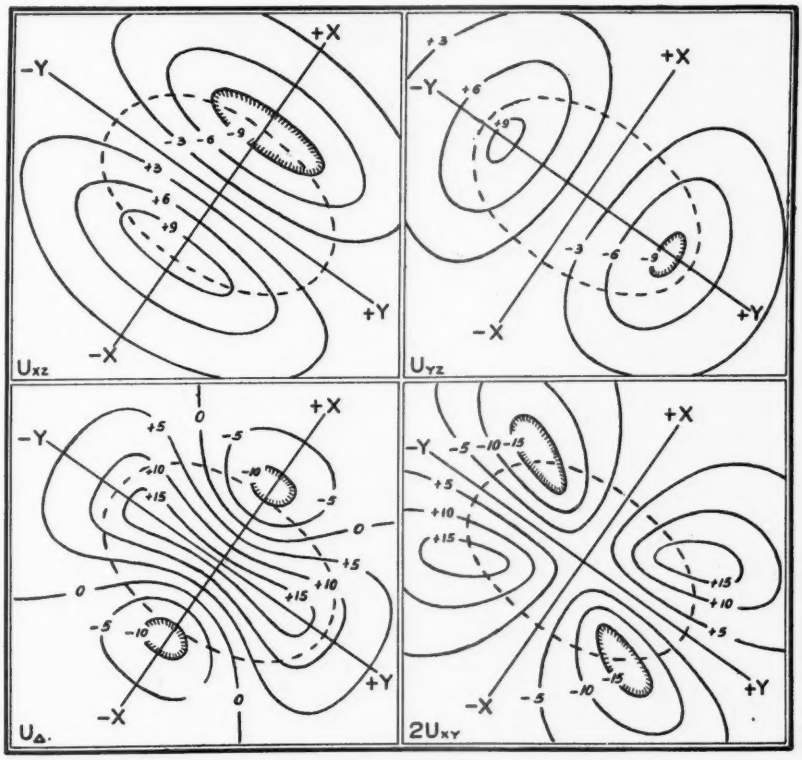

FIG. 1. Normal second derivative patterns for an elongated anticlinal dome with positive density contrast. Upper left, U_{zz}; upper right, U_{yz}; lower left, U_Δ; lower right, $2U_{xy}$.

maxima are in the first and third quadrants, the minima in the second and fourth, so that closures of like sign are diametrically opposed to each other. Thus, it takes 11 closures in the four second derivative maps, all in certain characteristic positions to each other and to the subsurface feature in question, and in certain quantitative relations to each other, in order to demonstrate satisfactorily the presence of a

positive mass anomaly in the subsurface, fitting the requirements of an elongated anticlinal dome.

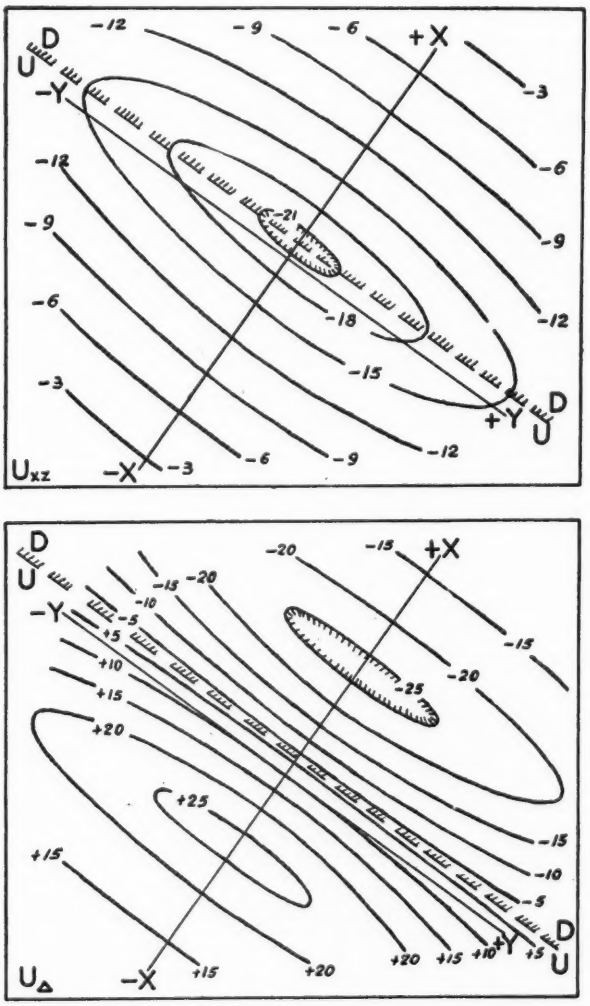

FIG. 2. Normal second derivative patterns for a vertical fault. Trace of fault shown by dotted line. Above, U_{xz}; below, U_Δ.

If we vary the subsurface conditions in Fig. 1 by assuming a negative density contrast of the same absolute magnitude as the positive contrast previously assumed, all we have to do to the pat-

terns is to reverse all signs. Otherwise, the patterns are identical. For a circular dome, the U_{xz} and U_{yz} patterns are alike, but the U_{yz} pattern is rotated clockwise through 90 degrees with respect to the U_{xz} pattern. For this case, the U_{Δ} pattern changes until it looks exactly like the $2U_{xy}$ pattern, but it is rotated clockwise through 45 degrees with respect to this true $2U_{xy}$ pattern, and both patterns lose the elongation shown in Fig. 1.

In the case of a fault parallel to the y-axis, we will generally observe U_{xz} and U_{Δ} patterns only, unless the throw of the fault diminishes rapidly in one or two directions from the point of maximum throw. The U_{xz} pattern will be an elongated maximum, if the fault is downthrown in the $-x$ direction, and a minimum of the same type, if the fault is downthrown in the $+x$ direction. In either of these cases, the U_{Δ} pattern will consist of an elongated maximum on the upthrown side and an elongated minimum on the downthrown side, with the zero line closely coinciding with the trace of the fault, and with the most rapid change of the values across the zero line. Similar patterns will result in the case of sudden facies changes involving an almost vertical density boundary, such as sands abutting a buried coral reef. It would lead too far to describe or illustrate other normal patterns. The patterns shown in the figures were derived from numerous actual patterns mapped in the field.

In marked contrast to the role which regional effects play in total gravity work, the second derivative patterns suffer almost no deformation from regional sources. Let us first consider the hypothetical case where the regional gravity change would be steady; in that case, the corresponding regional second derivatives would be constants. These constants may have any given value, over the extent of a given local anomaly, and this value would then merely be added to the contour values of a pattern, without deforming it in the least, and without changing its significance in the least. For example, in figure 1, it does not matter at all whether the relief of the U_{xz} pattern extends from $+9$ to -9, or from $+21$, to $+3$, or from -30 to -48 units, as long as we contour a maximum of 9 units above the regional level, and a minimum of 9 units below the regional level, in the same relationship as shown in Fig. 1. However, in actual surveys the regional second derivatives are generally not constants. Fortunately, the change is generally only a fraction of an Eoetvoes unit across the area of a local anomaly, and almost without exception only a very insignificant fraction of the Eoetvoes relief of a local anomaly.

Moreover, where the change is more rapid than usual, it will occur in one of the regional second derivatives only, so that the proper regional setting can be accurately estimated from the behavior of the others. It is obvious, for instance, that in zones showing the most rapid change of the regional U_Δ, the regional U_{zz} will show a minimum rate of change, and vice versa. It may be stated, therefore, that for qualitative work the regional eliminates itself in this method, and that for quantitative work it can be estimated within narrow limits. So much for the effect of the regional on the interpretation of local anomaly patterns.

Now, it may become desirable in the case of large connected surveys to ascertain the regional and to investigate it as fully as possible for its bearing on the regional geology. The new method is fully equal to this problem. At each local anomaly, a set of very accurate regional second derivatives can be determined, and where local anomalies do not occur, the average of all stations per unit of area may serve the same purpose. From these values, regional second derivative contour maps may be constructed, which will often bring out relationships between the regional gravitational field and the regional geology which are overlooked entirely in total gravity work. This, indeed, was one of the problems of Eoetvoes, and he used the same approach, if a different technique.

In gravimetrical work for geologic exploration, we are not only concerned with the task of isolating a local anomaly from the regional anomaly, but much more often we will have to disentangle several local anomalies *from each other and from the regional.* Obviously, this is the weakest point of all total gravity methods, because the gravity effect of a local subsurface feature occupies an area several times as large as that occupied by the geological feature, and thus, the gravity effects of several neighboring mass anomalies will merge readily. Consequently, the gravity effect of several subsurface features will be merged into a general high or low, as the case may be, at a distance of the structures from each other where the second derivatives still show separating characteristics, or even show them in enhanced form. For instance, a truncated anticline will generally be expressed by a single gravity high, whereas the second derivatives will often show the structural high as well as the buried topographical high on its flanks. This is especially important for the Mid-Continent area, for the correct diagnosis of seismic highs. Often so many local gravity features are merged that the process of estimating the regional gravity becomes a very hazardous one, resulting in the removal of "merged

local gravity" under the name of "regional," and there is the same danger in estimating the "regional gradient." However, in the method under consideration, the single features entering into a complex picture will be cleanly separated still under conditions where the task of disentangling them from gravity alone, or from the gradients alone, is entirely hopeless. Another advantage of the method is that often characteristics of structural deformation in the subsurface are apparent in the second derivatives where the corresponding gravity feature cannot show such criteria, and may therefore have an equal chance of representing a basement mass anomaly or a significant deformation of the sediments.

In case of general mapping, with only one redetermination of the second derivatives for the whole area, it becomes important to know how the deviation of the strike of a local anomaly from the chosen direction of the y-axis affects the local contour patterns. This is a somewhat involved subject going beyond the scope of this paper, and the problem shall only be mentioned here for the sake of completeness.

APPLICATION OF THE METHOD

It is not intended to advocate the use of this method for quantitative work; that is the proper place of the seismic methods. Instead, the method should be used qualitatively, that is, for the recognition of the type of structural deformations present in the subsurface, and the determination of their positions in relation to each other. This may be either general reconnaissance work for the high-grading of wildcat country to concentrate and reduce the cost of subsequent seismic or other detail work, or for the acquisition of acreage, or it may be supplementary work in conjunction with a seismic project. The new method is especially well adapted to the latter purpose, since the recognition of certain geological situations, such as faulting and truncation, is often much more direct and positive by this method than by any other geophysical method, including seismic reflection work. By the qualitatively correct recognition of structural details, the method is able to guide the correlation of seismic reflections in those places where the change in the stratigraphic equivalence of even correctly matched reflections may never be suspected from the seismic data alone. In this connection, the writer wishes to point out the possibility that several good seismic highs which were drilled with disappointing results may have been buried hills on the flanks of truncated structures. While the seismic data were good in many such cases, the interpretation may have been handicapped by the not

recognizable change in the stratigraphic position of the reflections. Of all known geophysical methods, the one described above would appear to have the best chance of correctly diagnosing such situations, and it would appear distinctly worth while, in the case of some recent seismic failures where the acreage is still held by the companies in question, to apply this method for the possibility of a solution of this type.

The contouring may also be resorted to as a preliminary for the selection of second derivative profiles, in order to carry out check calculations. In this manner much more representative profiles may be chosen than are provided by observed profile lines.

CONCLUSIONS

The new method is an amplification of the original torsion balance interpretations procedures, in that the investigation of the second derivatives is extended into the horizontal plane, by means of contouring these quantities. In contrast to present methods, which utilize the gradient only, and that in an indirect fashion through total gravity, the independent aspect of the gravitational field, which is furnished by the curvatures, is fully utilized, thus maintaining the principal advantage of the torsion balance over pendulum and gravity meter, which is: greatly increased resolving power in comparison to the latter. The fundamental requirements for the working of the method are (1) scattering of the control points over an area, instead of profile control, and (2) accurate field work, through the use of sensitive balances, good temperature control, long observation periods, good station selection, and adequate terrain correction. Those not willing to go to some pains in attaining high standards of field procedure would be better advised if they used the gravity-meter instead of the torsion balance, because a high probable error renders the method described ineffective or inapplicable. Many old torsion balance surveys have the control so arranged that contouring of the second derivatives is impossible, but some of these may be brought up to contour requirements at low cost by the addition of a few stations in the empty spaces between profiles.

The principal applications of the method are (1) in general reconnaissance work, for high-grading of an area in preparation for seismic and other detail work, or for the guidance of a leasing program; and (2) in direct conjunction with seismic work, for guidance of the interpretation of seismic data.

TRANSIENTS IN ELECTRICAL PROSPECTING*

PAUL F. HAWLEY†

The technique used in the older methods of electrical geophysical prospecting is well known. The measurements of current and potential drop which are made are the steady-state values, which can be readily measured on indicating-type meters. The factor of time is of very little importance.

Less attention has been paid to transient investigation of current and voltage applied to the earth. Max Müller[1] in Europe has made measurements on the decay time of potential between electrodes after current has suddenly been removed, thus obtaining data on the decay of ground polarization. Karcher and McDermott[2] reported on a method of determining the time constant of the surge of current into the ground when a circuit was closed between two grounded electrodes, measurements being made between other electrodes outside the first two. This was followed later by a paper by Statham[3] who used a modified configuration involving two current circuits and cancellation of the transient. A slightly different system has been disclosed by Blau[4] and Statham in two U. S. patents.

Although it has been generally known that several companies have experimented with electrical transients, no experimental data have been published. Accordingly, it was felt that a report of a preliminary investigation of electrical transient surveying which had been made by the laboratory of the Western Geophysical Company might be of general interest. This investigation was confined to the system outlined by Blau and Statham in the above mentioned patents.

This method is as follows: A source of constant voltage is suddenly applied between two electrodes driven into the ground some distance apart. In one type of measurement the resultant surge of current is recorded by suitable means. In the second type of measurement the potential surge between two other electrodes spaced in the field caused by the first two is recorded. In either case the wave fronts of the surges on the records are studied to see if there are any "nicks" in

* Paper read at Annual Meeting, New Orleans, La., Mar. 15, 1938.

† Western Geophysical Co., Los Angeles, California.

[1] For a list of references, see last page.

the curves. The presence of these nicks is said to reveal the presence of beds below the electrodes, the depth to a bed being proportional to the time after initiation at which the nick appears, and to the resistivity of the region above the bed.

In order to test this method, a recording system had to be devised which would be rapid enough to spread out the wave front to such an extent that the presence of nicks would be evident, and the time of their occurrence had to be measurable on the record. The switching arrangement to turn on the applied voltage had to be synchronized with the recording system so that the wave front would occur on the record.

Fortunately a high speed revolving drum camera constructed for another project was available. This camera comprises a six inch revolving drum around the periphery of which a strip of 35 mm. film is stretched, a light-tight housing for the drum, a small 6 volt motor to drive it, and a shutter whose action is synchronized with the drum rotation. After the shutter level is pulled, the shutter remains open for one complete revolution of the drum, then closes. Spare film is carried in a magazine on top of the camera, and loading is accomplished through a light-tight sleeved leather side to the camera.

It was realized that the speed of the transient was probably so high that any galvanometer type of oscillograph element was out of the question. Accordingly the camera was adapted to photograph the front of a cathode-ray oscilloscope. An f:2.0 lens was mounted between the shutter and drum in a focusing mount. A duMont oscilloscope with a three inch screen of the blue type was mounted four inches from the camera shutter. The deflecting voltage was applied to the horizontal plates only. The time axis was supplied by the drum rotation.

This system allowed a record of 18 inches of phenomena to be obtained, and was considered much superior to the alternative of photographing the face of the oscillograph with a still camera, using both time sweep and phenomena plates.

The amplifier system in the oscilloscope was not considered adequate for the present studies, so a special laboratory amplifier was used. This resistance-coupled amplifier had a maximum gain of 80,000 which was flat within 5% from 20 to 10,000 cycles, and a phase shift which varied so linearly with frequency that there was a maximum time lag between a 20 and a 10,000 cycle component of 2 microseconds. The amplifier gain was more than sufficient to give full

scale deflection with the currents used. The output of this amplifier was applied directly to the oscilloscope plates.

Preliminary tests using a 1000 cycle oscillation as the phenomena and Eastman Super X film as the recording medium showed that distortionless recording could be obtained at the quite high speed of 3000 inches per second. This figure is the speed with which the recording spot moves across the film. We believed that this would undoubtedly exceed any field requirement.

There were two problems to be met in designing the switching apparatus. First, the switch had to be absolutely chatter-free, so that the contact would be made as instantaneously as possible. Second, the switch had to close after the camera shutter opened. Both of these requirements were satisfied by using a gaseous discharge tube (thyratron) as the closing element in the circuit, and by tripping it from a pair of adjustable contacts built into the shutter mechanism. By this means the circuit could be closed at any point during the recording cycle. The breakdown time for a tube of this kind (885) is normally less than one microsecond. The tube was connected in series with a 315 volt bank of B-batteries and a current regulating rheostat to the current electrodes. No trouble with synchronization or faulty closing action was experienced.

The transient current was recorded by connecting the recording amplifier across a 10-ohm resistor in series with the current line, and recording the drop of potential across this resistor. Voltage transients were obtained by connecting the amplifier to the two lines from the intermediate or potential electrodes.

It was necessary to put a timing indication on the records. The method used was simply that of connecting an accurate 1000 cycle oscillator to the amplifier after each transient had been recorded, and making a second exposure on the film. Of course in order for this system to give accurate results, the camera speed had to remain constant for both exposures. This was checked repeatedly by recording the oscillator twice or more on the same film and measuring the film speed for each recording. The speeds always checked within 3%.

A general view of this apparatus mounted in the instrument truck is shown in Fig. 1. At the extreme left is the shielded amplifier, behind which is the 1000 cycle timing oscillator. In the back center is the oscilloscope, facing the high speed camera on the right. In front and to the right of the camera is the thyratron relay. The instrument with sloping panel in the center of the picture was used for steady state

measurements and has no bearing on this work. Connections to the lines are made through the panel on the upper right.

The truck was equipped with enough cable so that each current electrode could be spaced 6000 feet from the truck, thus giving a total spread of 12000 feet. The maximum spread between potential electrodes was 4000 feet. The Wenner configuration was used in all voltage transient tests.

FIG. 1. Initiating and recording apparatus for transients.

The field work was carried out in the San Joaquin Valley, about 25 miles northwest of Bakersfield. At this point in the valley the geological column is as follows: at the surface there is an 800 foot alluvial deposit, coarse sand and boulders. Then follows a 500 foot layer of alluvial or Upper Tulare fine sand, then 900 feet of Upper Tulare sand and sandy clay, then Etchegoin or Jacalitos shales, sands, and mudstones down to 5500 feet. Steady-state electrical tests show that there is a region of variable resistivity down to approximately 100 feet, followed by a layer of from 6000 to 9000 ohm-cm. resistivity down to around 500 feet, below which the sediments are of fairly constant

resistivity, of a value around 2100 ohm-cm. The lower limit of this region is not known.

The first transient tests made in this area showed that the buildup of both current and voltage transients was much faster than had been expected, and that higher recording speeds would be required. Progressive advancement in technique, such as the use of Agfa Ultra-Speed film, post-sensitized 6 to 12 hours with mercury vapor, and increasing the cathode-ray voltage and camera drum speed up to a maximum peripheral speed of 300 inches per second, resulted in obtaining records on which the maximum recording speed is approximately 8000 inches per second, with a faint but discernable trace. This was sufficient to spread out the wave front of the transient so that it could be studied.

In all, more than a hundred current and voltage transients were taken. These cover spreads between current electrodes of 12,000 to 1000 feet. Not all of the group were taken with sufficient speed to show the wave front in great detail, but at least half of the series are suitable. These records were enlarged so that along the time axis 0.001 sec. was stretched out to between 1 and 2 inches. At this size, the records could be studied with great detail.

Figures 2 to 5 show enlarged records of typical current transients obtained with spreads of 12000, 9000, 6000 and 3000 feet respectively. A current of 0.2 amperes was used for these four records. The corresponding voltage transients across the potential electrodes of the Wenner configuration are shown in Figs. 6 to 9. All these records are unretouched.

The buildup time for these waves naturally includes that of all the recording apparatus as well as that of the ground. Hence for each setup several records were taken with a direct short across the cable inputs at the truck. This gave the instrumental time constant, which was subtracted from the time constant read off the other record, to give the true buildup time for the ground circuit. The instrumental time constant averaged 20 to 23 millionths of a second. As time constant I refer to the time taken for the wave to build up to 70% of its peak value. The time constants of the ground circuit—from truck terminal to current electrode through the earth to the second current electrode and back to the truck—are interesting because of their extremely small magnitudes. Table I gives the average total and ground circuit time constants for spreads from 3000 to 12000 feet.

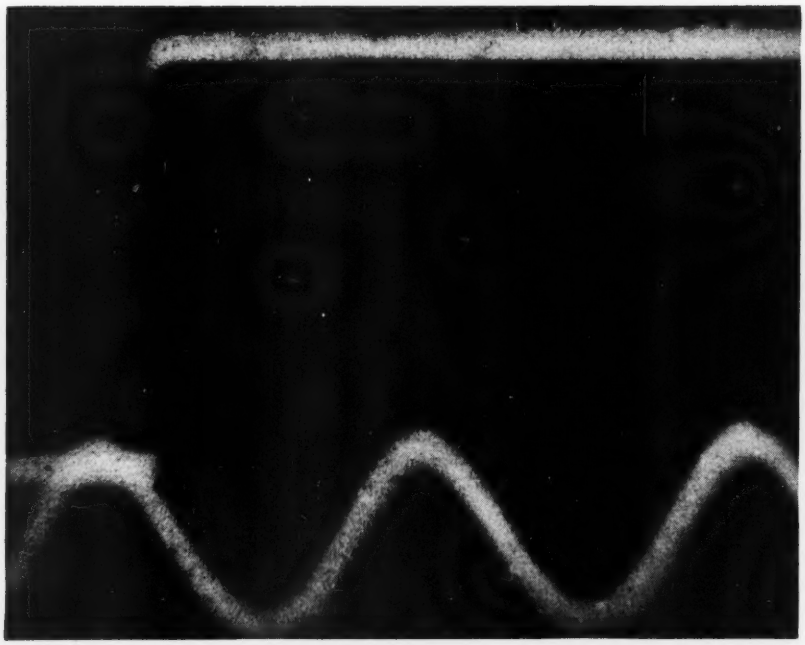

FIG. 2. Current transient for 12000 foot spread.

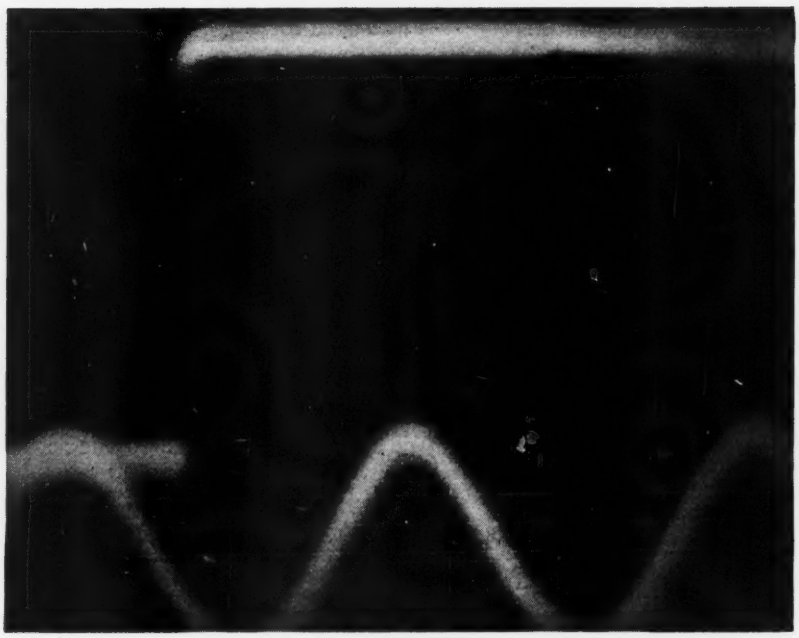

FIG. 3. Current transient for 9000 foot spread.

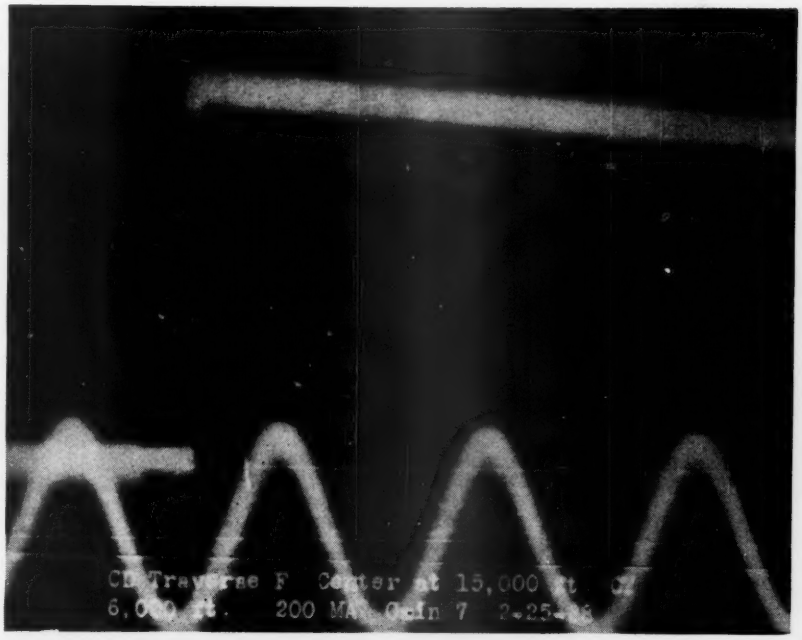

FIG. 4. Current transient for 6000 foot spread.

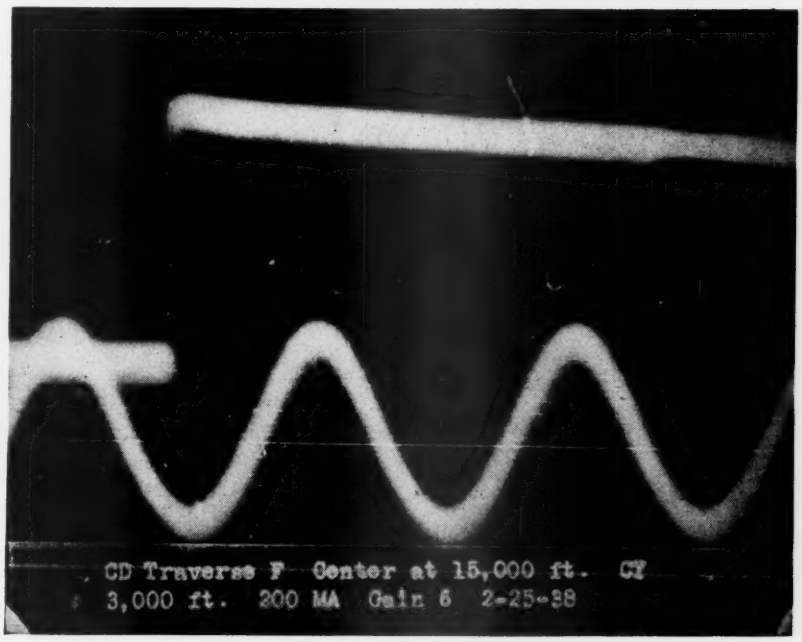

FIG. 5. Current transient for 3000 foot spread.

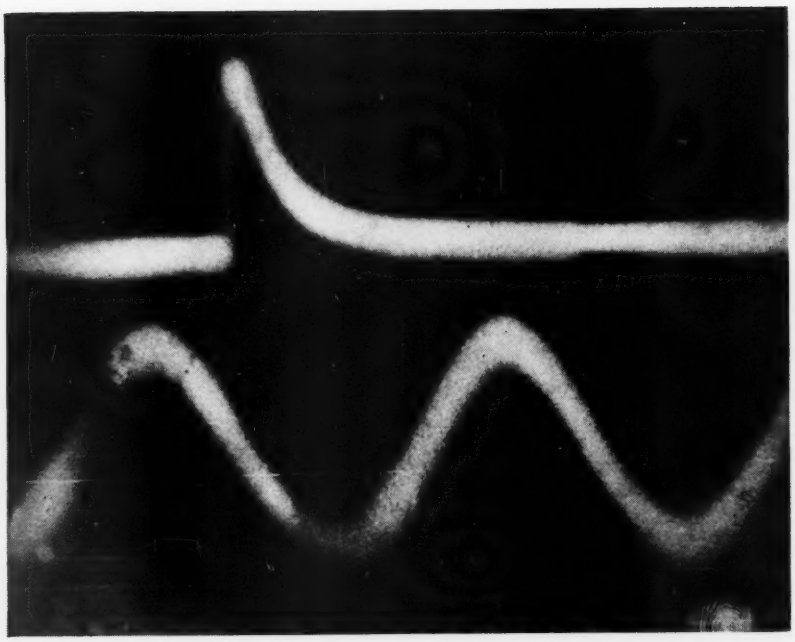

FIG. 6. Voltage transient for 4000–12000 foot spread.

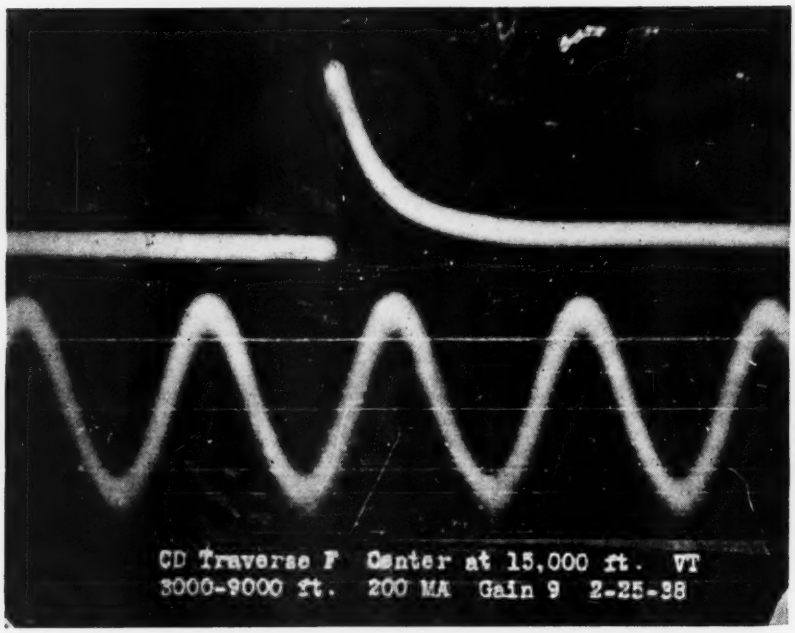

FIG. 7. Voltage transient for 3000–9000 foot spread.

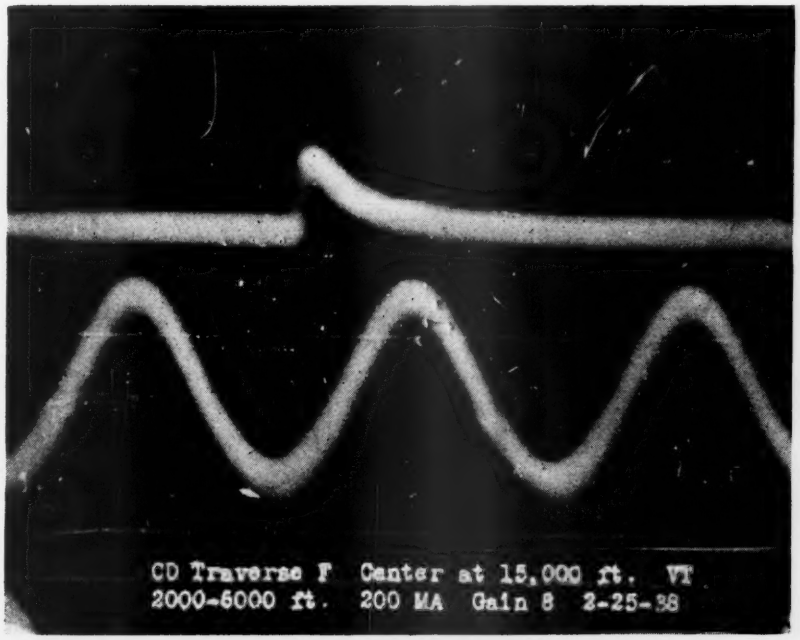

FIG. 8. Voltage transient for 2000–6000 foot spread.

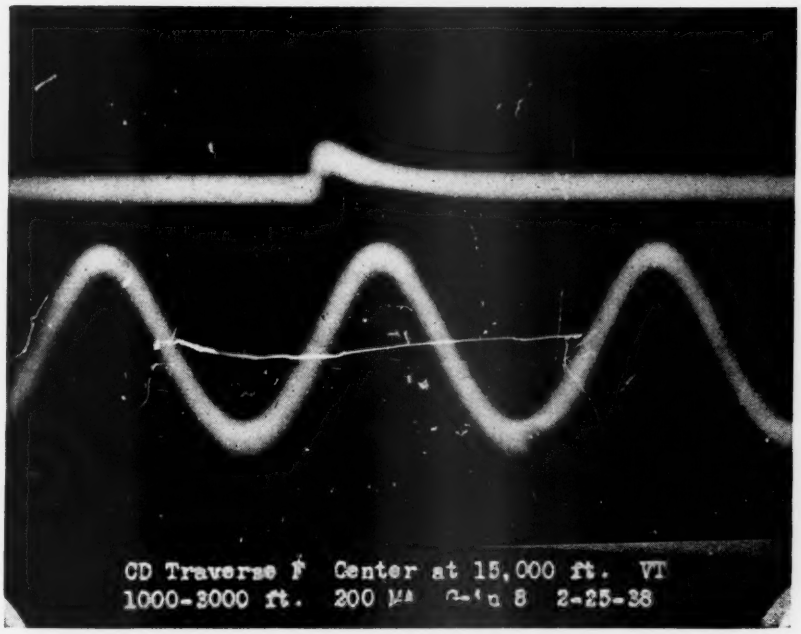

FIG. 9. Voltage transient for 1000–3000 foot spread.

TABLE I

Spread	Total Time Constant	Instrument Time Constant	Ground Circuit Time Constant
12000 ft.	53 microseconds	23 microseconds	30 microseconds
9000 ft.	36 microseconds	23 microseconds	13 microseconds
6000 ft.	31.5 microseconds	23 microseconds	8.5 microseconds
3000 ft.	27.5 microseconds	23 microseconds	4.5 microseconds

The voltage transient surge is quite different in form. The records show a practically instantaneous rise to a maximum value followed by an exponential die down. The time constant for the die down varied nearly linearly from 0.00035 seconds at 4000–12000 feet to 0.00015 seconds at 1000–3000 feet.

The wave forms of both the current and voltage transients can be explained as being the responses of inductive, highly damped circuits to unit functions of voltage. The time constant of the current transients, for example, is closely approximated by that of a semi-circular circuit whose diameter is that of the spread, and whose resistance is that found between the two stakes. In the case of the voltage transient, a nearly unit function of flux through the inductance of the ground circuit gives a rapid buildup of potential to a maximum value, after which the surge is dissipated through the resistance between potential electrodes, giving the exponential die down.

The records, examples of which are illustrated by Figures 2 to 9, have been carefully studied for the presence of the previously mentioned nicks. None has been found on any record, although the recording speed is sufficient to reveal a nick with a duration of 10 microseconds.

I have described apparatus with which the wave fronts of current and potential surges into the ground could be studied. The time constant of the current surges obtained in the San Joaquin Valley increased with distance to a maximum of 30 millionths of a second at a spread of 12000 feet. The time constant for the die down of the voltage transients also increases with distance to 0.00035 sec_r at 4000–12000 feet. None of the records obtained in the test area has shown the curves or nicks in the wave front which were postulated in the original description of the method. Furthermore, with the electrode configuration employed and in the area surveyed, the buildup of the current or voltage transients is entirely too rapid to permit any correlation between the data and known subsurface conditions.

Further investigation will be carried out in the near future with modifications of technique. Considering the importance which seems to be attached to this type of work at present, it is sincerely hoped that other investigations will also make known the experimental procedure and data of their studies, thus shedding light in a rather dark geophysical corner. It is felt that only in this way can the experimenters be free from the criticism, voiced by Blau[5] several years ago, that " . . . the discussions in geophysical papers are limited almost without exception to the results obtained."

I wish to express my gratitude to the members of the experimental electrical survey crew of the Western Geophysical Company and particularly to the party chief, Mr. Sexton, for assistance in obtaining the data.

REFERENCES

1. Müller, Max, Determination of reaction velocity of active electric processes in the earth. Zeits. f. Geophys. Vol. 8, No. 8, pp. 923–5.

2. Karcher, J. C., and McDermott, E., Deep Electrical Prospecting. A.A.P.G Bul., Vol. 19, Jan. 1935, pp. 65–77.

3. Statham, L., Electric Earth Transients in Geophysical Prospecting. Geophysics, Vol. I, No. 2, pp. 271–7.

4. Blau, L. W., and Statham, L., U. S. patents, 1,911,137 and 2,079,103.

5. Blau, L. W., Papers on Applied Geophysics, A.A.P.G. Bul., Vol. 17, No. I, pp. 87–91.

DETERMINATION OF THE POTENTIAL PRODUCTIVITY OF OIL-BEARING FORMATIONS BY RESISTIVITY MEASUREMENTS*

M. MARTIN,† G. H. MURRAY‡ AND W. J. GILLINGHAM‡

ABSTRACT

Electrical logging is now almost universally applied in oil and gas fields throughout the world. The usual practice is to record the self-potential and resistivity curves which, together, reveal the location and thickness of strata penetrated by the drill and a great deal as to their lithology and fluid content. The resistivity log thus obtained serves very well to disclose in detail formations penetrated and to distinguish between oil and water.

With the device used for ordinary electrical logging purposes, the true resistivity of the formation is not measured. The recorded resistivity is only an apparent value which is governed by several influencing factors, besides the true resistivity of the formation and its fluid content. As applied to the oil content of a formation, it is a qualitative measurement, merely showing the vertical extent of the oil accumulation.

Experience has shown that the electrical conductance of oil sands is due to connate water held by molecular forces to the sand grains. Research has disclosed a definite mathematical relationship between the true resistivity of an oil sand and the ratio of its oil and connate water.

This leads the way to a new practical application of electrical logging. By using a suitable combination of measuring devices, the true resistivity of an oil sand may be measured in an oil well. The true resistivity measurement, used in conjunction with other field and laboratory data, may in certain cases be used quantitatively to make a determination of the net oil content of a productive layer.

The method by which these measurements are obtained is described and actual examples are cited.

INTRODUCTION

Several publications (1)[1] have described a method of logging wells by electrical measurements and have given some of its applications. Since the publication of those papers a number of years has elapsed, during which, work in the great majority of the oil fields of the world has added considerable knowledge pertaining to the utility of the method. In the light of the vast experience thus gained, it would appear that the number of its applications can be considerably increased. Consequently it is interesting to note the results that have been definitely attained and to consider a possible new application that can be deduced therefrom.

The general nature of the electrical logs and their present applications are now well known throughout the petroleum industry. Two

* Paper read at the Annual Meeting, New Orleans, La., Mar. 15, 1938.

† Société de Prospection Électrique, Paris, France.

‡ Schlumberger Well Surveying Corporation, Houston, Texas.

[1] Numbers refer to bibliography at end of paper.

curves are usually recorded, which, together, reveal exactly the location and thickness of strata penetrated by the drill, and a great deal as to their lithology and fluid content. Oil is easily distinguished from salt water. The differentiation of oil and gas has certain difficulties and is only partially solved at present. Through correlations, these data elucidate the tectonics of a structure and finally enable the preparation of maps which show the horizontal and vertical extent of the oil and gas accumulations.

Research now indicates that electrical logging may be extended to some new and very useful applications.

NATURE AND SIGNIFICANCE OF RESISTIVITY MEASUREMENTS

The two electrical properties employed in electrical logging are on the one hand, the resistivity of the formations encountered by the well, and on the other hand, the self-potential which occurs in the earth and is usually designated as S. P. These two parameters are determined by means of apparatus immersed in the mud of the well, the principle of which has often been described in previous publications.

As far as the measurement of resistivity is concerned, it appears advisable to give some new facts about the exact meaning of this parameter. In the course of electrical logging one obtains a measurement which, if the measuring apparatus were situated in a homogeneous isotropic, infinitely large medium, would be equal to the resistivity of the surrounding medium. This is attained when the isotropic medium studied is sufficiently large compared with the dimensions of the measuring apparatus so that it can be considered as infinite as far as the distribution of potential is concerned. In actual practice the measuring device is lowered into the well which is filled with drilling fluid, the resistivity of which is not usually the same as that of the surrounding formations. Further, the well traverses a series of formations different both in lithology and in saturation, whose resistivities are different. The resistance measurements thus obtained under these conditions are evidently not equal to the resistivity of the medium surrounding the measuring device and sometimes differ considerably from their absolute values.

The apparent resistivity differs more from the true resistivity, the thinner the bed, the larger the diameter of the hole, and finally the greater the difference between the resistivity of the mud and the surrounding formations. The difference between real and apparent resistivity is increased opposite permeable horizons which are the

most interesting from a practical standpoint. Actually these beds are usually invaded by the fluids used in drilling, which create in the neighborhood of the hole a medium whose resistivity is quite different from that of the formation and which consequently introduces a considerable disturbance in the distribution of potentials. In substantiation of this fact there are the results of numerous observations in the field. Besides this, one can analyze the phenomena in a more or less approximate fashion by models in the laboratory. It is also possible, thanks to certain simplifying assumptions, to outline them mathematically. All these theoretical considerations lead to conclusions that are clearly confirmed by field results and which enable the selection of a suitable measuring device. For ordinary electrical logging purposes this device should not be so small that the effect of the formations is masked by that of the mud; on the other hand, it should not be too large, as a single average measurement would be obtained for too large a number of widely differing formations, which would render it impossible to distinguish in detail the different formations encountered.

As has been stated above, experience has shown that "apparent resistivity" is a parameter sufficiently characteristic for determination of the depth of the horizons and correlation work. This depends upon the fact that in a given field the drilling conditions are sufficiently uniform and that stratigraphy is sufficiently regular for the different formations to give on the electrical log easily recognizable forms. Besides this, the true resistivity of the porous formations, principally sands, are usually so different, according to whether the latter are saturated with oil or water, that the oil-bearing part of the formation can be clearly distinguished from the water-bearing part by its apparent resistivity.

The practical value of such results is considerable. The electrical data permit a delineation of the productive area. But thus employed, the results are only qualitative. Going further into the problem of the actual possibilities of the method shows that it is possible to employ them still further by touching on the question of the quantitative evaluation of the oil content of the formation. The experience obtained in recent years has actually shown that the true resistivity of the sands is governed, among other things, by the amount of oil they contain. The solution of the problem, therefore, rests finally on a determination of the true resistivity of the formations by the measurements made in the well.

It must be emphasized that a quantitative determination of oil content in a formation has little chance of being exact if based on resistivity as measured during a regular electrical survey, i.e., apparent resistivity; while the latter is indeed sufficiently different to permit a relatively exact differentiation between oil and water, it usually differs too much from the true resistivity for its absolute value to be used in quantitative determinations. For quantitative determinations electrical diagrams ought to be taken so that it is possible to deduce the absolute resistivity of the formations from them. Before explaining how to achieve this it is first necessary to examine the data regarding the relationship between the resistivity of the reservoir rocks and their saturation; afterwards the method by which this can be measured will be discussed.

DISTRIBUTION OF FLUIDS INSIDE SANDS

When electrical logging was first started in oil fields, the generally accepted opinion was that sands saturated with oil had an infinite "true resistivity." This conclusion was based on the fact that both the mineral of which the sand grains were composed and the oil surrounding them were insulators, electrically speaking. It was concluded, therefore, that if a measuring device were lowered opposite an oil-bearing strata, electrical current would be unable to enter the bed, and would be obliged to pass entirely through the drill hole. The difference of potential measured, according to this idea, would be equal to the potential drop caused by the passage of the current through the mud and consequently the apparent resistivity would be directly dependent on the resistivity of the mud. This rather simple explanation has not been confirmed by the results obtained. Practical experience quickly showed that if, in a given field, one found a certain relationship between the resistivity measured opposite oil-bearing strata and the resistivity of the mud for holes of the same size, the relationship was not directly proportional. In order to explain this anomaly, it was necessary therefore to assume that oil sands had a certain conductivity. Thus was suggested indirectly the presence of water in oil sands.

On the other hand, observations made during recent years by numerous observers (2) have shown, by actual examination of cores, the presence of connate water in oil sands, even in that part of the formation situated farthest from the edgewater zone. This connate water covered the sand grains as a capillary film—the remaining

space being filled with oil. The percentage of connate water in the pores, even at the top of the structure, in some cases exceeded ten per cent. It appeared to increase towards the flanks and the time would come when the water filled completely the pore space in the edgewater region. It is obvious, therefore, that according to this theory a sharp contact between water and oil does not exist, but a progressive diminution in the amount of water from the flanks to the top of the structure.

This phenomenon seems to depend upon the fact that the surface tension of water to the mineral forming the rock is greater (about three times) than that of oil. This same surface tension effect explains the fact that during exploitation, wells, at least those in the middle of the structure, produce practically dry oil—actually oil is given up while the water remains behind in the pores on account of the difference in surface tension.

This broad explanation is obviously subject to certain limitations. It can be accepted only if it is assumed that the formation is made up of sufficiently fine grains. If the rock is not homogeneous, and if certain zones of very large pores are present, the surface tension is insufficient for the water to rise up the grain walls and a well defined contact between oil and water exists. Similar conditions probably occur inside certain fissures which occur in calcareous formations and through which the fluids pass.

To return to the general case of sandy formations, experience has shown that gradually as the oil is produced, the water starts to occupy a larger and larger part of the pore space. First of all, it probably enters the zones of fine grains in which the oil is more quickly displaced, then the zones of coarse grains. Finally the time arrives when for a given diameter of pores, the pressure drop created by the wells on production is sufficient to overcome the surface tension; certain wells then commence to produce water.

Without being able to give an exact limit, since it depends on the size of the grains and the propulsive force of the fluids in the bed, it is to be noted that formations producing pure oil with a water saturation of 30% have been observed.

RELATIONSHIP BETWEEN THE RESISTIVITY OF A SAND AND ITS OIL CONTENT

It is well known that the resistivity of a rock is dependent upon the mineralized water that it contains, the mineral forming the rock

itself being usually insulating. From the above considerations, an oil sand consists of a rock in which the insulating constituent is made up partly of the mineral grains and partly of the drops of oil. The connate water exists as a film surrounding the grains, joining them together and thus insuring the conductivity of the whole. It is quite reasonable to assume that this conductivity will be greater, the higher the proportion of water in the pores. On the other hand, it is natural to think that for the same proportions of water and oil, the amount of water in a given volume of sand should be proportional to the free space between the grains and hence to the porosity. The conductivity of a sand, therefore, will depend upon its porosity, and it will be proportional to the conductivity of the adsorbed water, that is to say, to its ionic concentration. These considerations show that a knowledge of the resistivity of an oil-bearing formation can serve to determine its oil content if its porosity and the mineral content of its connate water are known.

Studies have been made in different laboratories to ascertain the nature of this relationship. We would mention here in this connection the results obtained in 1935 by the Petroleum Research Institute of Azerbaidjan (AZNI) at Baku (3). Since then the question has been taken up and studied extensively, in particular by Messrs. Jakosky and Hopper (4). Their results agree perfectly with those obtained by the Russian observers.

The experiments at Baku consisted in preparing samples of sands of given porosity which were saturated with varying proportions of water of known resistivity and oil. This method had the advantage of conforming to the current idea of the formation of oil fields, that is to say, migration of oil through a water-saturated reservoir rock. The testing instrument was a cylinder on the ends of which were placed two electrodes. The resistivity was measured very simply by using a Wheatstone Bridge.

A great number of experiments permitted the establishment of curves showing the relationship in question. Two of these curves made under the conditions enumerated below are shown on Fig. 1:

Curve I for a porosity of 45%,
Curve II for a porosity of 20%.

In both cases the water employed was a solution of NaCl of 12° Baumé.

The curves are plotted with the volume of pore space occupied by

the oil as abscissae (arithmetic scale) and the resistivity of the sample in ohms/m³. as ordinates (logarithmic scale).

An examination of the curves leads to the following conclusion:

As long as the proportion of oil is less than 80% of the pore volume, the resistivity is relatively low. On Curve II, for example, the sample with no oil at all gives a reading of 1.2 ohms, and with 80% oil, 20 ohms. Above this percentage, the resistivity increases rapidly. For 90% oil saturation, it reaches a value of 150 ohms, and for 92%, 1000s ohm.

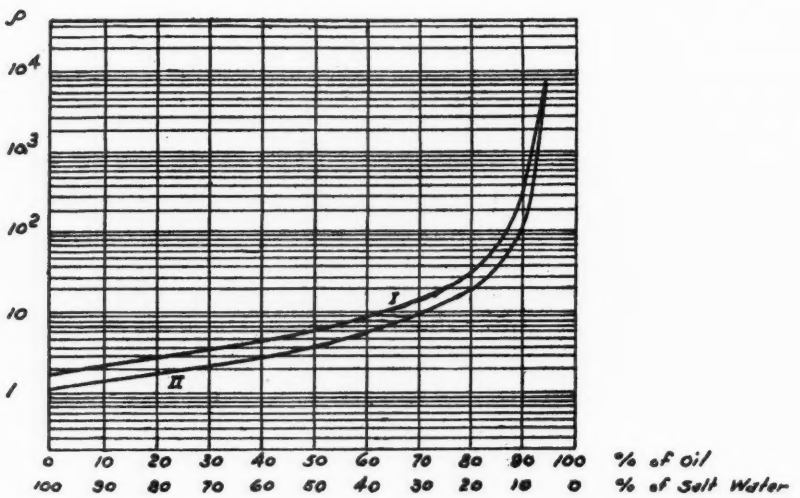

FIG. 1.

This shows that very rich oil sands, which on production will give nothing but dry oil, can have a resistivity which, although distinctly higher than that of a water sand, will, nevertheless, still be relatively low.

On the other hand, if the resistivity of the sample is designated by ρ and its oil saturation by s, it will be noticed that in that part of the curve between the abscissae 0.8 and 0.9 an increase of $d\rho$ of 100% corresponds to an increase of ds of about only 4%. This shows that the employment of resistivity for measuring oil saturation is extraordinarily accurate, *since a considerable error in the measurement of ρ involves an absolutely negligible error in the determination of s.* Conversely, an examination of the curves explains the considerable variations in resistivities measured opposite the oil-bearing parts of

a formation, even though the production is practically the same, for a slight change in oil saturation would produce a considerable variation in the resistivity.

PRACTICAL APPLICATION

It is rare that the taking of cores during drilling can give exact information about the fluid content. This difficulty arises from the fact that the core is always somewhat flushed by the drilling mud and the oil is partially expelled from it as the pressure is diminished. It results from these circumstances that the net oil content of an oil sand cannot be determined by analysis of the cores. Other means to evaluate the productivity of a reservoir formation must be sought.

Research has indicated that resistivity values closely approaching the true resistance of a formation may be obtained in a well with a suitable device. It therefore appears possible that this data may be combined with the S. P. diagrams to determine the net oil content of a sand body. This project is still in the research stage and is not sufficiently advanced to be applied as universally as electrical logging; nevertheless, the results already obtained indicate the possibility that it may be used to practical advantage under favorable conditions.

The quantitative determination of the oil content of a productive layer is accomplished by the electrical method in the following manner.

In the laboratory a set of curves similar to Fig. 1 is prepared beforehand, with a range of porosity percentage and water salinity sufficiently wide to cover all conditions which are likely to be found in a given field. The next step is to measure the porosity of the layer under evaluation and the salinity of a sample of the layer's formation water. In the field the true resistivity of the productive layer is measured as explained in subsequent paragraphs. The true resistivity value is then applied to the curve having the same porosity and salinity indices as the productive layer and the percentage of oil saturation is read on the corresponding abscissa. Knowing the percentage of oil saturation in a layer, from the resistivity diagrams, and its net productive thickness, from the S. P. log, Fig. 2, it is then a simple matter to compute the total volume of oil in place.

To apply the calculations to the entire oil accumulation after electrical measurements have been taken in a sufficient number of wells, it is expedient to prepare two maps on the same scale, from which the oil reserves may easily be estimated. On one map oil-sand

thickness contours are drawn; on the other, contour lines of equal resistivity. By converting the resistivity contours into terms of percentage of oil saturation from the laboratory curves, the amount of oil in each of these elements of surface may be determined. It is necessary then only to add these quantities to obtain the total of the oil in place.

This method has been actually applied to several oil sands in the Baku fields and the results obtained have been verified by production statistics. As an example, a series of resistance measurements

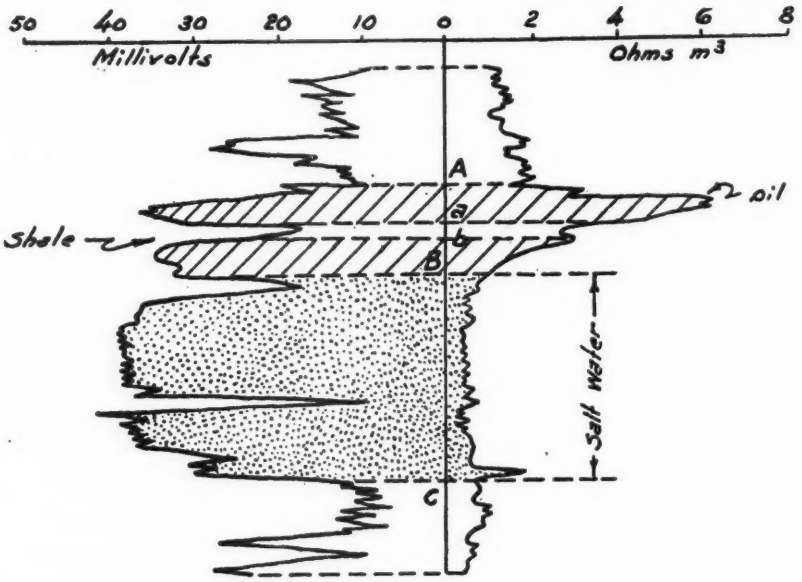

FIG. 2.

were made on the sixth horizon of Kaganovitch where electrical logging has been used since 1932.

A first determination was made by using the electrical logs of wells surveyed at the end of 1932 and the beginning of 1933. Fig. 6 illustrates the resistivity contours obtained at that time on the sixth horizon. Fig. 7 shows sand thickness contours of the same horizon. From these two maps, the total oil reserve was calculated to be 3,510,000 metric tons. A second set of resistivity readings was obtained in wells drilled during 1934–1935 from which a new resistivity contour map, Fig. 8, was prepared, and the total reserve was then calculated to be 2,280,000 metric tons. The difference between these figures, 1,230,000 metric tons, represents the estimated decrease

in reserve during the period under review. Actually, the wells produced 1,154,000 metric tons during that time. This last quantity differs only 8% from the figure calculated, which is an excellent confirmation of the accuracy of the method.

DETERMINATION OF TRUE RESISTIVITY

A special section has been kept for the discussion of this question so fundamental from the practical standpoint. It is necessary to state at the outset that the question of determining the true resistivity of the formations passed in the hole is still in the experimental stage.

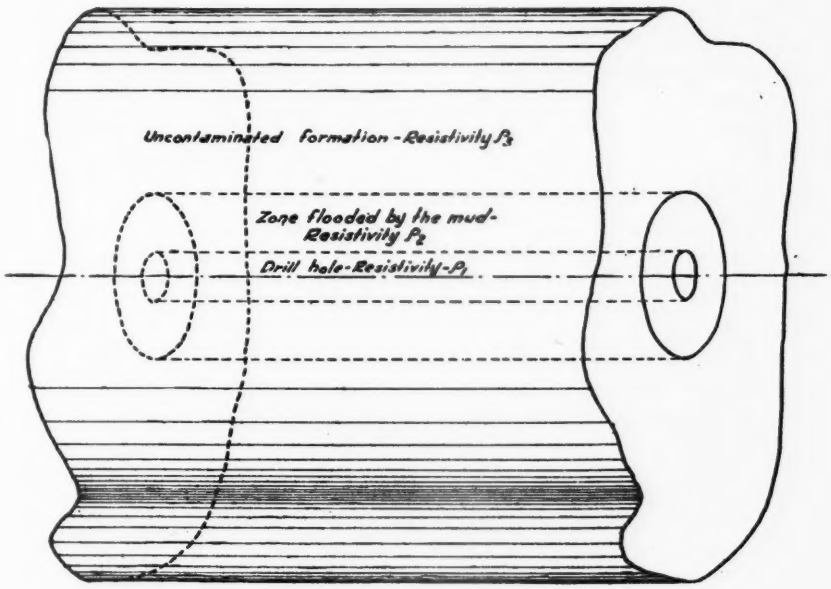

FIG. 3.

Without a doubt present conceptions will be perfected in the near future.

The problem consists in using a measuring arrangement sufficiently large that the influence of the mud is negligible. For this it must be assumed theoretically that one is dealing only with very thick formations. This last hypothesis is assumed in the reasoning that follows unless otherwise stated.

In keeping with this hypothesis, the general arrangement in space can be considered as follows, from the electrical point of view, Fig. 3,

a first medium of cylindrical shape is made up by mud, usually homogeneous and of resistivity ρ_1.

In the case of a permeable bed whose pressure is lower than that of the mud, a second medium is made up by the zone invaded by the mud. This zone is saturated to a great extent by the water of the mud which has filtered through the mud sheath. There may also remain some traces of oil if the formation is oil-bearing. The oil is flushed out more easily than the connate water which mixes with the invaded water changing its resistivity. It is quite difficult, therefore, to say what may be the resistivity of this invaded zone, even if the porosity of the bed is known. At any rate its resistivity ρ_2 is always greater than ρ_1. It is obvious that if the sand is very homogeneous the outer limits of this zone are a cylinder whose axis is the center of the hole.

Finally, a third ill-defined medium is constituted by the uncontaminated formation itself whose resistivity is ρ_3. If the bed is petroliferous, $\rho_3 > \rho_2$. If it is water-bearing $\rho_3 < \rho_2$.

It is possible by means of certain simplifying assumptions to calculate the relationship between the resistivity measured in the well (apparent resistivity), the true resistivity of the formation, the diameter of the hole, the resistivity of the mud, etc., and to represent this relationship graphically. Nevertheless, these theoretical calculations cannot replace entirely direct experimentation, as there is always at least one thing badly known, to-wit, the diameter of the invaded zone.

The complete experimental method, therefore, would consist of making a series of measurements opposite the same bed, Fig. 4, with measuring arrangements of successively increasing radii of investigation. In practice this is accomplished by increasing the electrode spacing. By plotting the spacing of the measuring electrodes as abscissae, and the corresponding apparent resistivities as ordinates, a curve of "lateral investigation," whose general shape is shown on Fig. 5, is obtained. This curve starts on the left at an asymptotic value equal to ρ_1, and finishes on the right at an asymptotic value equal to ρ_2.

This method has the serious defect of being very long and as a result quite costly. It is therefore impractical to apply it systematically to each well. Experience has shown that it is sufficient to record only a few lateral investigation curves in a district in order to determine the two best electrode spacings that will give the asymptotic

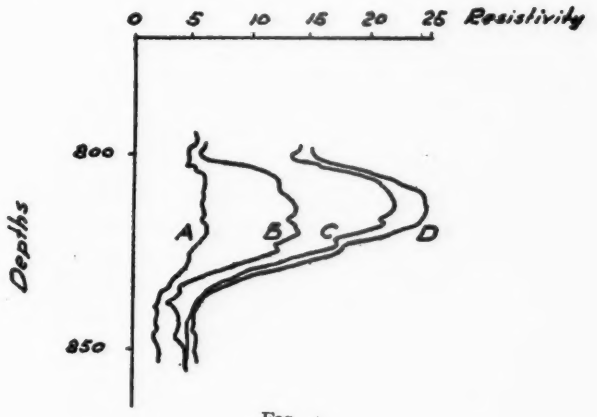
0
5
10
15
20
25
Resistivity
800
850
Depths
A
B
C
D

FIG. 4.

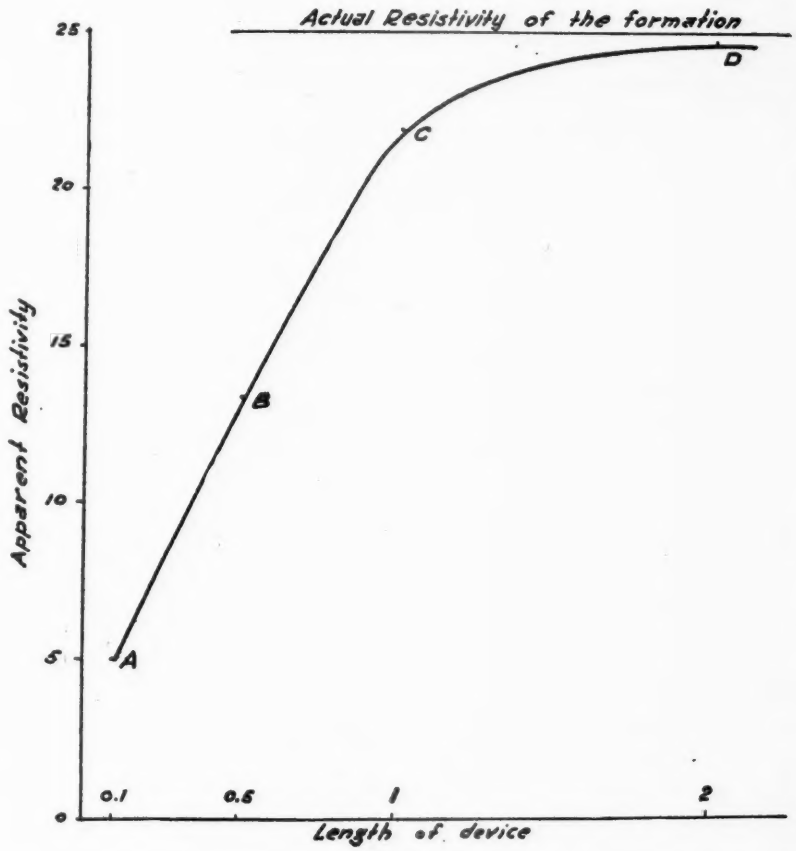
Actual Resistivity of the formation
25
20
15
10
5
0
Apparent Resistivity
A
B
C
D
0.1
0.5
1
2
Length of device

FIG. 5.

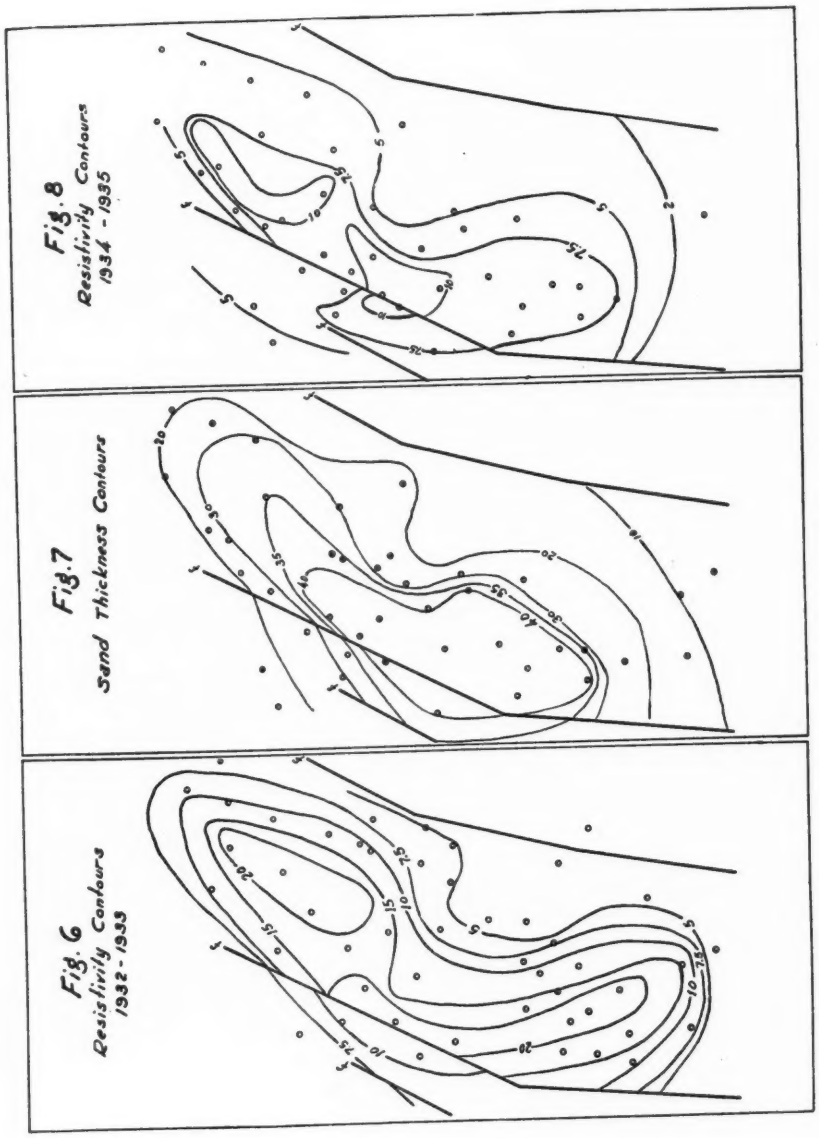
Fig. 8
Resistivity Contours
1934 - 1935
Fig. 7
Sand Thickness Contours
Fig. 6
Resistivity Contours
1932 - 1933

value of ρ_3 with sufficient accuracy and which henceforth can be used alone. To go further, it may be said that the results attained in the numerous different oil fields have shown that these best "spacings" are practically always the same in all the fields in a particular region.

It is important to note that the use of these two spacings can only give accurate quantitative results when applied to formations which are sufficiently thick. It is difficult to determine the minimum thickness necessary. Experience shows that for thickness greater than about fifteen feet, a value sufficiently close to the true resistivity can be obtained.

A considerable latitude in the choice of spacing is always permissible. Actually, the disturbing influence of the mud is greater the higher the resistivity of the bed. As long as the latter's resistivity is not too high (that is to say, for oil saturation less than 80%), it is quite easy to arrive at the true resistivity, even for relatively thin beds, as ten feet or fifteen feet. If the formation is very resistant (that is to say, for a saturation higher than 90%) it is more difficult to obtain the true resistivity accurately, but, as has been pointed out above, very great accuracy is useless, since a large error in true resistivity involves a negligible error in the determination of oil content.

At present it seems impractical to attempt true resistivity measurements on beds less than ten feet thick.

In conclusion, research has indicated that the field of electrical logging may be expanded to new applications which will be of practical value to oil operators. The method described is barely emerging from the research stage but it appears that with experience it will become a useful adjunct to ordinary electrical logging operations.

BIBLIOGRAPHY

1. (a) Electrical Coring; a Method of Determining Bottom-hole Data by Electrical Measurements. C. and M. Schlumberger and E. G. Leonardon, Transactions of the American Association of Mechanical Engineers, Vol. 110.
   (b) A New Contribution to Subsurface Studies by Means of Electrical Measurements in Drill Holes. C. and M. Schlumberger and E. G. Leonardon, Transactions of the American Institute of Mechanical Engineers, Vol. 110.
2. (a) Oil and Water Content of Oil Sand. Grozny, Russia, Bulletin of the American Association of Petroleum Geologists, Vol. 13, No. 7, July 1929, pp. 811–12.
   (b) The Connate Water Content of Oil Sands. Pyles and Jones, The Oil Weekly, November 16, 1936.
   (c) Interstitial Water Saturation in the Pore Space of Oil Reservoirs. A. Lewis and W. L. Horner, The Oil Weekly, October 19, 1936.

(d) Selective Wetting of Reservoir Rocks and Its Relation to Oil Production. Garrison, August 15, 1935.
(e) Influence of Connate Water on Estimation of Oil Reserves. R. L. Ginter, Oil and Gas Journal, October 10, 1937.
3. Utilization of Electrical Logging Data for the Determination of Oil Reserves. I. Kogan, Azerb. Neft. Khoziatzvo, October 11, 1935.
4. The Effect of Moisture on the Direct Current Resistivities of Oil Sand Rocks. Jakosky and Hopper, Geophysics, Vol. 2, No. 1, January 1937.
5. A Method of Determining Porosity; a List of Porosities of Oil Sand. D. B. Taliafero, T. W. Johnson, and E. J. Dewees, Report of Investigation, U. S. Bureau of Mines, September 1937.

LOCATING AND DETAILING FAULT FORMATIONS BY MEANS OF THE GEO-SONOGRAPH*

CURTIS H. JOHNSON†

ABSTRACT

Mapping of faults has previously presented great difficulties for the reflection method. These difficulties have often arisen from a confused reflection pattern, rather than from entire absence of reflections near the fault. The use of the Geo-sonograph in making a directional analysis of such confused patterns is described, and illustrated with several examples of faults located and mapped by this method.

Reflection seismograph exploration has now arrived at a state of maturity where the benefits derivable from its use are well established. It is, however, a widely conceded fact that the current type of seismo-

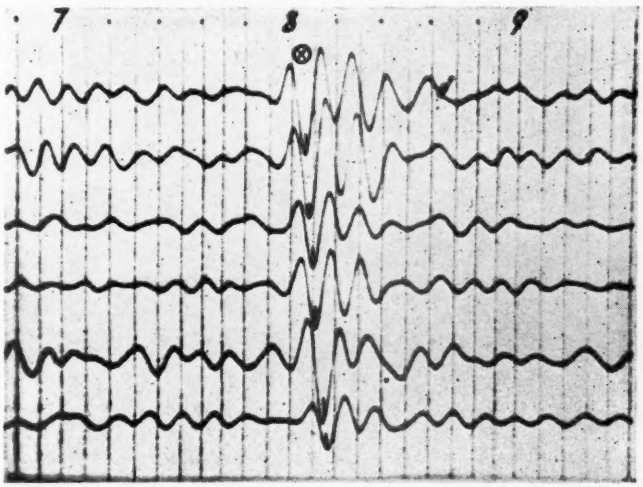

FIG. 1.

graph cannot operate in many regions, and obtains only marginal results in many others, due to the confused quality of the seismograms obtained.

Before discussing the appearance of confused seismograms, their causes, and cure, let us first have a look at a typical good seismogram. Fig. 1 illustrates such a record, and it seems to be characterized by

* Paper read at the Annual Meeting, Los Angeles, California, Mar. 18, 1937.

† Rieber Laboratory, Los Angeles.

a number of lineups, or groups of similar waves traceable continuously across from one side of the record to the other. A typical confused seismogram, however, might appear as in Fig. 2, where there is almost a complete absence of such lineups. The disconcerting feature about the confused seismogram is its tendency to appear whenever an interesting geological situation is approached. Opinions have been privately expressed by many geophysicists that interesting geological regions and confused records invariably go hand in hand.

Whether this be strictly true or not, it is generally observed that confused records and suspected faults very frequently go hand in hand. There are, of course, notable exceptions where, to the delight

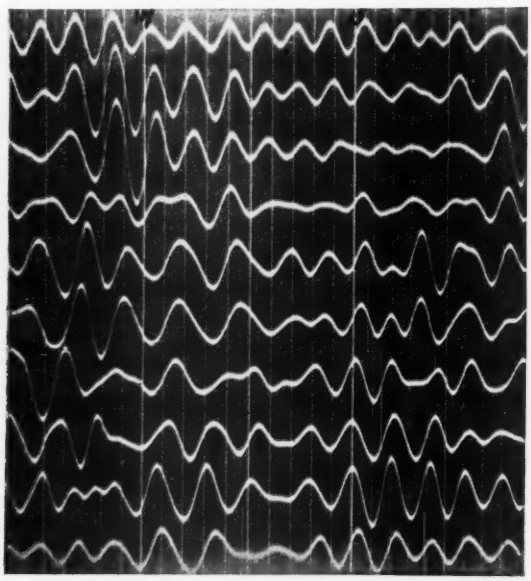

FIG. 2.

of the seismographer, minor displacements may actually be seen on a single seismogram. However, unreadable records and known faulting have been so commonly associated that the presence of confused records, has frequently been assumed, to good effect, as indicating the presence of a fault. Fig. 3 is a somewhat idealized profile, showing the delineation of the stratification up to a certain point—then a blank—then the continuation of the profile. There are many verified cases where the assumption that the "confused record" region, or "blank profile" region, should be interpreted as a fault has been

borne out by subsequent drilling. Obviously, the validity of such an assumption increases if several lines are shot in the same region, and

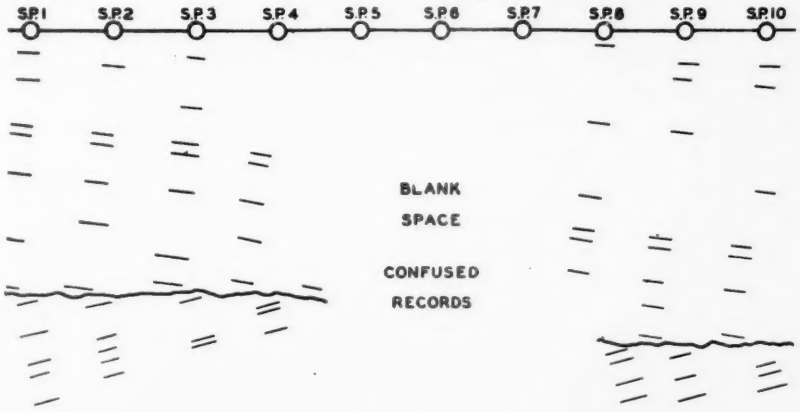

FIG. 3.

there appears a correlatable blank region on all of the series of lines, such as is here shown in Fig. 4. From the lineup of "bad record"

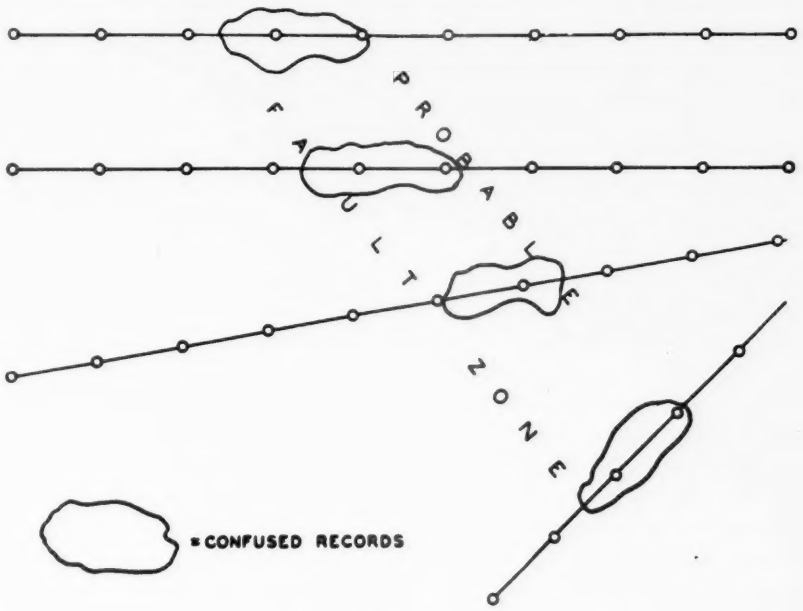

FIG. 4.

regions, or "blank profile" regions, the approximate trend of the fault is sometimes assumed.

It should be observed that there are two inadequacies in the "blank profile" or "no reflection" regions. First, the delineation of the stratification fails for some distance and second, the anomaly is not detailed. A complete solution of the problem would require a method capable of digging both the stratification and the anomaly out of the record. Fig. 5 shows the previously presented idealized profile,

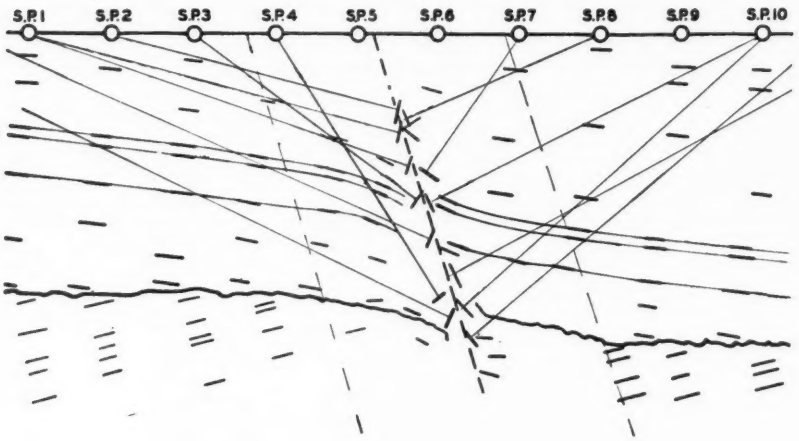

FIG. 5.

with the former blank space now detailed, showing stratification with a prominent key-bed and a prominent unconformity, together with an outlining of the fault surface partly by reflection and partly be diffraction.

In considering the possible causes of confused records near faults, we observe that the typical confused record (Fig. 2) is composed of frequencies characteristic of reflected waves but without any apparent pattern or set of lineups. Assuming, then, that the typical confused record in the neighborhood of a fault is predominantly of reflected wave frequency, we must rule out ground roll or air-borne unrest as a contributing factor. As a matter of fact, it is difficult to see why ground roll or air-borne unrest should be more prominent near faults than elsewhere.

Were these actually the cause of the confused records, the records could be very readily clarified by the simple process of frequency discrimination, for ground roll is usually of lower frequency than reflected waves, and air-borne unrest is usually of higher frequency.

Thus, the probability is that the confusion is caused by a multiplicity of compression waves arriving from the vicinity of the fault. Geometric considerations leading to the conclusion that waves will arrive from many directions over certain geologic structures, including fault regions, were presented by Frank Rieber in the form of an animated diagram at the March, 1937, meeting of the A. A. P. G. In a perhaps less striking but possibly more fundamental manner he has

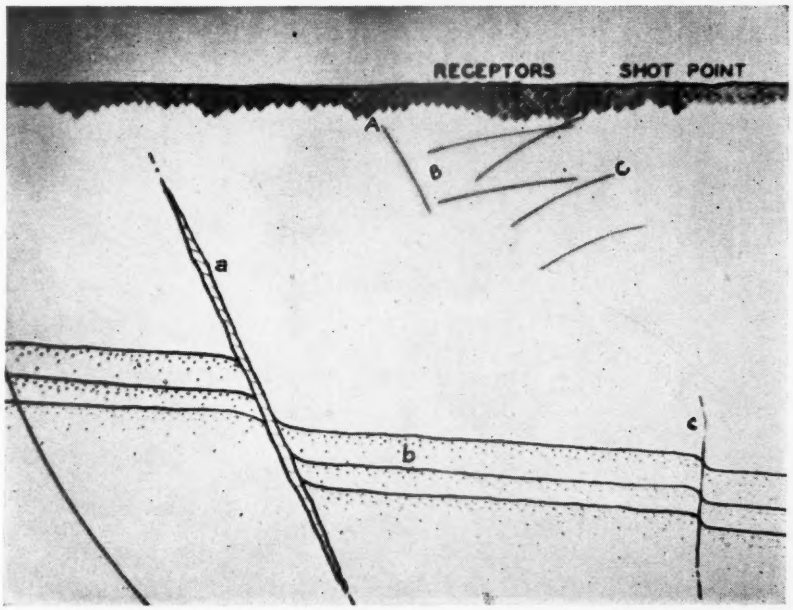

FIG. 6.

demonstrated in a previous paper,[1] the fact that multiple angles of arrival caused by diffractions, as well as reflections, from fault surfaces will produce crisscross arrivals at the surface.

Fig. 6 is one frame of the animated diagram showing geometrically the crisscross arrivals at the surface, "*A*" being a reflection from fault "*a*," "*B*" being reflections from strata "*b*" and '*C*" being diffractions from fault "*c*."

Fig. 7 is a sample strobogram taken from Rieber's previous paper,[1] illustrating the return of diffracted waves from fault corners.

[1] Visual Presentation of Elastic Wave Patterns Under Various Structural Conditions. Frank Rieber, *Geophysics*, Vol. 1. No. 2, July, 1936.

On the assumption that confused records are caused by crisscross arrivals, it is necessary to design some system for separating such crisscross waves out of a record. Beginnings along this line had been tried prior to the Geo-sonograph. The method of multiple recording,[2] while primarily designed to minimize the effect of ground roll, was useful, in a limited way, to clarify confused records, where the confusion was due to crisscross waves from a depth.

Fig. 8 combines parts of two of the illustrations from an article by E. E. McDermott.[2] It shows the effect of combining eight de-

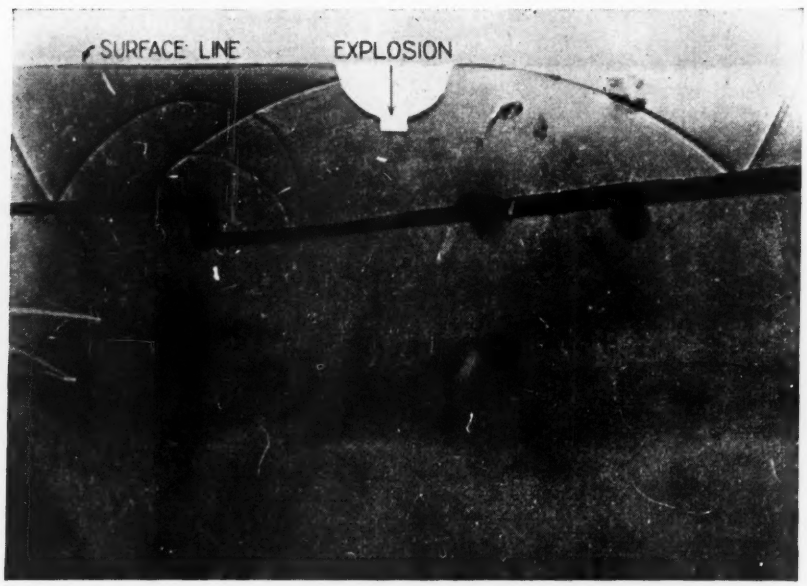

FIG. 7.

tector outputs, when the angle of arrival is respectively 5 degrees, 15 degrees and 25 degrees, with a detector spread of 100 feet, a frequency of 40 cycles per sec. and a velocity of 8,000 ft. per sec.

In Fig. 9 the magnitudes of the cumulations shown by McDermott are plotted as radii vectors pointing in the directions from which the waves reached the surface. The summation for waves arriving from other angles may be calculated analytically. The results of several

[2] The Use of Multiple Seismometers. E. E. McDermott, *Petroleum Engineer*, February, 1937.

such calculations are shown in Fig. 9 as lighter vectors than those obtained from McDermott's graphical solution. If we draw the envelope of all these vectors, it is evident that we have a polar curve representing the effective sensitivity of the detector group to waves of the reflected wave frequency.

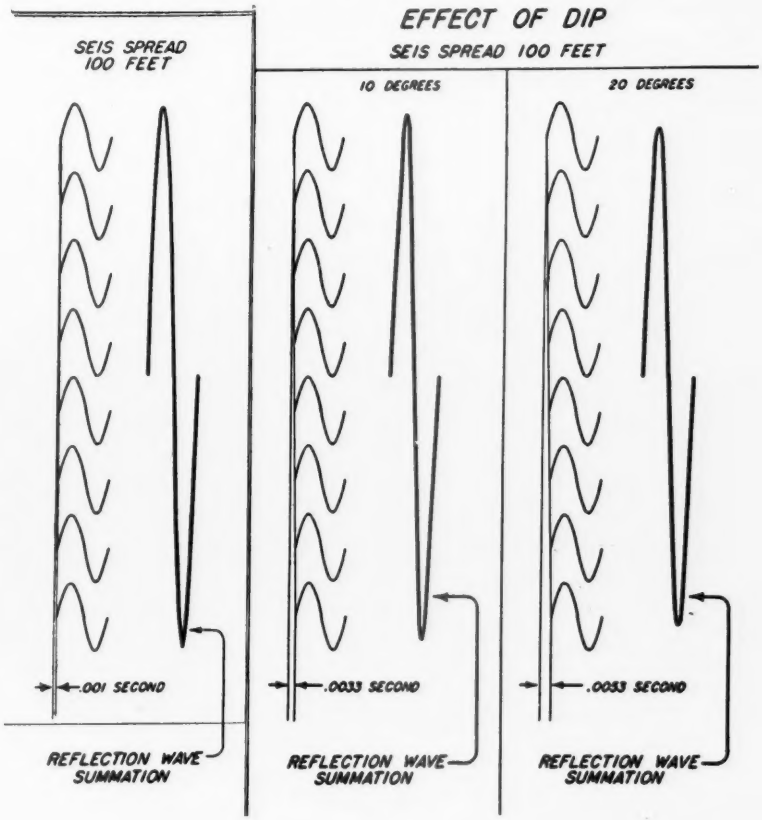

FIG. 8.

In Fig. 9 is drawn another polar sensitivity curve not designated by vectors. This curve, calculated throughout, illustrates the sharper effect obtained by using a 300 foot detector spread instead of one of 100 feet. Had a 600 foot spread been used, the corresponding sensitivity curve would have been still sharper.

Fig. 10 illustrates how such simple accentuation of vertical arrivals over arrivals from other angles might assist in detailing the

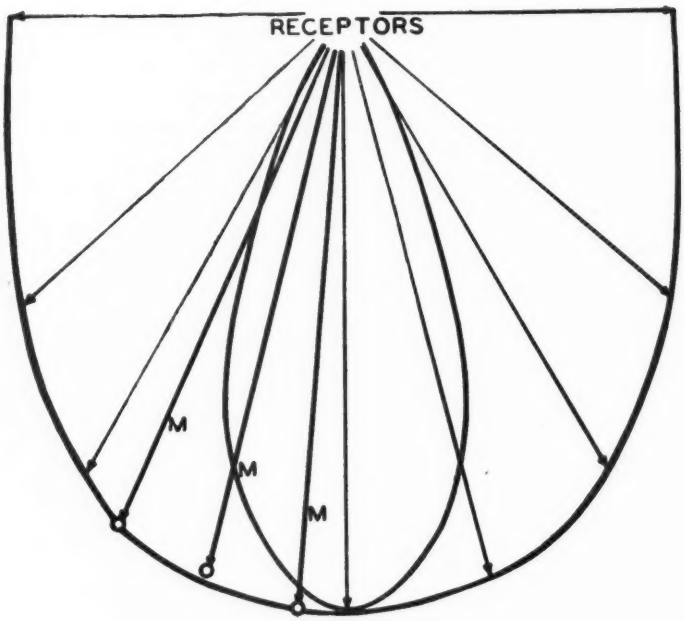

FIG. 9.

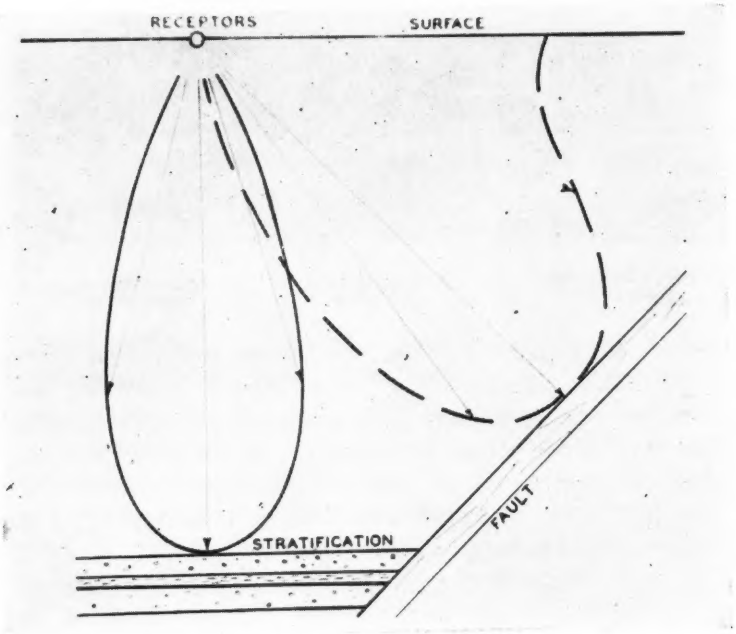

FIG. 10.

stratification near a fault, and, if outstanding key-beds were present, in finding the fault by means of its displacement. If the polar sensitivity curve could be pointed in turn at the stratification, and then at the fault surface (as shown by the dotted curve in Fig. 10), it might be possible to detail both of them. The story of the development of the Rieber Geo-sonograph is essentially a story of the development of a method by which this polar sensitivity curve could be rapidly and economically rotated to any desired direction, exploring for any one feature, while eliminating the effect of all others.

The rotatability of the polar sensitivity curve is accomplished in the Geo-sonograph method of directional analysis by cumulating in two steps, recording first a reproducible record of the output of each detector and later combining them not only in their original phase relationship, as is done in ordinary multiple recording, but also in any desired phase relationship. The finally perfected technique of directional analysis will not be described here, for it has been adequately described in various publications.[3,4]

For the present discussion it should be sufficient to show one variable density record with the corresponding visual seismograph record and the directional analysis obtained by means of the Geo-sonograph Analyzer from the variable density record. This is shown in Fig. 11 which illustrates a very simple, uncomplicated type of record. It serves to relate the ordinary seismograph record or seismogram, the sound film record (possibly called sonogram), and the directional analysis of the sonogram. Each of the traces on the seismogram is a reproduction of the corresponding sound track of the sonogram. Each of the traces on the directional analysis strip is, however, the sum (or multiple recording) of the outputs of all of the detectors.

The heavy trace is the combination of all the detector outputs unaltered in phase, and corresponds exactly to the result which would have been obtained had the detectors been connected in series to a common recording element. Each of the other traces of the directional analysis strip also represents the sum of the outputs of all of the detectors, but with a constant phase difference introduced between the outputs from adjacent detectors before cumulation. The traces near the heavy, or zero-phase cumulation, have small phase

[3] New Geophysical Method Provides Reliable Data for Structure Mapping. Wallace A. Sawdon, *Petroleum Engineer*, October, 1936.

[4] A New Reflection System with Controlled Directional Sensitivity. Frank Rieber, *Geophysics*, Vol. 1, No. 1. January, 1936.

differences introduced between the outputs of adjacent detectors before cumulating, while the traces farther away from the heavy, or zero, trace represent the cumulation when larger phase differences were introduced between the outputs of adjacent detectors.

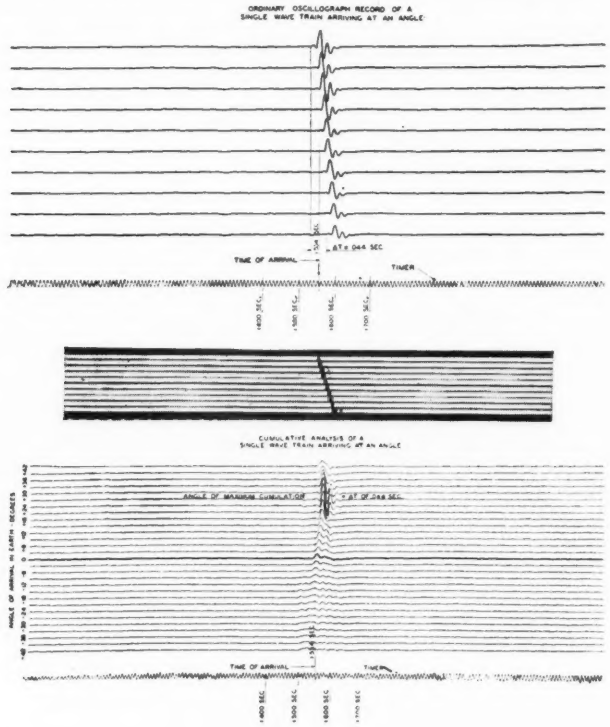
ORDINARY OSCILLOGRAPH RECORD OF A SINGLE WAVE TRAIN ARRIVING AT AN ANGLE
TIME OF ARRIVAL
TIMER
CUMULATIVE ANALYSIS OF A SINGLE WAVE TRAIN ARRIVING AT AN ANGLE
ANGLE OF MAXIMUM CUMULATION
TIME OF ARRIVAL
TIMER

FIG. 11.

Waves arriving at the surface of the earth at an angle reach the detectors at different times—or, in other words, there is a phase difference between the wave as it appears on the record obtained from one detector and the record obtained from an adjacent detector. This is the ordinary ΔT value ascertained visually on seismograms obtained in relatively simple shooting territory. The various traces on the directional analysis strip, representing, as they do different ΔT values, may be calibrated in terms of angle of arrival from the earth, as shown at the left hand side of the analysis strip. It is sufficient here to call attention to the large range of angles of arrival on the cumulative analysis strip which is unaffected by the waves recorded here. Clearly,

if another wave had arrived at an angle represented by one of these unaffected traces, it could have been almost as easily observed as if the waves now on the record had not been present.

Laboratory and field tests of the relative abilities of the analyzer and the visual method to extract two waves occurring on the record at nearly the same time and at different angles have been described by Frank Rieber in a previous publication.[5] This present paper will discuss some examples of results of shooting in complicated territory with the Geo-sonograph.

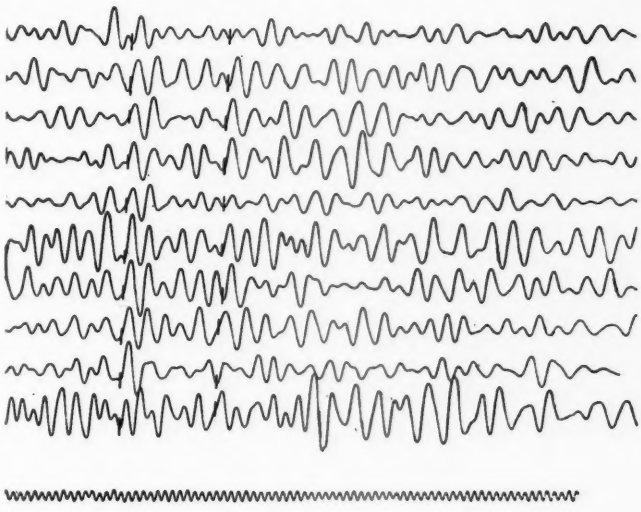

FIG. 12.

The first example of faults located in the field by the Geo-sonograph has not been verified by any other method to date. However, it is included in the presentation because it is an admirable illustration of a fault found by diffraction, and also because the results are so consistent as to hardly require substantiation by other means. These faults occur in territory characterized by relatively flat dips, where three-dimensional control is not vitally necessary as far as the stratification is concerned, but, as will be pointed out, without three-dimensional control these faults could not have been outlined.

[5] Complex Reflection Patterns and their Geologic Sources. Frank Rieber. *Geophysics* Vol. 2, No. 2, March, 1937.

A short distance away from these faults, the records are of a rather simple type and are suitable for ordinary seismograph recording, as shown in Fig. 12.

However, records obtained in the vicinity of the fault are of the confused type already discussed. One of these records, shown in Fig. 13, was taken only a little over half a mile from the previous record. Figure 14 shows how this confused record has been separated into its component parts by analysis.

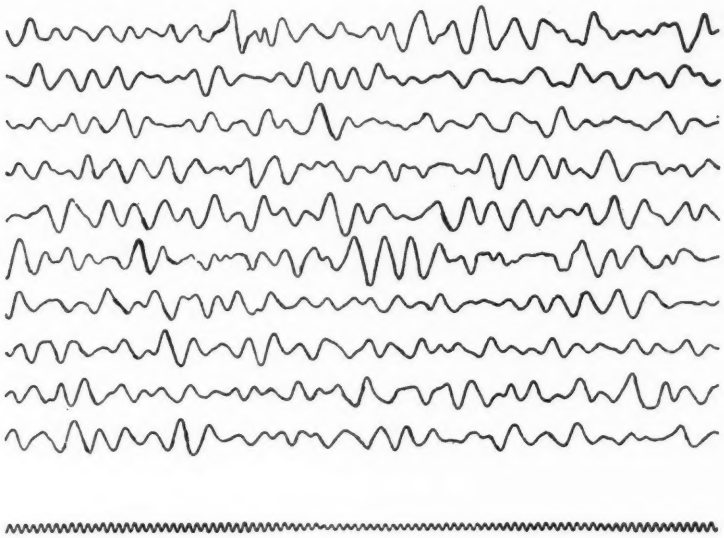

FIG. 13.

The profile obtained from records along this line is shown in Fig. 15. It should be noted that there is a fairly continuous set of flat dips, without any particularly outstanding key-bed. Neither are there any outstanding unconformities on this line from which a fault throw might have been determined. The detailing of the fault surface itself was the only method by which the fault could be located.

It should be noted from this figure that the diffracted waves apparently fall in no set pattern, and if this were assumed to be a true vertical profile of the line, no deductions as to the nature of the fault could be made. However, by a process of continuous three-dimensional control on the line of profile, which has been developed to go hand in hand with the Sonograph system of directional analysis,

the location of each of these diffractions to one side or the other of the line of exploration is known.

In a manner similar to plotting a strike and dip from three-dimen-

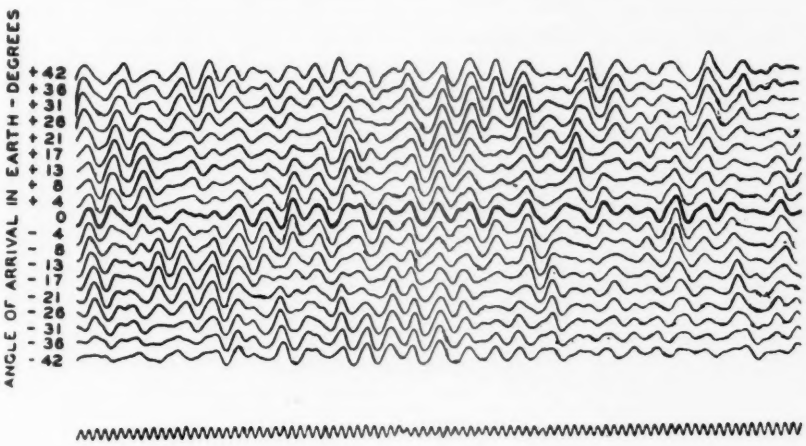

FIG. 14.

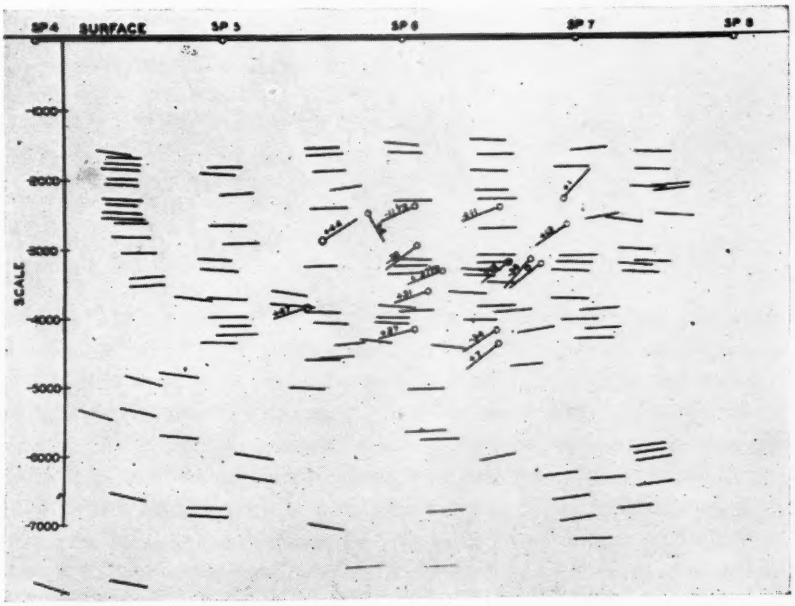

FIG. 15.

sional measurements the origin of the diffracted waves may be located three-dimensionally in space. Fig. 16 shows a plan view of the region, with the diffraction origin points plotted and the depths indicated. All but four of these points of origin fall on a pair of very nearly parallel surfaces, almost plane, which, in all likelihood, represent a pair of faults. Discarding the unexplainable points, we may draw approximate contours on the basis of the remaining points, as

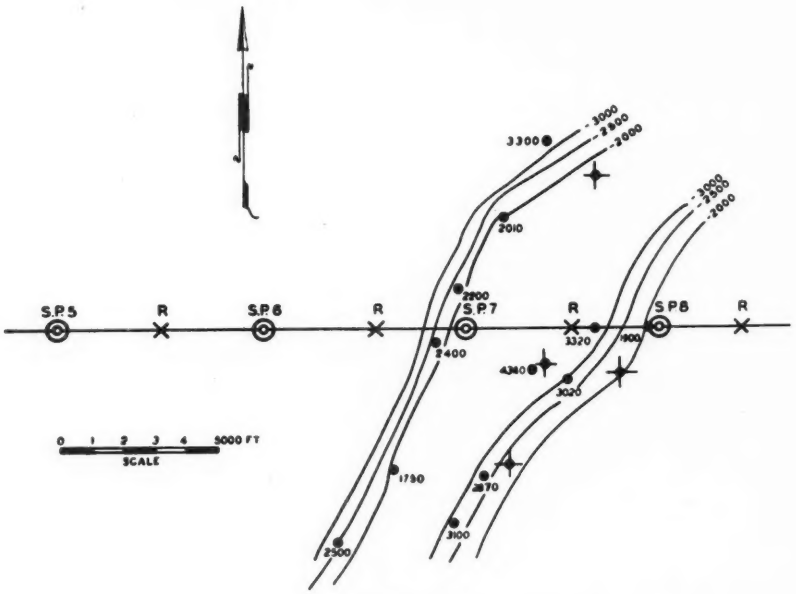

FIG. 16.

shown in Fig. 16, thus locating a pair of faults with a hade of about 40 degrees and a strike of about 50 degrees with the line of exploration.

Another example of field performance of the Geo-sonograph in highly faulted territory is shown in Fig. 17. Since the geophysical work was completed, surface geology confirmation has been released by the client for whom the work was done. Fig. 17 is a small-scale drawing of the profile in question, one of many in the region all contributing to the same ultimate interpretation. A quick scanning of the line reveals many complexities.

The unconformities and faults shown in the figures were all located prior to knowledge of the surface geology. The agreement with

surface geology is better than should be expected. Some of the unconformities are required by differences in line component of dip, while others were required by differences in cross-line component of dip. Some of the faults are indicated by dip changes (either line or cross-line components) while some are indicated by reflections or diffractions from fault corners or blocks in fault zones. Both faults and unconformities are supported by evidence from adjacent and cross lines though only this one section was released for publication.

Primarily the number of different directions of arrival at any one point on the surface should be noticed. Evidently any method of

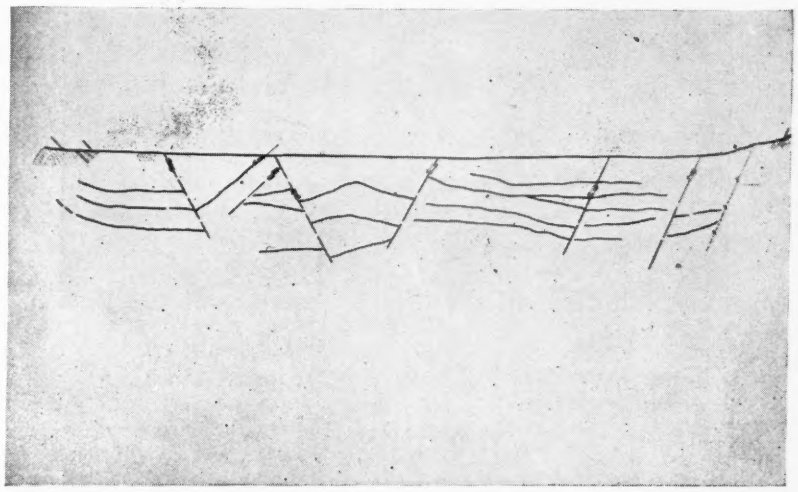

FIG. 17.

exploring this type of territory must feature directional separation to succeed.

For a third example of Geo-sonograph field performance, we are fortunate in having a direct comparison between results obtained by a Geo-sonograph field party and those obtained by a party employing what is conceded to be one of the better visual seismographs, in a typical faulted region, very similar to the one just shown. Typical records obtained by each party are shown in Figs. 18 and 19, where, for purposes of comparison, the Geo-sonograph record has been reproduced track by track in the equivalent visual form. Differences in the general appearance of the two records may be partly ascribed to dif-

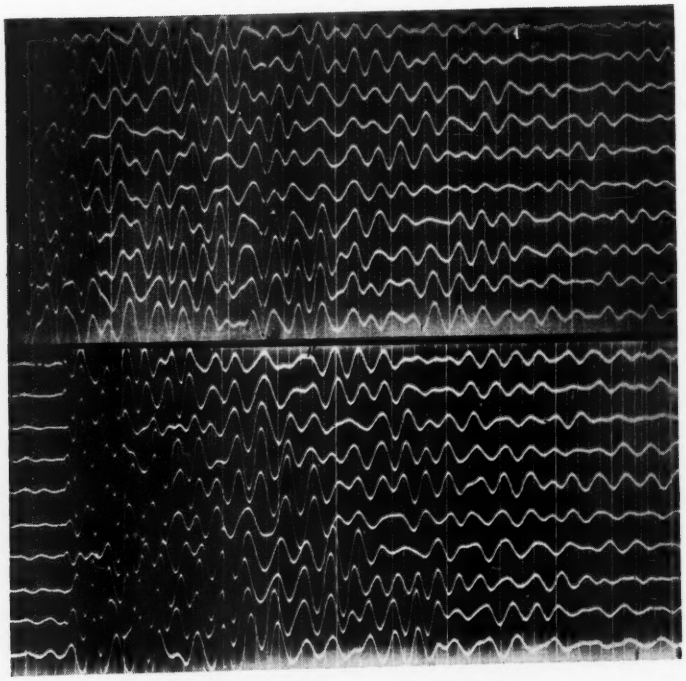

FIG. 18.

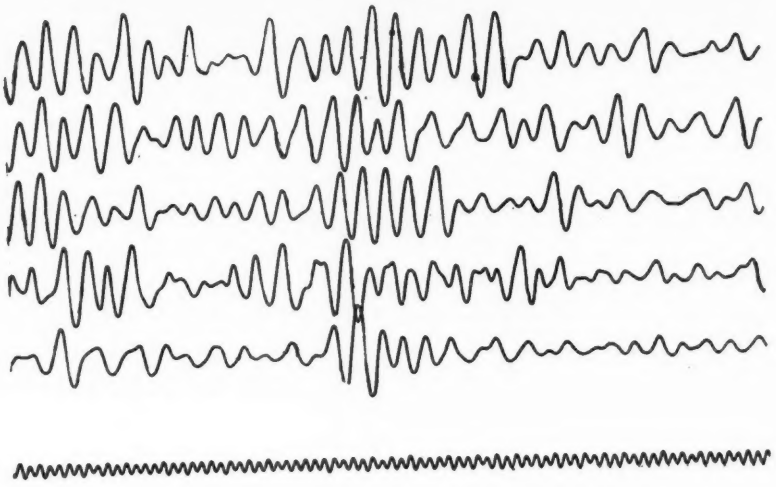

FIG. 19.

ferent time scales, but principally to differences in the recording instruments.

Since the Geo-sonograph achieves its results in two steps, the recording circuits may admit a large frequency and amplitude range which may be more narrowly limited in the step of analysis. The seismograph on the other hand, must completely limit frequency and amplitude ranges on the original record.

Overlooking these differences for the moment, it should be evident that neither record lends itself readily to visual interpretation,

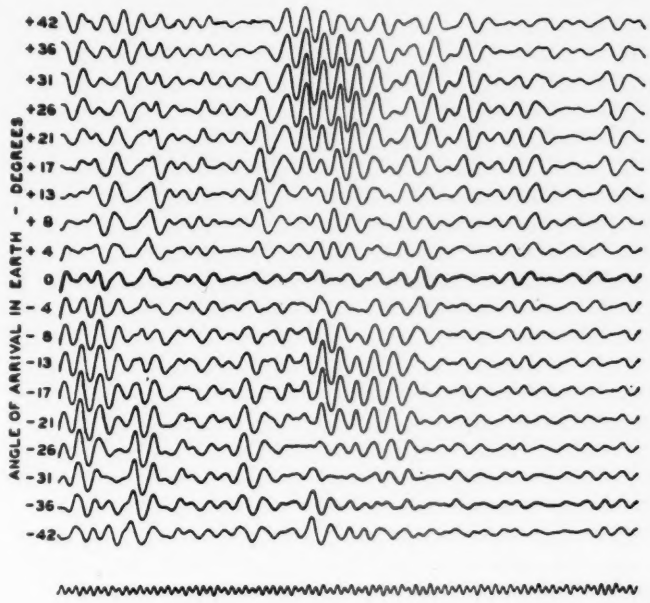

FIG. 20.

each in its own way being a typical confused record. Instead, from the original film record the cumulative analysis shown in Fig. 20 is made. On this record, certain features are strikingly evident, which were not noticeable at all on the visual record. These are, principally, a set of strong waves arriving from high angles together with others arriving from low angles. There cannot be the slightest suspicion that the interpreter of the Geo-sonograph cumulative record was searching for high angle waves because the fault was known to be present. Even the novice at reading these cumulative records can see that the

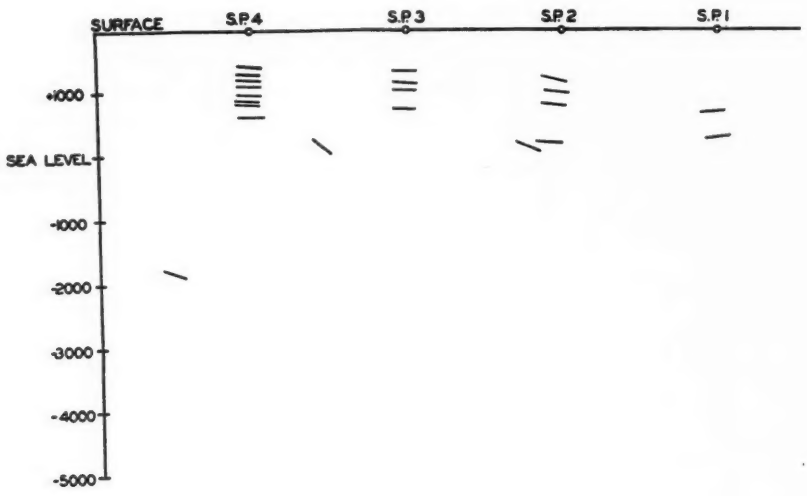
SURFACE
S.P.4
S.P.3
S.P.2
S.P.1
+1000
SEA LEVEL
-1000
-2000
-3000
-4000
-5000

FIG. 21.

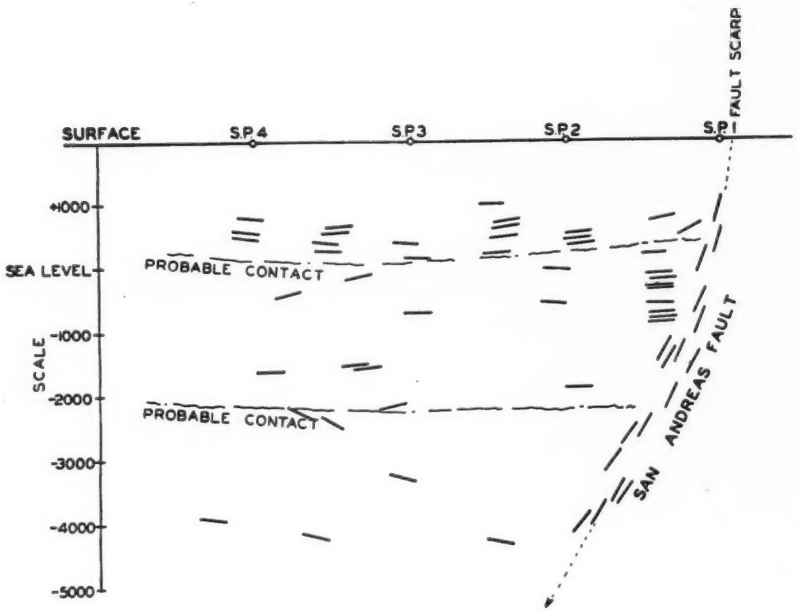
FAULT SCARP
SURFACE
S.P.4
S.P.3
S.P.2
S.P.1
+1000
SEA LEVEL
-1000
-2000
-3000
-4000
-5000
SCALE
PROBABLE CONTACT
PROBABLE CONTACT
SAN ANDREAS FAULT

FIG. 22.

high angle waves are as outstanding as any set of waves on the entire record.

Fig. 21 shows the profile which it was possible to obtain from the confused visual records. The complete absence of the fault, and the sparse reflections in the vicinity of the fault should be noticed. Fig. 22 shows the profile plotted from the results obtained from the Geo-sonograph cumulative record. Four advantages of this profile over that obtained by the seismograph are at once evident. First, the fault is very clearly outlined; second, reflections from stratification are practically as numerous near the fault as they are farther away; third, the reflections throughout the length of the line are more numerous on the Geo-sonograph profile than on the profile obtained from the seismograph records; fourth, the depth to which the stratification is mapped in this case is two or three times as great on the Geo-sonograph profile as on the seismograph profile.

In conclusion it may be observed that successful mapping of faulted areas with the Geo-sonograph is as much a vindication of the assumption that multiple angles of arrival cause "confused records" as of the method and apparatus employed to analyze the "confused record" into its components.

SUPPLEMENTARY NOTE (JUNE, 1938)

Since this paper was presented before the Society, much further experience with the Geo-sonograph has been obtained. In the light of this experience, the author believes the paper placed too much emphasis, in both theory and results, on diffractions as a major factor in Geo-sonograph performance. Far more impressive than its use of diffractions is the ability of the method to extract pertinent reflections from masking waves of undetermined origin and to separate two or more sets of pertinent reflections, relating each to its geologic origin. Thus, in filling in details in the "Blank Spaces" described in the paper, the extension of reflecting horizons far into the "Blank Spaces" and the separation of reflections arriving at the same time from strata on both sides of faults are more common occurrences than the detailing of the fault face by diffractions.

IN MEMORIAM: WENDELL BLESSING

Wendell Blessing, an associate member of the Society of Exploration Geophysicists, died Friday, May 20, 1938, in Houston, Texas, and was buried in South Park Cemetery in that city on Sunday, May 22, 1938. At the time of his death, he was a member of the insurance firm of Browning and Blessing. He is survived by his wife, two daughters, his parents, and a sister.

THE SOCIETY ROUND TABLE

MEMBERSHIP APPLICATIONS APPROVED FOR PUBLICATION

The Executive Committee have approved for publication the names of the following candidates for membership in the Society. This publication does not constitute an election, but places the names before the membership at large. If any member has information bearing on the qualification of these nominees, he should send it to the Secretary within thirty days. (Names of sponsors are placed beneath the name of each nominee.)

ACTIVE

James Affleck
L. L. Nettleton, G. B. Lamb, E. A. Eckhardt

John Frederick Anderson
W. G. Smiley, Jr., W. E. Hollingsworth, L. G. Ellis

Denys Howard Back
O. F. Sundt, L. F. Neuman, S. A. Judson

Charles Emery Buffum
A. L. Selig, D. Walling, C. J. Donnally

Lyman Chandler, Jr.
G. C. McGhee, J. A. Gillin, C. G. McBurney

Robert Leonard Craig
M. Riess, S. R. Marsh, A. B. Bryan

Thomas Anthony Elkins
L. L. Nettleton, G. B. Lamb, E. A. Eckhardt

Hubert Harold Evinger
L. L. Nettleton, G. B. Lamb, E. A. Eckhardt

F. Julius Fohs
E. De Golyer, E. McDermott, W. G. Saville

Maynard W. Harding
H. Hoover, Jr., C. G. Morgan, M. H. Gilmore

Benjamin Alfred Harris
J. H. Pernell, E. L. De Loach, R. Williams

Charles Henry Hightower
K. E. Burg, E. McDermott, H. B. Peacock

Alma Jones Hintze
W. H. Courtier, R. L. Doan, G. H. Westby

Aaron Elisha Holland
J. H. Pernell, A. N. Eby, W. E. Steele, Jr.

H. Wayne Hoylman
L. L. Nettleton, G. B. Lamb, E. A. Eckhardt

Roland F. Hughes
E. V. McCollum, H. R. Prescott, J. M. Crawford

John William Hull
J. L. Lake, E. E. Rosaire, P. W. Klipsch

Alvin Trousdale Jaques
P. W. Klipsch, R. Saibara, E. E. Rosaire

Edward Lipson
L. F. Neuman, O. F. Sundt, S. A. Judson

Joe Bernard Lovejoy
J. E. Jonsson, E. McDermott, P. Weaver
Weldon Gray McLarry
E. E. Rosaire, R. Saibara, S. S. West
Robert Du Wayne Miller
E. E. Rosaire, J. L. Lake, P. W. Klipsch
Herbert Horten Moody
L. F. Athy, H. R. Prescott, E. V. McCollum
Ralph Burgess Ross
E. A. Eckhardt, G. B. Lamb, C. H. Dresbach
John Joseph Rupnik
L. A. Scholl, Jr., G. D. Mitchell, Jr., R. L. Lay
Cyril Bertram Smith
J. H. Pernell, E. L. De Loach, R. Williams
Paul Ray Warren
L. F. Athy, H. R. Prescott, E. V. McCollum
James Roger Winnek
B. B. Weatherby, W. North, M. C. Born

ASSOCIATE

Joseph William Bastian
F. L. Bishop, J. W. Thomas, H. E. Banta
George Davenport
E. E. Rosaire, J. L. Lake, R. Saibara
Milton Burnett Dobrin
E. A. Eckhardt, B. Perkins, Jr., G. B. Lamb
John Adam Doering
E. E. Rosaire, P. W. Klipsch, J. L. Lake
Daniel Frank Elam
F. D. Bradbury, C. H. Wilson, J. J. Jakosky
Howard Fredrick Gemmell
G. B. Lamb, C. H. Dresbach, E. A. Eckhardt
James Turner Gilliam
F. W. Borman, L. Y. Faust, C. M. Ross
Harold Warren Haight
E. E. Rosaire, G. E. Wagoner, T. A. Manhart
Aurelous Vaden Hargis
J. E. Jonsson, B. Fisher, E. McDermott
Alred Arthur Hotard
N. N. Zirbel, D. F. Broussard, A. N. Eby
Roy Martin Langley
E. E. Rosaire, J. L. Lake, R. Saibara
George Ralph Merion
E. E. Rosaire, R. Saibara, L. Horvitz
Mansueto Joseph Pellillo
G. C. McGhee, J. A. Gillin, C. G. McBurney
Medwyn Dreyfus Sloane, Jr.
E. E. Rosaire, J. L. Lake, R. Saibara